



**Call: H2020-ICT-2016-2**

**Project reference: 760809**

**Project Name:**

**E2E-aware Optimizations and advancements for Network Edge of 5G New Radio  
(ONE5G)**

# Deliverable D5.2

## Final report on implementation and integration of PoC components into the PoCs and final PoC results

Date of delivery: 30/06/2019

Version: 1.0

Start date of project: 01/06/2017

Duration: 25 months

**Document properties:**

<b>Document Number:</b>	D5.2
<b>Document Title:</b>	Final report on implementation and integration of PoC components into the PoCs and final PoC results.
<b>Editor(s):</b>	Evangelos Kosmatos (WINGS)
<b>Authors:</b>	Gilberto Berardinelli , Rasmus Suhr Mogensen (Aalborg University) Matthias Mehlhose, Martin Kurras, Daniyal Awan (HHI), Cyril Collineau, Jean Dion (BCOM), Sergio Fortes, Carlos Baena, Ana Herrera García, Eduardo Baena, David Palacios, Carolina Gijón, María Luisa Marí-Altozano, Salvador Luna, Matías Toril, Raquel Barco (UMA), Emil Jatib Khatib (UMA, Aalborg University) Evangelos Kosmatos, Christos Ntogkas, Orestis Zekai, Andreas Georgakopoulos, Ioannis-Prodromos Belikaidis, Aspa Skalidi, Yiouli Kritikou, Panagiotis Demestichas, Panagiotis Vlaheas, Aimilia Badouna, Paraskevas Bourgos, Kostas Trichias, Eleni Giannopoulou, Konstantinos Tsoumanis, Ioannis Maistros, Evangelia Tzifa, Aikaterini Demesticha, Vera Stavroulaki (WINGS) Hanwen Cao (Huawei) Stelios Stefanatos (FUB)
<b>Contractual Date of Delivery:</b>	30/06/2019
<b>Dissemination level:</b>	PU <sup>1</sup>
<b>Status:</b>	Final
<b>Version:</b>	1.0
<b>File Name:</b>	ONE5G_D5.2_v1.0

**Abstract**

In this public report, we present the final results of WP5 within ONE5G project. WP5 covers the prototyping activities of the project targeting the definition, implementation, integration into testbeds and demonstration of a set of PoCs (Proof-of-Concepts) covering: a) both dense and scarcely populated

<sup>1</sup> CO = Confidential, only members of the consortium (including the Commission Services)

PU = Public

areas; b) a set of relevant verticals (e.g. smart city, factory of the future, automotive and agricultural applications); c) the main 5G service categories (eMBB, URLLC and mMTC) and; d) a selected set of technological components being proposed and investigated by the partners.

**Keywords**

Testbed, Proof-of-Concept, eMBB, URLLC, mMTC, Use case, PoC, technical components

## Executive Summary

In this public document, we report the final results of WP5 activities within ONE5G project. The objectives of WP5 are initially to select set of technological components being proposed and investigated by the partners in order to be implemented as technical component. Then to integrate these components into the partner testbeds and finally demonstrate a set of PoCs (Proof-of-Concepts) covering the two areas (Megacity and Underserved) addressed in the project. In addition, among the main objectives of WP5 is to link the provided prototypes with relevant verticals (e.g. smart city, factory of the future, automotive and agricultural applications).

In WP5, a set of five Proof-of-Concepts (PoCs) were defined and developed in order to validate the main ONE5G features and prove their benefits in realistic scenarios. The PoCs were built by implementing selected technical components proposed during the project timeframe by integrating these components into the available 7 partner testbeds of the project. These five PoCs cover different verticals in both “Megacities” and “Underserved Areas”, while some of them act as integrated PoCs including more than one testbed.

PoC#1 - Industrial PoC: This PoC targets URLLC services in an industrial area with large factories, in a “Megacities” scenario. The PoC integrates end-to-end (E2E) performance optimization techniques, small cells, multi-connectivity techniques (PDCP packet duplication, Single Frequency Network, coordinated multi-point transmission) for reliability enhancement, solutions for optimization of network resources in an end-to-end manner and network slicing management and negotiation in critical infrastructures.

PoC#2 - “Smart megacity”: This PoC focuses primarily on eMBB and mMTC service categories, in “Megacities” supporting a large number of users, services and cell densities. The PoC integrates E2E performance optimization techniques based on KPI to KQI mapping and monitoring, multi-node/multi-link, techniques context-aware multi-service solutions (e.g. RRM optimization), and enhancement of traditional load balancing techniques.

PoC#3 - Enhanced massive MIMO: This PoC targets eMBB services with a large number of users and dense cell deployment in “Megacities”. The PoC focuses on Massive MIMO technology in a multi-user and multi-cell environment and integrates technical components such as non-orthogonal multiple access (NOMA) and code design, novel antenna arrays (e.g. cylindrical arrays), sector, beam management and enhanced CSI acquisition techniques for Massive MIMO.

PoC#4 - “Underserved Areas”: this PoC focuses on low-cost network deployments and targets primarily mMTC and eMBB for agricultural applications. Technical components such as flexibility and fast reconfiguration of network elements and mechanisms for transmission path improvements and management of network slices are integrated.

PoC#5 - Automotive: this PoC targets URLLC for automotive applications in “Megacities”, but the scenario “Underserved Areas” could be considered as well, with less tight URLLC requirements. Technical components such as multi-antenna enhancement for improving reliability, and optimization of real-time processing in URLLC are integrated.

In addition to the aforementioned PoCs, two Integrated PoCs (IPoCs), meaning PoCs that utilise functionalities prototyped into different testbeds, were defined, implemented and demonstrated during the project.

---

IPoC#1 - Serving megacities and industrial areas through 5G technologies: integrated PoC between AAU, UMA and WINGS testbeds. The main goal of the integrated PoC is to prove the suitability of 5G technologies in supporting in a unified way the requirements in two challenging environments: a) industrial areas with large factories; b) highly populated areas, namely "Megacities".

IPoC#2 - Wireless control of industrial production: integrated PoC between AAU and UMA testbeds. This IPoC deals with a wirelessly controlled production line, addressing the capabilities of different radio technologies in supporting the latency demands. In addition, the IPoC showcases that end-to-end latency can be predicted using machine learning approaches..

# Table of Contents

<b>List of Figures</b> .....	<b>10</b>
<b>List of Tables</b> .....	<b>12</b>
<b>List of Acronyms and Abbreviations</b> .....	<b>13</b>
<b>1 Introduction</b> .....	<b>16</b>
1.1 Objective of the document .....	16
1.2 Structure of the document .....	19
<b>2 PoC#1: Industrial Proof-of-Concept</b> .....	<b>20</b>
2.1 Brief description of the PoC .....	20
2.2 List of technical components (TeCs) used in the PoC .....	20
2.3 TeC #1.1: Multi-connectivity for reliability improvement .....	21
2.3.1 Overview .....	21
2.3.2 Objectives .....	21
2.3.3 Architecture .....	21
2.3.4 Test/demo scenarios.....	22
2.3.4.1 Live demo .....	23
2.3.4.2 Measurement campaign for offline analysis.....	23
2.3.5 Validation .....	23
2.4 TeC #1.2: Reliable low latency communication in real industrial scenarios.....	25
2.4.1 Overview .....	25
2.4.2 Objectives .....	25
2.4.3 Architecture .....	25
2.4.4 Test/demo scenarios.....	27
2.4.5 Validation .....	27
2.5 TeC #1.3: Compressive sensing channel estimation in CRAN .....	28
2.5.1 Overview .....	28
2.5.2 Objectives .....	28
2.5.3 Architecture .....	28
2.5.4 Test/demo scenarios.....	29
2.5.5 Validation .....	30
2.6 TeC #1.4: Cloud control of low latency robot operations .....	31
2.6.1 Overview .....	31
2.6.2 Objectives .....	31
2.6.3 Architecture .....	31
2.6.4 Test/demo scenarios.....	32
2.6.5 Validation .....	32
2.7 Conclusion .....	32
<b>3 PoC#2: Smart-Megacity Proof-of-Concept</b> .....	<b>34</b>
3.1 Brief description of the PoC .....	34
3.2 List of technical components (TeCs) used in the PoC .....	34
3.3 TeC #2.1: Forward Error Correction component (FEC).....	35
3.3.1 Overview .....	35
3.3.2 Objectives .....	36
3.3.3 Architecture .....	36
3.3.4 Test/demo scenarios.....	38
3.3.5 Validation results .....	39
3.4 TeC #2.2: KPI-to-KQI metrics mapping .....	40
3.4.1 Overview .....	40
3.4.2 Objectives .....	40
3.4.3 Architecture .....	40
3.4.4 Test/demo scenarios.....	42

3.4.5	Validation .....	42
3.5	TeC #2.3: Prediction of network performance degradation.....	43
3.5.1	Overview .....	43
3.5.2	Objectives .....	43
3.5.3	Architecture .....	43
3.5.4	Test/demo scenarios.....	44
3.5.5	Validation .....	44
3.6	TeC#2.4: Enhancement of traditional load balancing techniques.....	45
3.6.1	Overview .....	45
3.6.2	Objectives .....	45
3.6.3	Architecture .....	45
3.6.4	Test/demo scenarios.....	45
3.7	TeC#2.5: Service-differentiated load balancing .....	48
3.7.1	Overview .....	48
3.7.2	Objectives .....	48
3.7.3	Architecture .....	48
3.7.4	Test/demo scenarios.....	49
3.7.5	Validation .....	50
3.8	TeC#2.6: Traffic steering management using context, user and cell level information .....	51
3.8.1	Overview .....	51
3.8.2	Objectives .....	51
3.8.3	Architecture .....	51
3.8.4	Test/demo scenarios.....	52
3.8.5	Validation .....	53
3.9	TeC #2.7: Ad-hoc deployment of services on edge cloud .....	54
3.9.1	Overview .....	54
3.9.2	Objectives .....	55
3.9.3	Architecture .....	55
3.9.4	Test/demo scenarios.....	56
3.9.5	Validation .....	56
3.10	Conclusion .....	56
<b>4</b>	<b>PoC#3: Enhanced massive MIMO Proof-of-Concept .....</b>	<b>57</b>
4.1	Brief description of the PoC .....	57
4.2	List of technical components (TeCs) used in the PoC .....	58
4.3	TeC #3.1: Machine learning-based adaptive nonlinear receive filtering in non-orthogonal multiple access (NOMA).....	58
4.3.1	Overview .....	58
4.3.2	Objectives .....	59
4.3.3	Architecture .....	59
4.3.4	Test/demo scenarios.....	60
4.3.4.1	Live Demo .....	60
4.3.5	Validation .....	62
4.3.6	Conclusion .....	67
<b>5</b>	<b>PoC#4: Underserved areas Proof-of-Concept .....</b>	<b>68</b>
5.1	Brief description of the PoC .....	68
5.2	List of technical components (TeCs) used in the PoC .....	68
5.3	TeC #4.1: Rx and Tx Digital Front Ends (Rx/Tx DFE) .....	68
5.3.1	Overview .....	68
5.3.2	Objectives .....	69
5.3.3	Architecture .....	69
5.3.3.1	Rx DFE.....	69
5.3.3.2	Tx DFE .....	71
5.3.3.3	Associated testbeds.....	72
5.3.3.4	Position of the TeC in the protocol stack .....	72

5.3.3.5	Technology used.....	73
5.3.3.6	Interfaces .....	73
5.3.4	Test/demo scenarios.....	73
5.3.4.1	Test overview .....	73
5.3.4.2	Test setup parameters .....	73
5.3.5	Validation .....	74
5.4	TeC #4.2: Slice negotiation between the vertical side and the operator side.....	74
5.4.1	Overview .....	74
5.4.2	Objectives .....	74
5.4.3	Architecture .....	75
5.4.4	Test/demo scenarios.....	76
5.4.5	Validation .....	77
5.5	TeC #4.3: Network slice creation supporting the vertical requirements in an area-based and time-based manner .....	79
5.5.1	Overview .....	79
5.5.2	Objectives .....	79
5.5.3	Architecture .....	80
5.5.4	Test/demo scenarios.....	81
5.5.5	Validation .....	81
5.6	Conclusion .....	82
<b>6</b>	<b>PoC#5: Automotive Proof-of-Concept .....</b>	<b>83</b>
6.1	Brief description of the PoC .....	83
6.2	List of technical components (TeCs) used in the PoC .....	84
6.3	TeC #5.1: Flexible SDR Architecture Supporting Joint Performance-Complexity Optimization .....	84
6.3.1	Overview .....	84
6.3.2	Objective.....	85
6.3.3	Architecture .....	85
6.3.4	Test/demo scenarios.....	86
6.3.5	Validation .....	86
6.4	TeC #5.2: Short Packet Structure for Ultra-Reliable Machine-type Communication.....	86
6.4.1	Overview .....	86
6.4.2	Objective.....	87
6.4.3	Architecture .....	87
6.4.4	Test/demo scenarios.....	88
6.4.5	Validation .....	88
6.5	TeC #5.3: Multi-connectivity beamforming for enhanced reliability .....	88
6.5.1	Overview .....	88
6.5.2	Objectives .....	88
6.5.3	Architecture .....	89
6.5.4	Test/demo scenarios.....	89
6.5.5	Validation .....	89
6.6	TeC #5.4: Tele-operated Driving Solution .....	90
6.6.1	Overview .....	90
6.6.2	Objective.....	90
6.6.3	Architecture .....	91
6.6.4	Figure 6-7. The overall architecture of the Tele-Operated Driving System from TU MünchenDemo/Test scenario.....	91
6.6.5	Validation .....	91
6.7	Conclusion .....	91
<b>7</b>	<b>Integrated PoCs .....</b>	<b>93</b>
7.1	IPoC#1: Serving megacities and industrial areas through 5G technologies .....	93
7.1.1	Description.....	93
7.1.2	Architecture .....	94

---

7.1.3	Test/demo scenarios.....	94
7.1.3.1	Megacity scenario.....	94
7.1.3.2	Industrial scenario .....	95
7.1.4	Validation .....	95
7.1.5	Conclusion .....	96
7.2	IPoC#2: Wireless control of industrial production .....	96
7.2.1	Description.....	96
7.2.2	Architecture .....	97
7.2.2.1	Data gathering for ML.....	98
7.2.2.2	Machine Learning.....	98
7.2.2.3	Estimator.....	98
7.2.3	Test/demo scenarios.....	99
7.2.3.1	Client .....	99
7.2.3.2	Server.....	101
7.2.4	Validation results .....	102
7.2.5	Conclusion .....	102
<b>8</b>	<b>Conclusion .....</b>	<b>103</b>
	<b>References .....</b>	<b>105</b>

## List of Figures

Figure 2-1. Test scenario with four cells. When multi-connectivity is activated, the smart UE can be served by two cells.....	22
Figure 2-3. ECDF of the estimated SINR for the different multi-connectivity options. ....	24
Figure 2-5. Wireless communication at MES level. ....	26
Figure 2-8. Configuration of RRH positions relative to the UE of interest. ....	29
Figure 2-9. Received power profile of the measurements. The nominal distribution is the one expected theoretically, while the crosses refer to individual measurements. The actual one deviates from the theoretical one due to hardware imperfections. ....	30
Figure 2-11. Normalized MSE for each RRH. ....	30
Figure 3-1. Generic FEC enabler .....	35
Figure 3-2. FEC position on a Physical Layer architecture .....	37
Figure 3-3. Graphical User interface for the FEC CNUM testbed.....	38
Figure 3-4. FEC qualification loopback.....	39
Figure 3-5. Decoding curves plotted on FPGA Board .....	39
Figure 3-8. KQI prediction.....	43
Figure 3-9. Comparison of real and predict indicators in training phase .....	45
Figure 2-22. Scenario of enhancement of traditional load balancing.....	46
Figure 3-14. Initial scenario .....	49
Figure 3-15: Distribution of users in the scenario .....	50
Figure 3-17. Distribution of users in the scenario .....	53
Figure 3-18. Initial situation.....	53
Figure 3-19. QoE evolution of each cell. ....	54
Figure 3-20. TeC Architecture .....	55
Figure 4-1. NOMA Uplink System Model Setup for the PoC .....	57
Figure 4-2. NOMA Uplink System Model.....	60
Figure 4-3. NOMA demonstration setup – array view.....	61
Figure 4-4. NOMA demonstration setup – bird-eye’s view.....	61
Figure 4-5. Graphical user interface for the NOMA MIMO testbed .....	62
Figure 4-6. Result 1 - (top plot) SER performance, (bottom plot) total sum goodput .....	63
Figure 4-7. Result 2 - (top plot) SER performance, (bottom plot) total sum goodput .....	64
Figure 4-8. Result 3 - (top plot) SER performance, (bottom plot) total sum good put .....	65
Figure 4-9. Result 4 - (top plot) SER performance, (bottom plot) processing time .....	66
Figure 5-1. Rx DFE overview .....	69
Figure 5-2. NB-IoT implemented in In-band. ....	70
Figure 5-3. Filter bank transfer function .....	70
Figure 5-4. NB-IoT Digital Front End – Rx side .....	71

---

Figure 5-5. NB-IoT Digital Front End – Tx side .....	72
Figure 5-6. Position of the Rx and Tx DFE in the protocol stack .....	72
Figure 5-7. Test scenario .....	73
Figure 5-8. Architecture and interfaces of Slice Negotiation TeC .....	75
Figure 5-9. Overall scenario architecture .....	76
Figure 5-10. Experimentation/demonstration architecture .....	77
Figure 5-11. Slice negotiation process - scenario 1 .....	78
Figure 5-12. Slice negotiation process - scenario 2 .....	79
Figure 5-13. Architecture and interfaces of TeCs .....	80
Figure 5-14. Traffic load patterns for the residential and office areas respectively .....	81
Figure 5-15. Slice negotiation results .....	82
Figure 6-1. Flexible SDR Architecture .....	85
Figure 6-2. Self-contained Frame Structure .....	87
Figure 6-3. End-to-end ping to test the round-trip end-to-end delay .....	88
Figure 6-4. Setup for performance evaluation with real-time channel emulator .....	89
Figure 6-5. Field test of air interface performance .....	89
Figure 6-6. Performance gain with Rx MRC diversity .....	90
Figure 6-7. The overall architecture of the Tele-Operated Driving System from TU München	91
Figure 7-1. IPoC#1 architecture .....	94
Figure 7-2. General overview of the proposed MLaaS scheme. ....	97
Figure 7-3. Hardware connections in a demo setup. ....	99
Figure 7-4. Client Modules .....	100
Figure 7-5. Live prediction in the client GUI .....	101
Figure 7-6. Training and demo controls .....	101

## List of Tables

Table 1-1. TeCs per PoC .....	16
Table 1-2. Testbeds relations .....	19
Table 3-1. FEC parameters in WiFi and NR systems .....	36
Table 3-2. Demonstration scenario .....	38
Table 3-3: Inputs and outputs of the prediction system. ....	44
Table 3-3. Throughput statistics comparison .....	47
Table 3-4. Network and experiments setting of PoC#2.6 .....	50
Table 3-5: Initial mean QoE of each cell .....	50
Table 3-6: Balanced mean QoE of each cell .....	51
Table 3-7. HOM configuration mechanism from previous TeC .....	54
Table 3-8. HOM configuration with the use of contextualized indicators .....	54
Table 3-9. Latency results .....	56
Table 5-1. Resource blocks per NB-IoT bands .....	70
Table 7-1. Accuracy measurements. ....	102

## List of Acronyms and Abbreviations

<b>Term</b>	<b>Description</b>
<b>ADC</b>	Analog to Digital Converter
<b>AP</b>	Access Point
<b>API</b>	Application Programming Interface
<b>BS</b>	Base station
<b>CAPEX</b>	Capital expenditure
<b>CCDF</b>	Complementary Cumulative Distribution Function
<b>CDF</b>	Cumulative Distribution Function
<b>C/I</b>	Carrier to Interference Ratio
<b>CIC</b>	Cascaded integrator comb filter
<b>C/N</b>	Carrier to noise ratio
<b>CM</b>	Configuration Management
<b>CR</b>	Coding Rate
<b>CRC</b>	Cyclic Redundancy Check
<b>CSS</b>	Chirp Spread Spectrum
<b>CSI</b>	Channel State Information
<b>CQI</b>	Channel Quality Indicator
<b>dB</b>	Decibel
<b>DFE</b>	Digital Front End
<b>DOF</b>	Degree of Freedom
<b>eMBB</b>	Enhanced Mobile Broadband
<b>E2E</b>	End To End
<b>FEC</b>	Forward Error Correction
<b>FIR</b>	Finite impulse response filter
<b>FM</b>	Fault Management
<b>FoF</b>	Factories of the Future
<b>FPGA</b>	Field Programmable Gate Array
<b>GPU</b>	Graphics Processing Unit
<b>GSPS</b>	Giga Samples per Second
<b>GUI</b>	Graphical User Interface
<b>HARQ</b>	Hybrid Automatic Repeat reQuest
<b>HETNET</b>	Heterogeneous Network
<b>HOM</b>	HandOver Margin
<b>HTTP</b>	Hypertext Transfer Protocol

---

<b>IIO</b>	Industrial I/O
<b>IoT</b>	Internet of Things
<b>IPF</b>	Image Processing Functionality
<b>IPoC</b>	Integrated Proof of Concept
<b>IRC</b>	Interference Rejection Combining
<b>IP</b>	Intellectual Property
<b>JSON</b>	JavaScript Object Notation
<b>JT</b>	Joint Transmission
<b>KPI</b>	Key Performance Indicator
<b>KQI</b>	Key Quality Indicator
<b>LBT</b>	Listen Before Talk
<b>LDPC</b>	Low Density Check Code
<b>LIDAR</b>	LIght Detection And Ranging
<b>LLR</b>	Log Likelihood Ratio
<b>LTE</b>	Long Term Evolution
<b>LoRa</b>	Long Range
<b>MAGW</b>	Multi-Access GateWay
<b>MCS</b>	Modulation and Coding Scheme
<b>MEC</b>	Multi-access Edge Computing
<b>MES</b>	Manufacturing Execution System
<b>MIMO</b>	Multiple-in Mutliple-out
<b>ML</b>	Machine Learning
<b>MLB</b>	Mobility Load Balancing
<b>MMSE</b>	Minimum mean square error
<b>mMTC</b>	Massive Machine Type Communication
<b>MML</b>	Man-Machine Language
<b>MRC</b>	Maximum Ratio Combining
<b>NMS</b>	Network Management System
<b>NOMA</b>	Non-Orthogonal Multiple Access
<b>NR</b>	New Radio
<b>OAI</b>	Open Air Interface
<b>OBU</b>	OnBoard Unit
<b>OPEX</b>	Operational expenditure
<b>OTA</b>	Over-The-Air
<b>PCB</b>	Printed Circuit Board
<b>PCIe</b>	Peripheral Component Interconnect Express
<b>PLC</b>	Programmable Logic Controllers
<b>PDCP</b>	Packet Data Convergence Protocol

---

<b>PDSCH</b>	Physical Downlink Shared Channel
<b>PHY</b>	Physical Layer
<b>PM</b>	Performance Management
<b>PoC</b>	Proof of Concept
<b>PUSCH</b>	Physical Uplink Shared Channel
<b>QAM</b>	Quadrature Amplitude Modulation
<b>QoE</b>	Quality of user Experience
<b>QoS</b>	Quality of Service
<b>RAT</b>	Radio Access Technology
<b>REST</b>	Representational State Transfer
<b>RF</b>	Radio frequency
<b>RKHS</b>	Reproducing kernel Hilbert space
<b>RRH</b>	Remote Radio Head
<b>RRM</b>	Radio Resource Management
<b>SDR</b>	Software defined radio
<b>SER</b>	Symbol error rate
<b>SFN</b>	Single Frequency Network
<b>SSH</b>	Secure Shell
<b>SIC</b>	Signal Interference Cancelation
<b>SINR</b>	Signal-to-Interference-plus-Noise Ratio
<b>SNR</b>	Signal-to-noise ratio
<b>SoC</b>	System-on-Chip
<b>TeC</b>	Technical component
<b>ToD</b>	Tele-operated driving
<b>UE</b>	User Equipment
<b>URLLC</b>	Ultra-Reliable Low Latency Communications
<b>USRP</b>	Universal Software Radio Peripheral
<b>V2X</b>	Vehicle-to-everything
<b>VHDL</b>	Vhsic Hardware Description Language
<b>WiFi</b>	Wireless Fidelity
<b>WP</b>	Work Package

# 1 Introduction

This document is the final deliverable of Work Package 5 (WP5) for the ONE5G project. It presents the project achievements related to the implementation of the technical components (TeCs) developed/proposed in WP3 and WP4, the integration of the TeCs into the Proof-of-Concepts (PoCs), the demonstration of PoCs during conferences and events and finally the validation of the PoCs.

## 1.1 Objective of the document

During the first months of the project, we started our implementation/integration activities by defining the Proof-of-Concepts (PoCs) that can best demonstrate the project use cases and fulfill the project objectives. The outcome of these activities was the definition of 5 PoCs described in detail in deliverable D5.1 [ONE5G-D51].

In parallel, we continued our activities by identifying for each PoC the technical proposals from the technical work packages (WP3 and WP4) that: a) were feasible to become prototypes within the project period; b) could serve as representative proposals for showcasing the project topics developed in the technical work packages. In this direction, an initial list of technical components (TeC) which were candidates for PoC implementation and integration into the 5 PoCs was described in milestone M5.1 of the project.

Then, a next step was to filter the aforementioned list of TeCs (and accounting for the amount of resources planned in the project for this work) to conclude to a subset of TeCs in a way that: a) the selected TeCs are a representative set of project technical proposals; b) after implemented and integrated in the PoC, they can demonstrate the main innovation of the PoC, with respect to the related vertical scenario and the project in general. The outcome of this activity was the final list of TeCs planned to be implemented and integrated into the testbed forming the defined PoCs. This list of TeCs was presented in detail in milestone M5.2 and deliverable D5.1 [ONE5G-D51].

Then, we continued our activities by implementing the selected TeCs and integrating them into the available testbeds, demonstrating them in conferences and events and finally validating them. All the aforementioned activities are presented in detail in the current document.

Therefore, this document presents the TeCs that were implemented, integrated into the partner testbeds, demonstrated and validated during the project duration. A summary of the implemented/integrated TeCs is provided in Table 1-1. In this table, for each PoC, the included TeCs are presented, together with the TeC Provider (the partner which proposed the mechanisms and algorithms of the TeC) and the Testbed Owner (the partner which actually implemented the TeC and integrated it into its testbed). In addition, the relation of the TeCs described in this document and the TeCs reported in D5.1 is presented, since in some cases the TeCs described in this document includes more than one elementary TeCs mentioned in D5.1.

**Table 1-1. TeCs per PoC**

PoC	Vertical	TeC #	Technical component title	Relation to TeCs described in D5.1	TeC Provider	Testbed Owner
1	Factory of the Future	1.1	Multi-connectivity for reliability improvement.	<ul style="list-style-type: none"> <li>• Macroscopic transmit diversity (i.e. multiple base stations transmitting the same signal)</li> <li>• Packet duplication at PDCP level</li> <li>• Packet duplication at physical layer, with single-frequency-network (SFN) type of transmission</li> </ul>	AAU	AAU
		1.2	Reliable low latency communication in real industrial scenarios	No direct relation with TeCs defined in D5.1. New TeC defined during the project.	AAU	AAU

		1.3	Compressive sensing channel estimation in CRAN	<ul style="list-style-type: none"> <li>Acquisition of downlink channel state information by means of low-overhead non-orthogonal reference sequences, and compressed sensing algorithms at the user</li> </ul>	FUB	AAU
		1.4	Cloud control of low latency robot operations	<ul style="list-style-type: none"> <li>Optimization of real-time processing in URLLC</li> <li>Multi-connectivity beamforming for enhanced reliability</li> <li>Short Packet Structure for Ultra-Reliable Machine-type Communication</li> </ul>	HWDU	HWDU
		1.5	Slice negotiation between the vertical side and the operator side.	<ul style="list-style-type: none"> <li>Implementation of slice negotiator entities both on Factory owner and Operator sides</li> </ul>	WINGS	WINGS
		1.6	Creation of new network slices in order to support the vertical requirements	<ul style="list-style-type: none"> <li>Network slice creation supporting the FoF requirements in an area-based and time-based manner</li> <li>Creation of end-to-end network slices (5G network and cloud resources)</li> <li>Activation of mMTC network slices for non-critical tasks inside the factory</li> <li>Activation of URLLC network slices in cases of emergencies</li> </ul>	WINGS	WINGS
2	Smart megacity	2.1	FEC (Forward Error Correction)	<ul style="list-style-type: none"> <li>Flexibility and fast reconfiguration of network elements according to the requested service requirements</li> </ul>	BCOM	BCOM
		2.2	KPI-to-KQI metrics mapping	<ul style="list-style-type: none"> <li>QoE-to-KQI and KQI-to-KPI metrics mapping</li> </ul>	UMA	UMA
		2.3	Prediction of network performance degradation	<ul style="list-style-type: none"> <li>Prediction of network performance degradation</li> </ul>	UMA	UMA
		2.4	Enhancement of traditional load balancing techniques	<ul style="list-style-type: none"> <li>Enhancement of traditional load balancing techniques</li> </ul>	UMA	UMA
		2.5	Service-differentiated load balancing	<ul style="list-style-type: none"> <li>Service-differentiated load balancing</li> </ul>	UMA	UMA
		2.6	Traffic steering management using context, user and cell level information	<ul style="list-style-type: none"> <li>Traffic steering management using context, user and cell level information</li> </ul>	UMA	UMA
		2.7	Ad-hoc deployment of services on edge cloud	No direct relation with TeCs defined in D5.1. New TeC defined during the project.	WINGS	WINGS
		2.8	Slice negotiation between the vertical side and the operator side	<ul style="list-style-type: none"> <li>Implementation of slice negotiator entities both on vertical side and operator side</li> </ul>	WINGS	WINGS
		2.9	Creation of new network slices in order to support the vertical requirements	<ul style="list-style-type: none"> <li>Creation of new network slices (including 5G network and cloud resources) in order to support the vertical end-to-end requirements</li> <li>Management of already established slices in order to continuously fulfil the vertical requirements</li> </ul>	WINGS	WINGS
3	Enhanced massive MIMO	3.1	Machine learning-based adaptive nonlinear receive filtering in non-orthogonal multiple access (NOMA)	<ul style="list-style-type: none"> <li>Non-orthogonal multiple access and code design</li> <li>Multiple data path transmission and multi-source synchronization</li> <li>MIMO planar antenna arrays and subarrays</li> </ul>	HHI	HHI

				<ul style="list-style-type: none"> <li>Change the configuration of the SDR platform using M-MIMO simulations based on QuaDRiGa channel model and measurement data</li> <li>Transmission of raw I/Q data in time domain over packet based 10G Ethernet</li> </ul>		
4	Agricultural	4.1	Rx and Tx Digital Front Ends (Rx/Tx DFE)	<ul style="list-style-type: none"> <li>Flexibility and fast reconfiguration of network elements according to the requested service requirements</li> </ul>	BCOM	BCOM
		4.2	Slice negotiation between the vertical side and the operator side	<ul style="list-style-type: none"> <li>Slice negotiation between the vertical and the operator</li> </ul>	WINGS	WINGS
		4.3	Network slice creation supporting the vertical requirements in an area-based and time-based manner	<ul style="list-style-type: none"> <li>Creation of new network slices (including 5G network and cloud resources) in order to support the vertical end-to-end requirements</li> <li>Management of already established slices in order to continuously fulfill the vertical requirements</li> <li>Creation of time-based and area-based network slices</li> </ul>	WINGS	WINGS
5	Automotive	5.1	Flexible SDR Architecture Supporting Joint Performance-Complexity Optimization	<ul style="list-style-type: none"> <li>Robust synchronization and channel equalization in URLLC</li> <li>Optimization of real-time processing in URLLC</li> </ul>	HWDU	HWDU
		5.2	Short Packet Structure for Ultra-Reliable Machine-type Communication	<ul style="list-style-type: none"> <li>Flexible short frame structure and frequency bandwidth</li> <li>Flexible pilot pattern</li> </ul>	HWDU	HWDU
		5.3	Multi-connectivity beamforming for enhanced reliability	<ul style="list-style-type: none"> <li>Multi-connectivity beamforming for enhanced reliability</li> </ul>	HWDU	HWDU
		5.4	Tele-operated Driving Solution	<ul style="list-style-type: none"> <li>Robust synchronization and channel equalization in URLLC</li> <li>Optimization of real-time processing in URLLC</li> </ul>	HWDU	HWDU

Another important note is that according to Table 1-1, some PoCs (PoC#1, PoC#2 and PoC#4) are constituted of several testbeds, therefore they are involving multiple partners. This means that different (non overlapping) parts of the PoCs (e.g. different TeCs) were implemented and integrated into different testbeds.

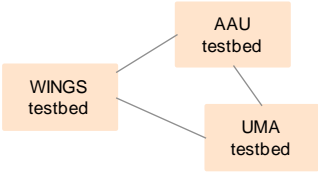
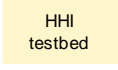
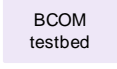
In addition, some TeCs (e.g. TeC#4.2 and TeC#4.3) were reused in more than one PoCs serving similar functionalities but in a different context. These TeCs are presented only once in the document. In detail, TeC#1.5 and TeC#2.8 are presented only in TeC#4.2, while TeC#1.6 and TeC#2.9 are presented only in TeC#4.3.

In addition to the implementation of the aforementioned PoCs, we went one step forward by defining, implementing and demonstrating Integrated PoCs (IPoCs), meaning PoCs that utilise functionalities prototyped into different testbeds. The following IPoCs were developed and demonstrated (described in detail in section 0):

- IPoC#1: Serving megacities and industrial areas through 5G technologies: integrated PoC between AAU, UMA and WINGS testbeds. Demonstrated in MWC2019.
- IPoC#2: Wireless control of industrial production: integrated PoC between AAU and UMA testbeds. Demonstrated in EuCNC2019.

In order to further explain the motivation of the aforementioned integration activities and also to explain the reason for selecting not to integrate between other partners, the following Table 1-2 was generated. The table summarizes the relations between the available partners testbed.

Table 1-2. Testbeds relations

Testbeds	Motivation and level of integration
 <pre> graph LR   WINGS[WINGS testbed] --- AAU[AAU testbed]   WINGS --- UMA[UMA testbed] </pre>	<p><b>Motivation for integration:</b> To demonstrate the validity and performance of project innovations (reliability enhancement for URLLC, e2e network optimization, slice management) and their feasibility through prototyping into megacity and industrial contexts.</p> <p><b>Level of integration:</b> AAU testbed and UMA testbed realizes the Megacity and industrial area enhanced functionalities controlled by slice management functionalities of WINGS testbed.</p>
 <pre> graph LR   AAU[AAU testbed] --- UMA[UMA testbed] </pre>	<p><b>Motivation for integration:</b> to demonstrate the usage of prediction techniques to improve communication's reliability in industrial scenarios.</p> <p><b>Level of integration:</b> AAU testbed realizes the industrial area reliability enhancement driven by prediction techniques based on ML realized in UMA testbed.</p>
 <pre> graph LR   HHI[HHI testbed] </pre>	<p><b>Motivation for non integration:</b> HHI testbed focused on massive MIMO topics, which are not related with the interests of other testbed partners. In addition, integration on massive MIMO is not feasible without the two testbeds to be collocated.</p>
 <pre> graph LR   BCOM[BCOM testbed] </pre>	<p><b>Motivation for non integration:</b> BCOM testbed focuses on technical proposals for lower layers (e.g., Tx/Rx DFE) than the ones addressed by the other testbeds, therefore a remote integration with other testbeds is not feasible.</p>
 <pre> graph LR   HWDU[HWDU testbed] </pre>	<p><b>Motivation for non integration:</b> In HWDU testbed, V2X related technical proposals are integrated and since no other partners are related with V2X, an integration did not appear useful.</p>

## 1.2 Structure of the document

This document is organised into 8 sections. The current section is an introduction of the document and the summary of PoCs and their respective TeCs. Sections 2 to 6, describe the five PoCs respectively. Each PoC section is divided into sub-sections describing different aspects of the TeC. Each subsection is structured as follows:

- A brief description of the PoC
- The list of technical components selected for the PoC
- TeC overview: a short summary describing the technological component
- Objective of the TeC: the main objectives of the TeC
- TeC architecture: the main building blocks and their interfaces
- Test/demo scenarios: description of a set of scenarios under which the TeC will be tested, demonstrated and evaluated.
- Validation: the validation process followed for the TeC and the validation results
- Conclusion: the main outcomes of the PoC

Section 7 presents the two integrated PoCs. Each subsection is structured as follows:

- Description: a brief description of the IPoC
- Architecture: the architecture, the main building blocks and interfaces
- Test/demo scenarios: the testing and demonstration scenarios
- Validation: the validation process followed

The document concludes with section 8, which summarizes the content and main findings.

## 2 PoC#1: Industrial Proof-of-Concept

### 2.1 Brief description of the PoC

The aim of this PoC is to test and validate E2E performance optimization techniques and enhancements for reliability improvements in industrial areas. Initially the scope of this PoC included also cell-less aspects, therefore the initial name was "Cell-less Megacity PoC". However, during the course of the project, the interest of cell-less aspects was assessed by the partners as having a lower priority as other technologies targeting the Industry vertical, and were consequently replaced by these new technical components, to strengthen the focus on this vertical. The PoC was therefore renamed "Industrial PoC". The vertical scenario is assumed to be an industrial area with large factories.

In particular, this PoC addresses solutions for supporting services demanding high reliability for industrial automation use cases, efficient support of large number of communication links via reduction of the overhead needed for channel estimation, control of robots operation in the cloud, and support of different services via network slice negotiation.

Though the scope of the individual TeCs considered in this PoC is in some cases rather diverse, these TeCs represent a pool of solutions addressing the needs of the targeted vertical scenario, whose scopes may range from the support of low latency highly reliable communication to the efficient multiplexing of different services on the same radio interface.

Three testbeds are used in this PoC:

- a) the multi-link/multi-node and CRAN (centralized RAN) testbed (AAU);
- b) Platform for vertical service delivery through 5G – IoT and big data - technologies (WINGS);
- c) Cloud Robot Testbed (Huawei).

For more information on the used testbeds and on this PoC, please refer to Chapter 2 of the ONE5G document D5.1 [ONE5G-D51]. In this deliverable and extra TeC has been included (Reliable low latency communication in real industrial scenarios), which was not envisioned in the first year of the project, and whose feasibility for realization became possible during the project time.

### 2.2 List of technical components (TeCs) used in the PoC

The following TeCs are used in this PoC:

- **Multi-connectivity for reliability improvement.** This TeC is related to "Multi-connectivity with packet duplication: operations and enhancements" (section 3.2.1 of D3.2 [ONE5G-D32]).
- **Reliable low latency communication in real industrial scenarios.** It is an additional TeC not related to the technical WPs [MRB+19].
- **Compressive sensing channel estimation in CRAN.** This TeC is related to "CRAN performance under low-overhead channel estimation" (section 4.1.1 of D4.2 [ONE5G-D42]).
- **Cloud control of low latency robot operations.** This TeC is related to "URLLC Enabled by GF Access, HARQ, and Frame Design" (section 2.2 of D4.2 [ONE5G-D42]).
- **Slice negotiation between the vertical side and the operator side.** This TeC is related to "Time-variant optimal slicing negotiations" (section 3.2.3 of D3.1 [ONE5G-D31]). The TeC is described in section 5.5 of the current document.

- **Creation of new network slices in order to support the vertical requirements.** This TeC is related to "Network slice management based on mobility and traffic patterns" (section 4.2.3 of D3.2 [ONE5G-D32]). The TeC is described in section 5.5 of the current document.

## 2.3 TeC #1.1: Multi-connectivity for reliability improvement

### 2.3.1 Overview

Radio cells densification is foreseen as a valid solution for improving spectral efficiency and reliability of the wireless links in the light of upcoming 5G NR services [MPT+13]. Such density translates to the existence of multiple strong links that can be exploited by a device running a demanding wireless application.

Multi-Connectivity has recently drawn significant attention as a promising solution for exploiting the redundancy of the radio links [MLL+18]. Differently from single connectivity, where a device is always connected to a single point of transmission/reception (e.g., an Access Point (AP)) and its performance is therefore depending on the quality of a single radio link, in multi-connectivity multiple APs can simultaneously configure radio resources to a given terminal, introducing link diversity. This can be beneficial, for instance, in case of severe interference or blockage in a specific link. Multi-connectivity is then envisioned to offer relevant benefits for services targeting reliable communication. The price to pay is a larger resource utilization for the users benefiting from the multi-connectivity solutions, which translates to an overall network throughput penalty.

### 2.3.2 Objectives

The objective of the TeC is to verify the potential of downlink multi-connectivity in improving the link quality of specific "smart" user equipment (UEs) with respect to traditional single link connection. We consider dense scenarios characterized by a number of small cells located at a short mutual distance, and therefore generating a harsh interference environment which may compromise the link performance in case of single connectivity, jeopardizing the possibility of achieving a reliable connection. Introducing multi-connectivity is expected to lead to significant performance improvement for the UEs suffering from harsh fading or interference conditions. Different techniques are analyzed and compared: packet duplication, Single Frequency Network (SFN), and non-coherent joint transmission (JT). Two different receiver types will be considered: Maximum Ratio Combining (MRC) and Interference Rejection Combining (IRC). The MRC receiver is able to strengthen the desired signal but is interference-unaware, while the IRC receiver is able to suppress a number of interfering streams by projecting them over an orthogonal subspace with respect to the desired signal. Our analysis will also address the trade-off between link performance improvement of the UEs benefiting from multi-connectivity, and its impact on the overall network performance.

### 2.3.3 Architecture

The multi-link multi-node testbed by AAU is used for implementing this TeC. The usage of the AAU testbed for this TeC is twofold:

- Live demonstration, with the possibility of verifying the instantaneous performance of the targeted techniques in live scenarios
- Offline analysis. The testbed is used to collect a large set of radio channel measurements in specific scenarios/environments, which are post-processed to emulate the multiple multi-connectivity configurations, and analyze their performance.

The TeC is targeting the verification of physical layer (PHY) solutions for multi-connectivity (Single Frequency Network (SFN), non-coherent Joint Transmission (JT)), but also packet duplication techniques at higher layer (HL), e.g. Packet Data Convergence Protocol (PDCP).

The general architecture consists of a testbed server connected to a number of nodes.

The nodes -Access Points (APs) and User Equipment (UEs) are implemented physically as Windows PCs and a Universal Software Radio Peripheral (USRP) RIO board connected through PCIe bus. The USRPs are controlled and programmed using Labview Communications Suite. In the software developed in Labview, the nodes have an HTTP interface which allows communication with the exterior. Since our focus is on the downlink, the APs operate as transmitters, and the UEs as receivers. The UEs measure the channel responses from each AP, and report such measurements to the testbed server. The testbed server emulates the different multi-connectivity techniques based on such measurements as well as the receiver types, and calculate the relevant KPIs. Such KPIs can be displayed live over a Graphical User Interface (GUI).

### 2.3.4 Test/demo scenarios

The testbed emulates a network with four cells, each cell composed by one AP and one UE. Each node in the network (UE or AP) is multi-antenna capable (MIMO 2x2). Out of the 4 cells, two are smart cells (offering the multi-connectivity options) and the others are background cells, i.e. only meant for assessing the overall network throughput.

Our focus is on the downlink only, with 1 smart UE (benefiting from multi-connectivity), and 3 UEs associated to 3 cells in single cell mode. A pictorial representation of the scenario is depicted in Figure 2-1.

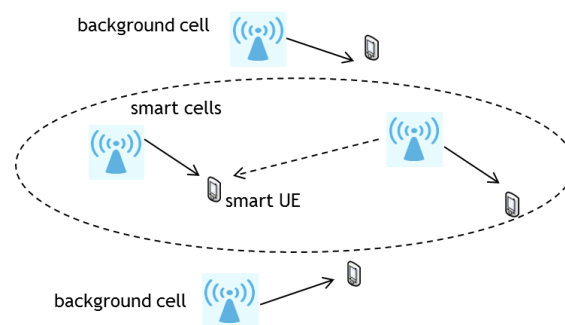


**Figure 2-1. Test scenario with four cells. When multi-connectivity is activated, the smart UE can be served by two cells.**

In the default mode, the network operates in single cell mode, i.e. also the smart UE is served by a single AP. Different multi-connectivity options can be then set for the smart UE. The UEs can be set to operate with MRC or IRC receivers. The goal of the test is to assess the benefits of multi-connectivity in terms of Signal-to-Interference plus Noise Ratio (SINR) improvement for the smart UE, and its impact on the overall network throughput.

The main KPIs that we are calculating are throughput and reliability. Throughput is calculated based on the instantaneous SINR by using Shannon mapping. Reliability is also reflected by a measured SINR value; i.e. an SINR lower than a predefined threshold for guaranteeing correct data reception translates to a packet loss.

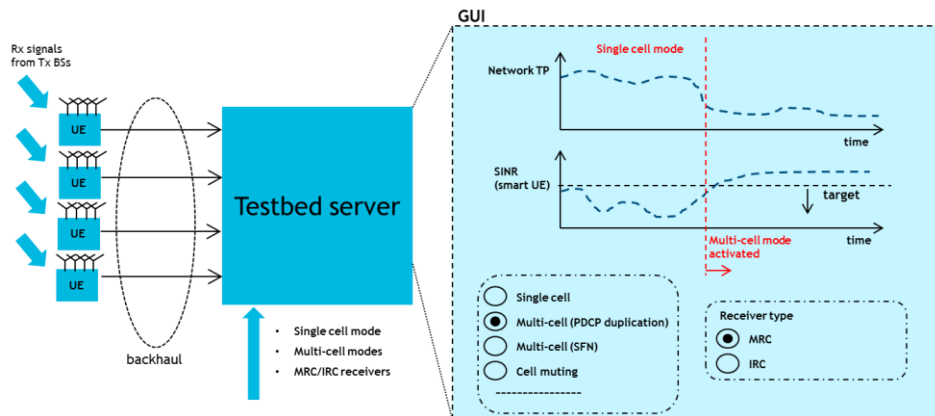


**Figure 2-2. Measurements collection and GUI display. Improvement of reliability for the smart UE**

### 2.3.4.1 Live demo

As mentioned in section 2.3.3, this TeC has been evaluated via live demonstration and offline analysis.

In the live demonstration, the testbed runs in the Aalborg University laboratory and the mentioned KPIs are calculated real time in the testbed server for different receiver types or multi-connectivity solutions, based on the channel measurements reported instantaneously by each UE. The GUI shows the live KPIs, highlighting the trade-off between reliability of the smart UE and overall network throughput, for the instantaneously selected configurations. This is pictorially shown in Figure 2-2.

This live demo was presented at EuCNC2018, as well as during the intermediate project review in September 2018.

### 2.3.4.2 Measurement campaign for offline analysis

The offline analysis mentioned in Section 2.3.3 is based on channel measurements followed by offline emulation of the multi-connectivity techniques. Measurement campaigns have been run in two real industrial scenarios, which we denote as Factory A and Factory B. Such scenarios are rather diverse in terms of machinery clutter. In particular, Factory A has a light amount of clutter, with sparsely distributed machinery. As a consequence, line-of-sight communication conditions are more probable. Factory B is instead characterized by a significant amount of clutter which translates to a high probability of obstructed radio communication conditions.

Measurements have been taken by using 12 SDR nodes, where 4 nodes are configured as transmitters, and the other 8 nodes as receivers. Each node consists of 2 USRP RIO devices (2x2 MIMO capable) and a host PC that runs the measurement software. The system operates at a 3.5 GHz carrier frequency is used, with a 18 MHz transmission bandwidth.

The transmitter locations are deployed at the corners of each factory scenario. The receivers are distributed over 24 predefined positions via several redeployments. In this way, a large number of measurements can be obtained. Panel antennas with 60 degrees aperture are used for the transmitter nodes, and omnidirectional dipole antennas for the receiving nodes. The transmit antennas are set at a 2.6 m height, while different heights per terminal are set for the receive nodes (1.75 m and 0.25 m). Such different heights are meant to emulate the diverse positions of industrial devices like sensors and actuators in the factory environment. For further details on the measurements and on the offline processing, we refer to [KAB+19].

### 2.3.5 Validation

The results presented here are obtained from the offline analysis based on measurements on the two considered scenarios, and are meant at assessing statistically the potential performance gain of the multi-connectivity techniques.

Figure 2-3 shows the Empirical Cumulative Distribution Function (ECDF) of the SINR of the smart UE in the two different scenarios and receiver types (MRC and IRC).

The multi-connectivity solutions (red, purple and yellow lines) clearly lead to a higher SINR gain with respect to single connectivity (blue line) in Factory A. In particular, the gain is in the order of ~8 dB at a  $10^{-2}$  percentile for the physical layer multi-connectivity solutions compared to the ~1-2 dB gain in Factory B. By assuming for example a 0 dB SINR threshold for correct packet detection, in Factory A transmission appears to be successful for all the measured samples in case physical layer multi-connectivity is used, while in Factory B a remaining failure rate persists. The better performance in Factory A is due to the presence of LOS conditions, which allow to translate a potentially detrimental interfering link to an useful one when multi-connectivity is used. In contrast, the massive presence of obstructers in Factory B diminishes the benefits of multi-connectivity, since the receiver is already unlikely to experience significant interference even in single-connectivity mode. As expected, both SFN and JT clearly outperform HL duplication. This is due to the fact that in HL duplication, both primary and secondary AP still suffer from their mutual interference since they transmit the duplicated packets at different time instants. However, the physical layer duplication improvements come at a significantly higher cost. It is worth to observe that no significant gain of JT with respect to SFN is visible. The usage of an IRC receiver has a minor benefit with respect to MRC in Factory A while its impact is negligible in Factory B. Supporting reliable communication has an impact on the overall network capacity: the maximum throughput in the network is estimated to be about 36 % lower when comparing the multi-connectivity with respect to single connectivity. We refer to [KAB+19] for additional results and analysis.

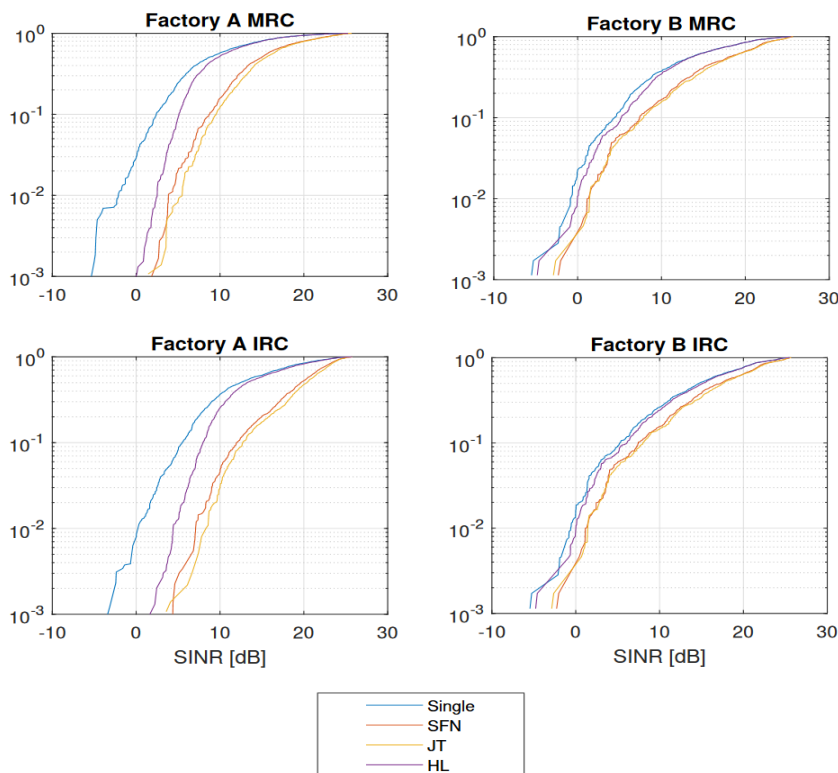


Figure 2-3. ECDF of the estimated SINR for the different multi-connectivity options.

## 2.4 TeC #1.2: Reliable low latency communication in real industrial scenarios

### 2.4.1 Overview

Wireless technologies are identified as a major enabler of the Industry 4.0 vision, since they lead to massive capital expenditure (CAPEX) and operational expenditure (OPEX) reduction with respect to a traditional wired setup, besides enabling new use cases (e.g., support of mobile robots) translating to higher flexibility, improved product customization and – ultimately – productivity increase [CWS+17]. The usage of wireless solutions for applications such that manufacturing execution system (MES) – which controls the overall manufacturing operations – or closed loop control require however a guarantee of bounded communication latency in order to ensure correct and timely execution of operations. The latency requirements are application specific; while closed loop control may require physical layer latencies in the order of ms and below, MES command may demand latencies in the order of ~100 ms. The feasibility of existing radio solutions in supporting industrial automation use cases has to be verified. Also, it is envisioned that the usage of multiple radio interfaces with packet duplication can contribute in reducing the latency performance.

### 2.4.2 Objectives

The objective of this TeC is to verify the suitability of existing radio technologies (namely LTE and WiFi) in supporting MES connectivity in industrial automation. Also, the TeC aims at investigating the potential benefits of using a multiaccess technique that benefits from the combined application of different radio technologies. This TeC leads to a first assessment of the potential of wireless technologies for industrial automation, and paves the way for future investigation dealing with more challenging use cases such as support of closed loop control, where 5G NR is needed.

### 2.4.3 Architecture

This TeC has been implemented in the AAU Smart Production Lab. We consider a manufacturing line consisting of multiple Festo modules with conveyor belts and various manufacturing equipment, shown in Figure 2-4. Each module is split up into two stations containing a switch, multiple Programmable Logic Controllers (PLCs) and fieldbus technologies, screen and a port for external Ethernet connections. A PC running a MES is used to keep track of different products in production based on radio-frequency identifier (RFID) tags in product carriers. When a carrier passes a scanner, the PLC reports this to the MES, that returns a response on the action to be taken according to the product state e.g. drill a hole or place circuit board. In this manufacturing line the time sensitive communication is represented by the PLC and fieldbus, in contrast to the delay tolerant inter- module and MES communication.

In this TeC we focus on replacing Ethernet connection for communication at MES level with wireless, while keeping communication at PLC level still wired. The concept is pictorially depicted in Figure 2-5. The inter module and MES communication consists of a mixture of Layer 2/3 traffic, that is latency tolerant and with low bandwidth requirements.

Backwards compatibility is to be taken into account when designing a network architecture for MES communication support, such that no existing equipment needs to be modified or replaced. This requires that the wireless network is self-contained and configurable independently of the wired network. This is obtained by designing a multi-access gateway which provides seamless integration along with low latency, high availability and reliability.



**Figure 2-4. Manufacturing line in AAU Smart Production Lab.**

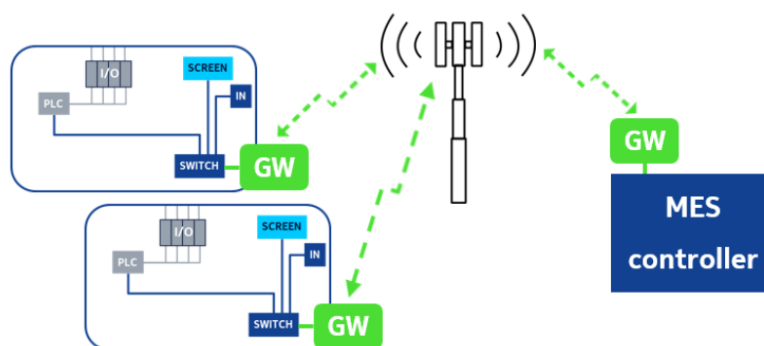


**Figure 2-5. Wireless communication at MES level.**

For the connectivity between gateways we leverage both LTE and Wi-Fi. The LTE connectivity is provided by one of the major mobile operators in Denmark via its commercial wide area network. A dedicated APN is deployed in the operator's core network that allows for UE-to-UE communication as well as assignment and configuration of static IPs. In the used configuration the traffic between gateways is routed in the core and not forwarded to the public internet; this means that it effectively creates a private network using the public infrastructure. This is similar to network slicing in 5G, although without prioritized resource allocation in the radio access network (RAN). Integrating LTE with Wi-Fi provides the additional benefit of having fallback options, thereby increasing the availability and reliability of the overall system.

The block diagram of the multi-access gateway (MAGW) is shown in Figure 2-6. Such gateway design does not only aim at fulfilling the communication requirements previously stated but also includes network configuration-oriented functionalities such as DHCP and routing, such that an existing network can be replicated using only these gateway devices.

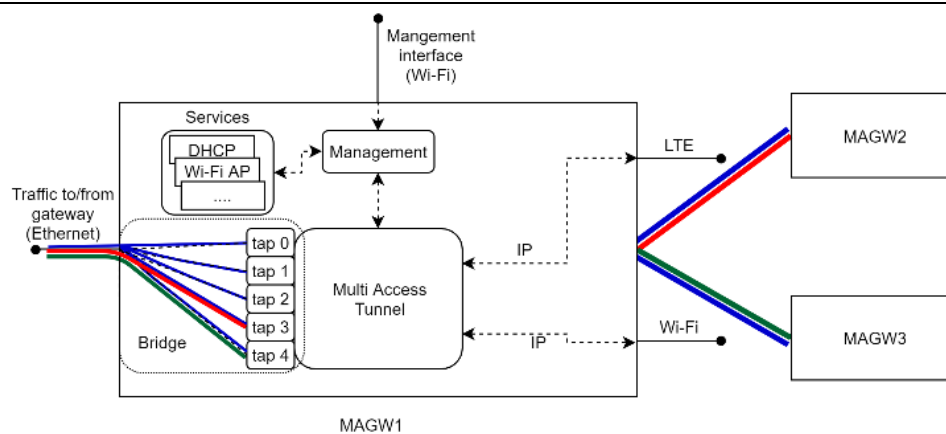


Figure 2-6. Block diagram of multi-access gateway.

## 2.4.4 Test/demo scenarios

The measurement setup for the evaluation of the LTE and WiFi performance consists of time synchronized packet sniffers that are placed at the gateways on each module and the MES PC. In the measurement setup there are two different cases, for regular Ethernet, and for wireless connectivity, respectively.

For WiFi, we consider both options of interference-free and interference-prone channels. Interference is generated by adjacent Wi-Fi networks that are not related to the manufacturing lines. The interference is created by using the same channel as the one used by the university network (channel 132) and starting different traffic flows from 5 devices (streaming service, file download and periodic traffic) while the manufacturing line is running. For the interference-free case we select a channel where only our gateways are transmitting data (channel 161).

A test run consists of the production line producing the same product type for 30 minutes. This corresponds to 17k to 20k measurements, with an average load of 6.2 kb/s, when aggregating all the samples to and from the MES. For each test approximately 90 % of the size packets transmitted wirelessly are 88 to 108 bytes (excluding technology specific overhead for Wi-Fi and LTE). This means that no distinction is being made for the individual modules and the results should be interpreted as the overall communication performance for the whole production line.

## 2.4.5 Validation

Figure 2-7 shows the empirical complementary cumulative distribution function (CCDF) for the different wireless technologies along with the baseline Ethernet. While Ethernet provides a significant better latency and consistent performance even at the 99.99th percentile, we stress that the type of communication that needs to be facilitated is delay tolerant. If we compare Wi-Fi with public LTE there is a clear performance significant difference in latency for the interference-free scenario. However, when interference is introduced, Wi-Fi exhibit a 10x delay degradation compared to interference free Wi-Fi and approximately  $\sim 2.5x$  compared to the public LTE connection. The reason for this performance degradation lies in the fact that the random back off that is a part of the Listen Before Talk (LBT) mechanisms are triggered more often and the increased collision probability due to the increased traffic. When enabling packet replication over both radio interfaces we observe an improvement in latency for both Wi-Fi cases. For standalone LTE it is a  $\sim 4x$  and  $\sim 5x$  improvement respectively. Such large improvement, even in interference conditions, is due to the fact that the latency performance of LTE and Wi-Fi are uncorrelated and therefore present the possibility of a diversity gain. For further details, we refer to [MRB+19].

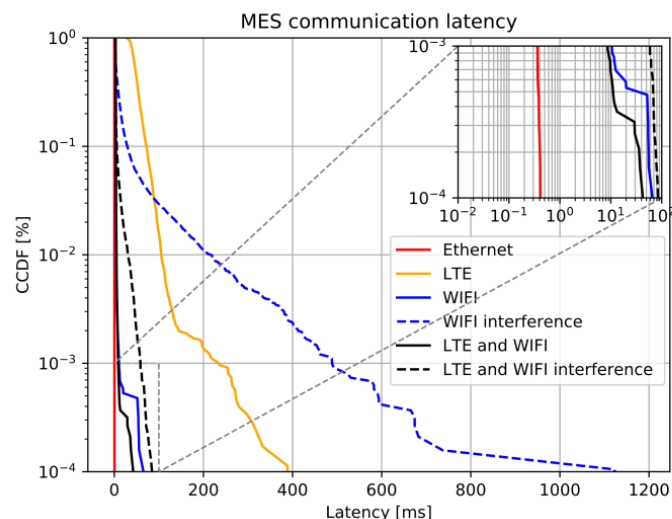


Figure 2-7. One way latency behaviour for various technologies

## 2.5 TeC #1.3: Compressive sensing channel estimation in CRAN

### 2.5.1 Overview

Accurate channel estimation is a fundamental precondition for coherent data detection. In current radio standard, including 5G NR, channel estimation is based on the transmission of reference sequences (i.e., sequences known by both transmitter and receiver) from which the channel response can be estimated. In order to ensure a fair coexistence among multiple transmitters and accurate channel estimation in spite of potential interference, reference sequences are usually designed as orthogonal. Nonetheless, channel estimation based on orthogonal reference sequences is not scalable to very dense deployments where many Remote Radio Heads (RRHs) may be simultaneously active. This is because the usage of orthogonal reference sequences leads to an overhead which is proportional to the number of RRHs. Compressive channel sensing can reduce the overhead for accurate channel estimation by enabling the usage of low-overhead non-orthogonal reference sequences. The compressive sensing solution presented in ([ONE5G-D41], section 4.1.3) and [SW+18] leverage the randomness of the RRH positions for enabling channel estimation with short non-orthogonal reference sequences.

### 2.5.2 Objectives

The objective of this TeC is to validate the potential of non-orthogonal training combined with compressed sensing algorithm at the receiver. The goal is to obtain satisfactory performance in terms of Mean Square Error (MSE) of the channel estimation with limited training overhead by exploiting the path loss diversity of the multiple RRH links.

### 2.5.3 Architecture

The TeC is validated by using the AAU multi-link multi-node testbed. We considered a setup consisting of multiple USRP transmitters and a single USRP receiver. The system geometry (position of the transmitters and distance from the receiver) is arranged such that predefined expected pathloss levels for each transmitter are obtained. All links are in line of sight conditions.

The experimental approach consists in running a large set of measurements and processing them offline. During the measurement phase, transmitters are sending a specific narrowband reference sequence in a time interleaved fashion. In this way, measurements are interference-free and allow for a reliable estimate of the channel response to be used as a reference for MSE calculation.

Each receiver records the received reference sequence. The multiple receive signals are then summed up and used as an input for the offline analysis, using the techniques presented in [ONE5G-D41] and [SW18]. In particular, the global channel vector representing the channel responses from all the transmitters is estimated by using the standard  $\ell_1$ -norm minimization approach.

#### 2.5.4 Test/demo scenarios

We implemented in the AAU laboratory the transmission of downlink reference sequences in a CRAN system consisting of 12 RRHs and a single UE. Each RRH is set at a fixed distance from the UE of interest. A typical configuration of the RRH distribution is shown in Figure 2-8. It is worth mentioning that the performance of the considered scheme depends only on the distances of the RRHs to the UE and not on their actual position on the Cartesian plane. Note that, in this configuration, the UE is located in the very close vicinity of 3 RRHs, and is therefore expected to receive strong power from them. The other RRHs are located further away. Consequently, their received power is expected to be significantly lower. This is the fundamental observation motivating the consideration of low-overhead, non-orthogonal training sequences, as justified in [SW+18].

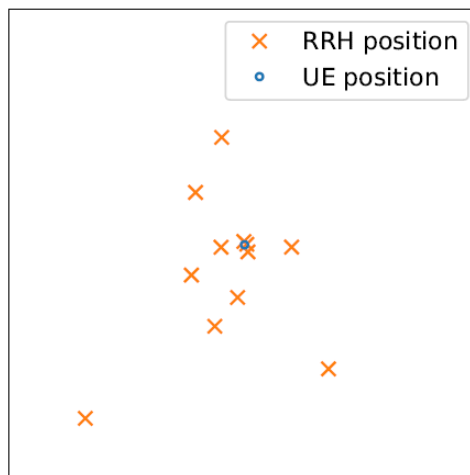


**Figure 2-8. Configuration of RRH positions relative to the UE of interest.**

Each RRH is assigned a unique pilot sequence randomly selected out of a large set of sequences. The sequences have a length of 9 resource elements; since an orthogonal design would lead to a sequence length at least equal to the number of RRH, the presented approach leads to a 25% overhead reduction compared to the conventional approach. In particular, the sequences are generated from a  $9 \times 12$  random permutation matrix with unit-modulus elements and designed such that its *coherence* [CEN+10] is minimum. This property is important in a compressive sensing estimation framework towards estimating sparse vectors from a small number of measurements.

The RRHs transmit their reference sequences in a time interleaved fashion as described in section 2.5.3. The experiment is repeated 18 times with random sequence assignments to each RRH. Measurements have been run at a 5 GHz carrier frequency, over a channel which has been verified to be interference-free. The superposition of all the received signals is then emulated offline in order to verify the capability of the compressed sensing solution in resolving the multiple channel estimates from the superimposed non-orthogonal training sequences.

### 2.5.5 Validation

Figure 2-9 shows the received channel power of each RRH, normalized to the received power of the strongest RRH, for each of the 18 random pilot assignments measured (the power of one assignment is shown with marks connected by lines). The RRHs are labeled according to their received power, i.e., RRH 1 is the strongest RRH, RRH 2 is the second strongest, and so on. In general, the received power distribution does fairly match the nominal one; the limited fluctuations are due to the uncertainties in reproducing the exact pathloss conditions in the practical setup, as well as to the hardware imperfections of the SDR devices.

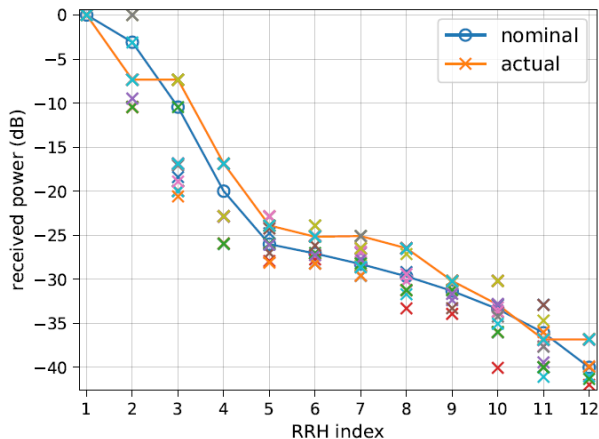


**Figure 2-9. Received power profile of the measurements. The nominal distribution is the one expected theoretically, while the crosses refer to individual measurements. The actual one deviates from the theoretical one due to hardware imperfections.**

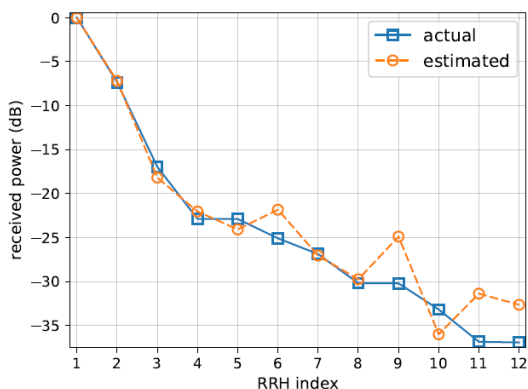


**Figure 2-10. Normalized receive power of the channel estimates for each RRH, for a given pilot assignment.**

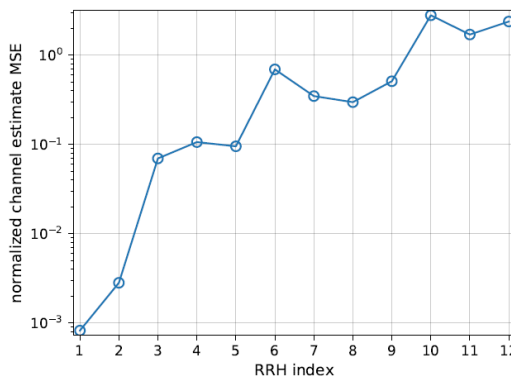


**Figure 2-11. Normalized MSE for each RRH.**

Figure 2-10 shows the power of the resulting channel estimates, normalized to the power of the strongest actual channel, for a random pilot assignment. Note that the first 3-4 strongest channels are very accurately estimated. The weaker RRH channels exhibit larger error in their estimates with a couple of RRHs with significant error. However, note that the signals from these RRHs are weak, hence their contribution to the received signal is weak, meaning that they will either not be employed in the data transmission stage or a very accurate channel estimate is not required as the signal itself will be “buried” in noise. We note that similar observations were made for all other 17 pilot assignments considered. This is also seen in Figure 2-11, depicting the, average over pilot assignments, normalized MSE of each RRH. As remarked, the strongest

RRHs show very good normalized MSE performance (below  $10^{-1}$ , likely to lead to negligible performance degradation in terms of data rate when channel estimates are used for coherent detection). This suggests that reliable channel estimation of multiple strong RRHs in a CRAN setting is possible with small-length training sequences.

## 2.6 TeC #1.4: Cloud control of low latency robot operations

### 2.6.1 Overview

In industrial automation for future factory, there is an increasing demand to softwarize and centralize the control functionality from local unit such as Programmable Logic Controller (PLC) in to highly flexible cloud framework.

The cloud robot concept PoC is based on a customized version of the Robotino mobile robot system provided by Festo [Robotino]. The whole setup consists of:

- The mobile platform carrying a robotic arm with 4 degrees of freedom
- The robotic arm lifts a plate with resistive touch sensor which can sense the position of a ball carried on top
- The controlling logic software located in the remote cloud
- The 5G testbed supporting the URLLC communication between the controlling software as the robot

### 2.6.2 Objectives

The goal is to keep the ball stably balanced, even when the robot platform is moving around. This demands a tight closed-loop control with cycle time of 2ms. Due to the limited processing power of the robot, all the raw sensing data from the plate is sent to the remote controller which actually requires high throughput while low-latency requirement should be satisfied.

### 2.6.3 Architecture

In this TeC, the following configurations was applied for adapting the data traffic requirement of the cloud robot application [HW+18], which differs from the configuration for Tele-operated Driving (ToD) use case in PoC #5:

- higher modulation and coding scheme (64QAM, 2/3 coding rate) is used to adapt the high data rate demanded for delivering the raw sensing data from the carrying board
- since the moving speed of the robot is not as high as a car, lower density of reference signal is configured giving more resource to data

This TeC contains full stack from PHY up to application layer. Most of the implementation is focused in enabling radio connectivity in PHY and MAC while higher layers an implemented in a simplified way.

The following technologies are enabling the TeC:

- Sensing and actuating functions of Robotino platform
- Separation of control and executing functions of Robotino platform
- Flexible SDR architecture and enhancement for high mobility and high reliability features of 5G radio testbed, especially in PHY/MAC layer
- Multi-connectivity beamforming for enhanced reliability  
The advanced receiver in the 5G testbed can automatically steer the receiving beam to the transmitter based on the estimated channel information, which is mathematically equivalent to the maximum-ratio combining (MRC) technique.

- Short Packet Structure for Ultra-Reliable Machine-type Communication  
The 5G testbed is configured to use 0.25ms self-contained frame structure to support the low latency required by the fast close-loop control of the remote robot.

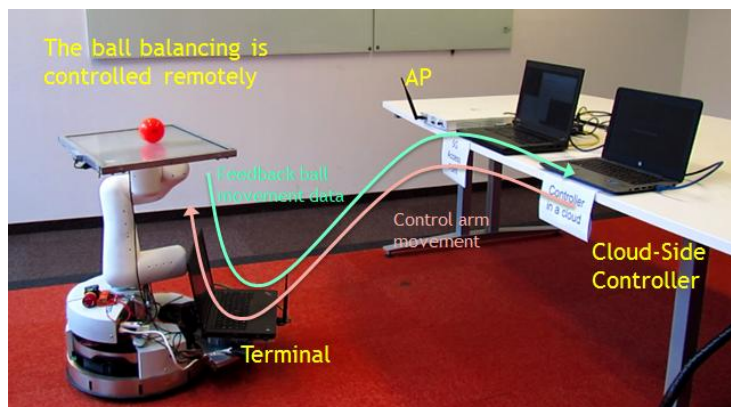


**Figure 2-12. Cloud Robot PoC TeC**

The internal interface between 5G testbed and Robotino system is standard 1Gb Ethernet. Packet Capture (PCAP) interface is used in the 5G testbed to capture and inject Ethernet frames from and to the Robotino's onboard processor. No external interface is necessary in this TeC.

## 2.6.4 Test/demo scenarios

The TeC was tested and validated in an indoor 5G radio testbed in which the Robotino platform was deployed, which is exhibited in Figure 2-12. It includes the Robotino system attached with the tray for carrying the ball, the 5G testbed (access point and terminal parts) and the controller.

## 2.6.5 Validation

The validation of the cloud robot system is performed in three aspects:

1. Latency  
The artificial latency is imposed to the data packets upon the existing <1ms one-way latency from the 5G testbed. The validation shows that when the overall latency is increased to 5ms, instable movement of the robot arm can be observed, which leads to the failure of balancing the ball.
2. Link Reliability  
It can be validated by reducing the transmitting power of both BS and UE to emulate a cell-edge scenario with degraded link quality. The test results show the reduced stability of the robot balancing the ball. When the 2x2 antenna diversity is enabled, the stability is significantly increased.
3. System durability  
The cloud robot is put in the running status continuously balancing the ball while moving randomly. Test results show that the whole system can run without the ball falling for several hours during an exhibition event.

## 2.7 Conclusion

This PoC demonstrated the capabilities of the ONE5G solutions in dealing with the communication demands of industrial scenarios including reliable communication and support of services with diverse requirements.

The potential of multi-connectivity solutions in improving the reliability of the communication link has been assessed. Different multi-connectivity solutions have been studied; physical layer

solutions such as SFN and non-coherent JT, as well as higher layer duplication. Results obtained from the offline analysis prove the capability of multi-connectivity solutions in improving the receive SINR especially in scenarios characterized by high LOS probability. Physical layer multi-connectivity solutions outperform high layer duplication, at the expense of a higher cost. The penalty of multi-connectivity in terms of maximum throughput in the considered network has also been estimated.

Besides “single technology” multi-connectivity, the benefits of having multiple radio interfaces for improving reliability and latency of the communication link in real industrial scenarios has been demonstrated.

Further, it has been proved how scenarios characterized by dense deployments of RRHs can benefit from low overhead non-orthogonal reference sequences for coherence channel estimation, provided compressed channel sensing solutions are used at the UE.

The advantages of technology components such as multi-connectivity beamforming and short packet structure in supporting low latency high reliable communication also appear in the cloud robot concept TeC, based on a customized version of the Robotino mobile robot system provided by Festo.

Finally, the potential of slice negotiation between vertical and operator and creation of multiple network slices for the support of diverse services within an industrial setup has also been addressed.

## 3 PoC#2: Smart-Megacity Proof-of-Concept

### 3.1 Brief description of the PoC

The scenario is assumed to be a smart megacity, consisting on highly populated areas with very high throughput demand and connection densities [ONE5G-D21]. The involved TeCs present set of solutions to optimize the network where traditional solutions are not suitable, focusing primarily on technical components associated with high data throughput, proper of eMBB services. For more information about this PoC, please refer to chapter 3 of ONE5G document D5.1 [ONE5G-D51].

The TeCs focuses on the guidance of optimization process beyond the classic paradigms in this scenario. Firstly, advanced schemes for Forward Error Correction of eMBB traffic are developed in this framework. Secondly, the focus is put on the use of E2E information, both estimated and measured, for optimization. Novel techniques based on forecasting of the metrics are also applied as well as context-awareness procedures ([FAB+15],[FAF+16],[FBA+15]) to further refine the optimization mechanisms based on not only network information, but also on information such as the position of users clusters.

Additionally, network virtualization and slicing of resources between different verticals inside the PoC is also a main characteristic envisaged for this scenario. In this line, different TeCs address the slice negotiation process for supporting the efficient and tailored allocation of resources.

To cover these TeCs three main testbeds were used.

- MIMO multi-rat testbed: for the implementation, integration and validation of the FEC related components.
- Full indoor commercial LTE network: UMAHetnet [ONE5G-D51] [FSP+19] which allows for reconfiguration and online measurements of performance both E2E and at network layer in a complete picocell-based commercial-like LTE deployment.
- Platform for vertical service delivery through 5G - IoT and big data- technologies [ONE5G-D51]: which allows for the generation and assessment of network slicing scenarios.

### 3.2 List of technical components (TeCs) used in the PoC

The following TeCs are used in this PoC:

- **Forward Error Correction component (FEC).** This TeC is related to "Flexible and Fast Reconfigurable HW Architecture for Multi-Service Transmission" (section 3.6.2 of D4.2 [ONE5G-D42]).
- **KPI-to-KQI metrics mapping.** Not direct relation to technical WPs (it was a development specific for WP5). It can be considered related to section 4.3.1 "Context-aware proactive QoE traffic steering through multi-link management" of D3.1 [ONE5G-D31].
- **Prediction of network performance degradation.** This TeC is related to section 4.2.2 " Network performance prediction enhancement through feature engineering" of D3.1 [ONE5G-D31].
- **Enhancement of traditional load balancing techniques.** This TeC is related to section 4.3.1 "Context-aware proactive QoE traffic steering through multi-link management" of D3.1 [ONE5G-D31].
- **Service-differentiated load balancing.** This TeC is related to section 4.3.1 "Context-aware proactive QoE traffic steering through multi-link management" of D3.1 [ONE5G-D31].

- **Traffic steering management using context, user and cell level information.** This TeC is related to sections 4.3.1 "Context-aware proactive QoE traffic steering through multi-link management" and section 4.2.2 "Social events information gathering, association and application to cellular networks" of D3.1 [ONE5G-D31].
- **Ad-hoc deployment of services on edge cloud.** This TeC is related to "Optimized functionality placement and resource allocation in CRAN/DRAN context" (section 4.4 of D4.2 [ONE5G-D42]).
- **Creation of new network slices in order to support the vertical requirements.** This TeC is related to "Time-variant optimal slicing negotiations" (section 3.2.3 of D3.1 [ONE5G-D31]). The TeC is described in section 5.5 of the current document.
- **Network slice creation supporting the vertical requirements in an area-based and time-based manner.** This TeC is related to "Network slice management based on mobility and traffic patterns" (section 4.2.3 of D3.2 [ONE5G-D32]). The TeC is described in section 5.5 of the current document.

### 3.3 TeC #2.1: Forward Error Correction component (FEC)

The Forward Error Correction (FEC) is one of the most complex components on a modem transceiver, while being specific for each standard. A flexible and fast reconfigurable component is a key technology to address multiple standards and services with the same modem. The FEC is part of the "Flexible and fast reconfigurable" hardware IP initially proposed in ONE5G document D5.1 [ONE5G-D51].

#### 3.3.1 Overview

The FEC (Forward Error Correction) sublayer includes the channel coding, with enhanced coding scheme like LDPC (Low Density Parity Check) or polar code, the channel adaptation, as the coding rate and QAM (Quadrature Amplitude Modulation) mapping of the data symbols. These parameters correspond to the Modulation and Coding Scheme (MCS) and adjusted regarding to the Channel Quality Indicator (CQI) and the allocated resource blocks, in order to optimize the spectral efficiency. The FEC architecture shown on Figure 3-1 is versatile enough to address several physical layers (LTE, WiFi, NR).

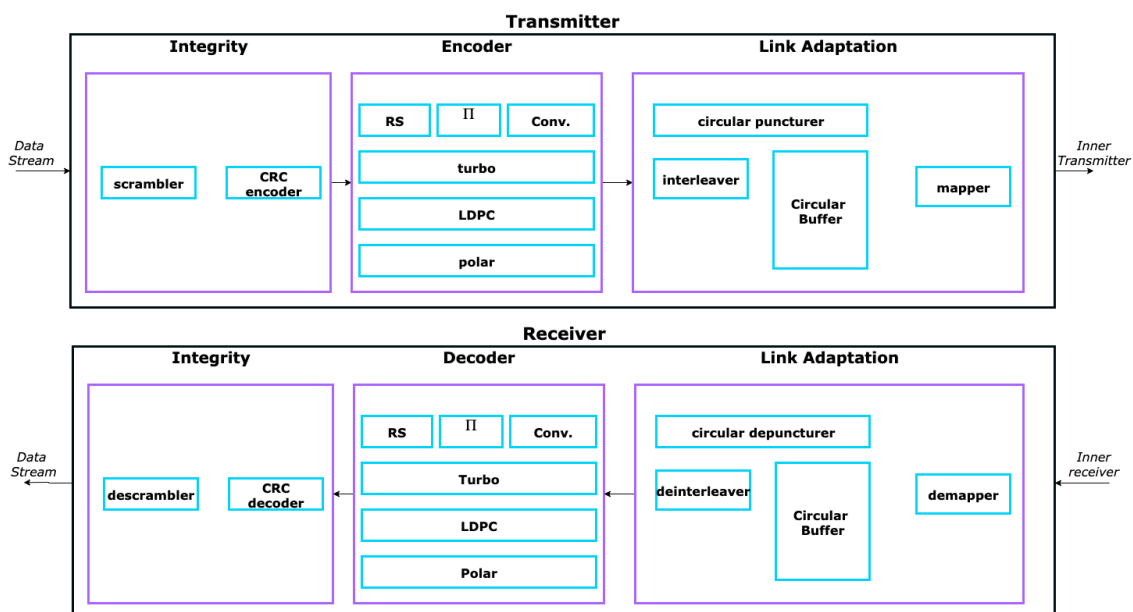


Figure 3-1. Generic FEC enabler

WiFi IEEE 802.11ac [IEEE-80211ac] and 3GPP New Radio (NR) [3GPP-38212] standards operate different mapping schemes (up to 256QAM) and adapt several coding rates. The focus of the FEC technical component stands in PDSCH and PUSCH NR and WiFi IEEE 802.11ac channels, whose configurations are summarized in **Table 3-1**. Additional characteristics are given in D4.1 [ONE5G-D41] section 3.1.3.

	NR PUSCH	NR PDSCH	WiFi
<b>Coding</b>	LDPC	LDPC	LDPC
<b>HARQ</b>	Yes	Yes	Yes
<b>Segmentation</b>	Yes	Yes	Yes
<b>Coding rates</b>	0.12 – 0.96	0.12 – 0.96	0.5 – 0.83
<b>Modulation</b>	$\frac{\pi}{2}$ BPSK QPSK 16/64/ 256 QAM	QPSK 16/64/ 256 QAM	BPSK QPSK 16/64/ 256 QAM

**Table 3-1. FEC parameters in WiFi and NR systems**

The data stream channels like PUSCH or PDSCH are protected with LDPC codes and its throughput is optimized with segmentation pattern. It assumes a large number of configurations. LDPC coding scheme gathers two base graphs holding 8 indexes and 51 expansion factors each. PDSCH and PUSCH outline almost 27 MCS (Modulation and Coding Scheme) representing a specific modulation and a coding rate. The data flow is also adapted with the allocated resource blocks. WiFi VHT (Very high throughput), usually known as IEEE 802.11ac, is protected by convolutional or LDPC coding. It gathers 12 LDPC matrices for up to 9 MCSs.

### 3.3.2 Objectives

The technical component has to code and to decode a High Throughput bit stream compatible with the standardization (NR or WiFi) and fully compatible with any MCS. Objectives are to switch randomly the Radio technology with a low impact on the reconfiguration side. In any case, the component aims at reaching 100 Mbps, with less than one millisecond latency. For many use cases, a single component aggregates several services in parallel with no impact for the user.

### 3.3.3 Architecture

The FEC transmitter and receiver are compliant with the physical layer specified for both uplink and downlink. The component forms the outer transceiver of a modem as shown on Figure 3-2. This component interacts with the Digital Front End part.

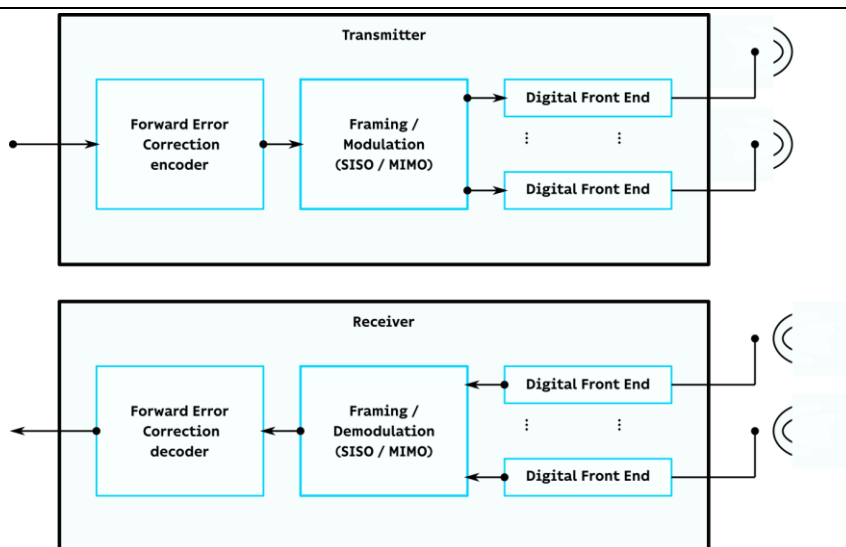


**Figure 3-2. FEC position on a Physical Layer architecture**

The component is coded in VHDL and runs on FPGA (Intel or Xilinx). It respects the standardized Intel Avalon streaming or ARM AXI4 streaming handshake.

It is integrated in a first standalone setup, which enables to draw some performance curves directly on board.

A second setup transmits on board several video on UDP streams, where each video corresponds to a specific PHY layer. This setup tests the flexibility of the component in a random way. The Graphical User Interface for this setup is represented on Figure 3-3. This Figure shows the characteristics of two users using specific systems and different systems and MCS. The received mapped signals are drawn for each one. Random data, considered as a third user, is inserted to reveal some BER performance, drawn in the middle panel. The received videos are played for each user on the right. They are well received and separated, which secures the robustness of the component.

The technical component has been successfully integrated into the following testbeds:

- Virtex6 FPGA Board
- Reflex ARRIA10 Board
- BCOM multi-RAT Platform

Virtex6 FPGA and Reflex ARRIA10 testbeds enables the capability of the component in a standalone process. The BCOM multi-RAT Platform embeds an OFDM chain, which tests the component with on air transmission.

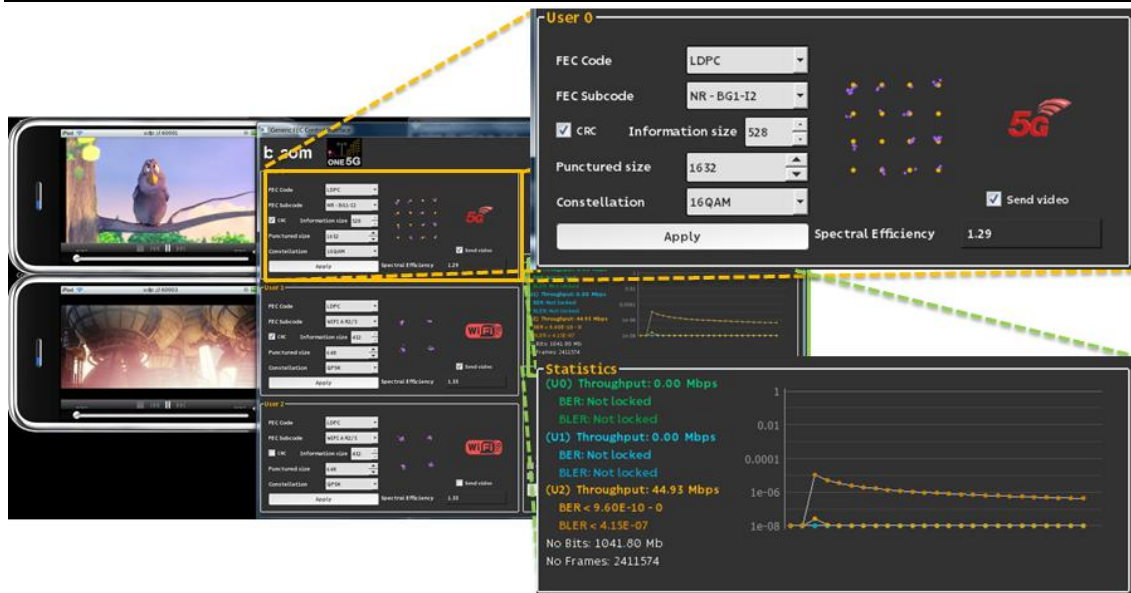


Figure 3-3. Graphical User interface for the FEC CNUM testbed

### 3.3.4 Test/demo scenarios

The Hardware FEC component handles several simultaneous user services with different Radio Access Technologies. The first configuration (5G NR) is a PDSCH received stream corresponding to MCS 10. The second configuration (Wi-Fi) corresponds to MCS 4. Table 3-2 summarizes the characteristics for each configuration.

A single transmitter processes two different high definition videos in an interleaved way, so that both services are seamlessly sent. In the same way, the receiver decodes both services independently.

	Configuration 1	Configuration 2
Physical Layer	5G NR	Wi-Fi
Coding	LDPC BG 2 Index 2	LDPC BG 2 Index 1
Expansion factor	24	27
MCS	PDSCH 10	4
Information length (in bits)	528	432
Coding rate	1/3	3/4
Modulation	16QAM	QPSK
Spectral efficiency (in bits/s/Hz)	1.29	1.50

Table 3-2. Demonstration scenario

### 3.3.5 Validation results

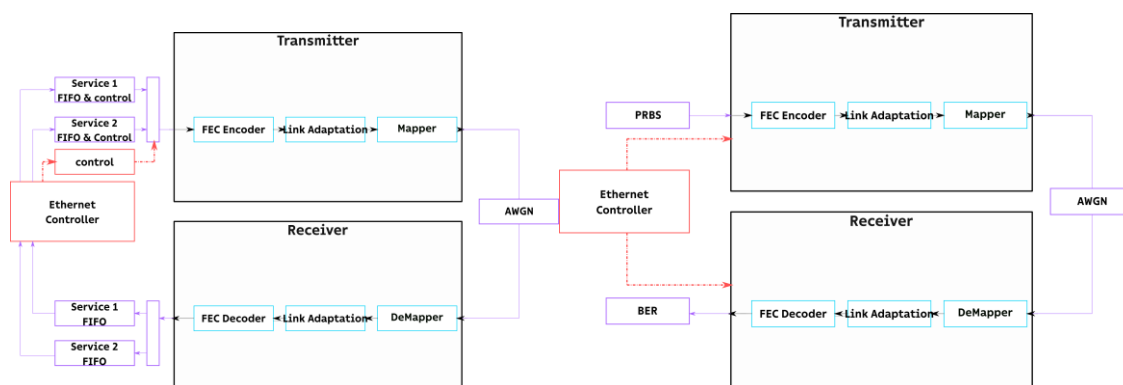


Figure 3-4. FEC qualification loopback

The standalone component is validated over a Reflex ARRIA10 board. The operation consists in a loopback (see Figure 3-4) integration of the transmitter and the receiver side. A dummy data set, independent and identically distributed and provided by a PRBS module, is sent to the FEC transmitter, with a set of parameters (typically the data length and the MCS). The data stream is coded and mapped. The resulting I/Q symbols are noised with a parametric AWGN channel and the stream feeds the receiver. The data is demapped and decoded. The resulting sequence is then compared with the initial one.

A second loopback provides several data stream corresponding to several configurations. Each stream is fed by a PRBS or by a video stream. With a low level of noise, the transmitted data shall not be degraded. The comparison of in/out data set validates the slow reconfiguration between systems of the component with no packet loss. Figure 3-5 draws the Bit Error Rate (in continuous lines) and Packet Error Rate (in dashed lines) corresponding to two users and padding transmitted in the same time. The curves are equivalent to the expected performances of dedicated component with these configurations.

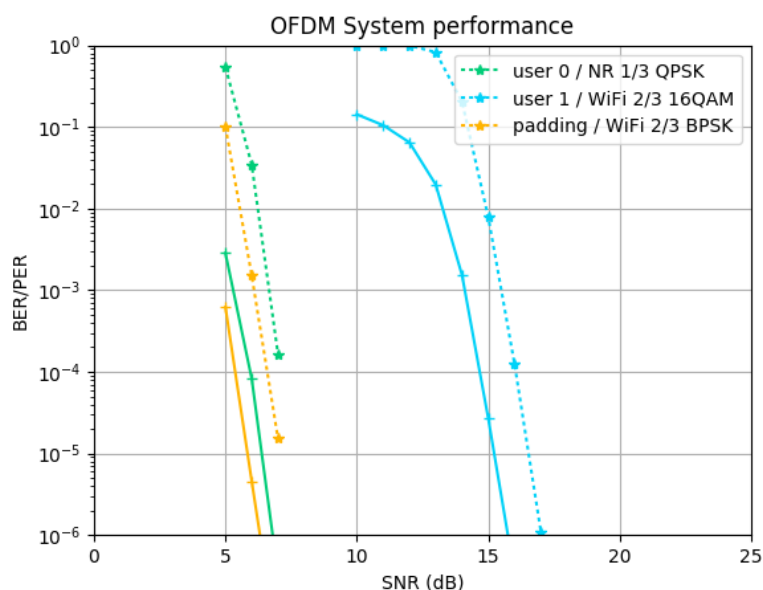


Figure 3-5. Decoding curves plotted on FPGA Board

The proposed testbed consists then in sending two distinct videos corresponding to two distinct services. The videos are sent to the BCOM multi-RAT Platform through UDP streams and the data feeds two FIFOs. The received streams feeds also two FIFOs before been sent back with UDP stream to a video viewer.

## 3.4 TeC #2.2: KPI-to-KQI metrics mapping

### 3.4.1 Overview

In recent years, mobile communications traffic has experienced an important increase due to the growing number of users demanding mobile services. Services such as web browsing or video transmission are widely used in the mobile network. For example, [Cisco-FaM] reports more than 82% of the world's mobile data traffic will be video by 2021. In this sense, users demand a better quality of experience (QoE). Traditionally, optimization techniques have been based on improving classic KPIs (such as throughput, delay, etc.).

These are insufficient in the new telecommunication environment where the focus is placed on the performance provided to specific services and applications. This has given way to new techniques based on improving the specific service Key Quality Indicators (KQI) metrics perceived by users, as they are described in section 2 of the WP2 deliverable [ONE5G-D21], e.g. video stalling, resolution, download time.

However, service-level KQIs cannot typically be directly measured from the users. In previous times, KQIs could be sometimes obtained via deep packet inspection of higher-layer protocol messages. However, the introduction of encryption mechanism makes difficult to obtain the KQIs. Considering client-side applications, these are not under the operator's control, and having "online" measurements of the KQIs being experienced in the network is nearly unachievable.

### 3.4.2 Objectives

Taking into account the previous indications, the main objective of this TeC is to define modelling/mapping mechanisms able to translate from the classic lower layers indicators (e.g. RSRP, RSRQ, load...) to KQI metrics at application-layer. These focuses on KQIs for the FTP service: total file transfer delay (s), The evaluation of the "estimated" or "indirect" KQIs will be done by comparing them with measured KQIs gathered from an experimental UE which is able to access application-layer indicators

### 3.4.3 Architecture

The implementation of this technical component implies the gathering of metrics from lower and higher network layers (from the testing UEs). Performance management (PMs) / Configuration management (CMs) data (performance and configuration measurements, e.g. KPIs) are obtained from lower layers such as NAS/RRC/PDCP/RLC/MAC/PHY and KQIs/QoE from application layers. Additionally, other metrics such as network/transport metrics can be taken into account.

This TeC has been implemented using Matlab and Python in order to process counters and traces from the network. This program connects to the UMAHetNet Network (based on commercial LTE core eCN600+12 picocells [ONE5G-D52]), to obtain the lower layer metrics, through the REST interface described later. Additionally, SSH2 is used as technology enabler

---

<sup>2</sup> SSH (Secure Shell) is a network communication protocol that enables two devices to communicate and share data. The communication between the two devices is encrypted.

for the connection to the testing UEs. The REST interface allows the program to gather measurements and perform actions in the network in a transparent manner with regards to the original management tool of the network, based on U2000 [U2000] (Huawei network commercial management tool) functionalities.

The technical component is set with the following interfaces:

- **REST interface.** A REST API has been defined to gather measurements and perform changes in the UMAHetNet. The RESTful interface gives access to the following internal functions:
  - Performance Management: query PM (performance management)/CM (configuration management)/FM (fault management) variables for the e-NodeBs and core, filtering by network element and date/time.
  - Configuration Management: modify the configuration of the eNBs and core, using MML (Man-Machine Language) commands. MML is a language used typically in the configuration interface of mobile telecommunications equipment. More information can be found in the ITU-T Z300 recommendation series.

To use the REST API, a set of URLs will be provided for authentication and access, as well as documentation for the request formats and JSON output.

- **SSH interface.** This interface is connected to the experimental UE and through it, metrics from different services can be obtained.
- **GUI interface.** This interface allows the final user to visualize the results of the experiments.

Figure 3-6 shows the interconnection between these elements.

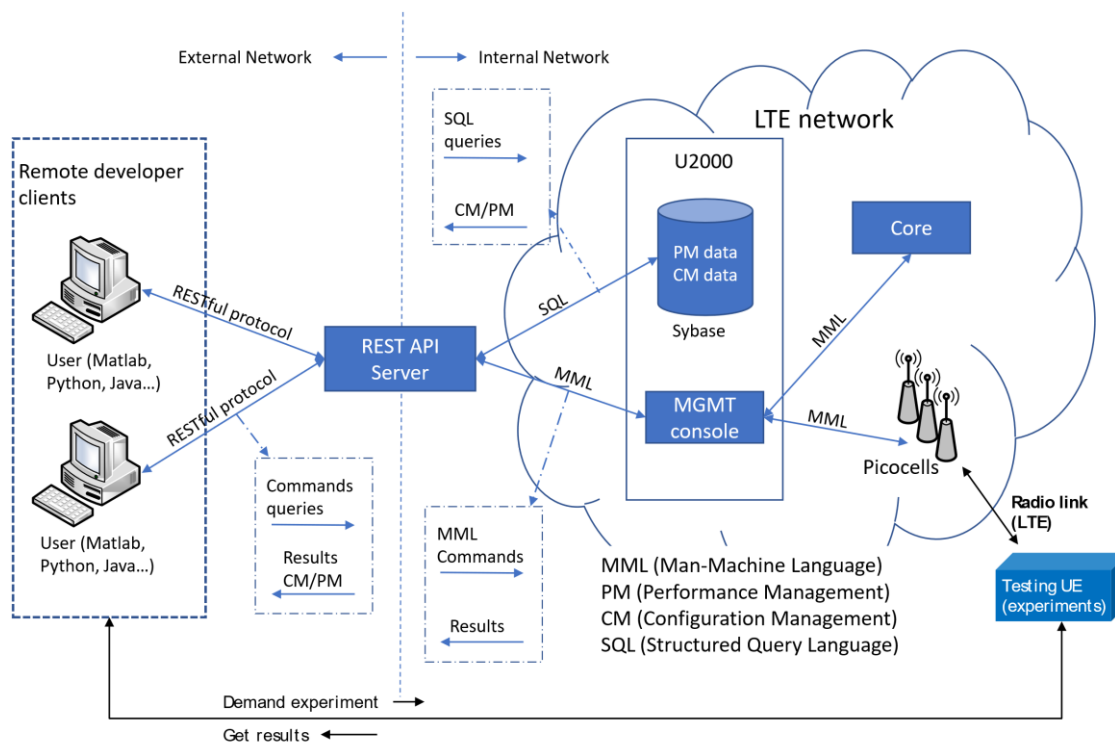


Figure 3-6. Test architecture

### 3.4.4 Test/demo scenarios

The test scenario in which this TeC is evaluated comprises the UMAHETNET, accessible through the REST API, a testing UE and a remote client, running the mapping script.

The objective of the demonstration is to validate if the estimated KQIs, computed from the network counters and traces, correspond with the KQIs obtained from the experimental UE. In order to achieve this, the following methodology has been adopted:

1. Launch a limited service, that requires a low number of network resources, and validate that the KPI and the KQI/QoE metrics, both computed and measured, reveal an optimal performance.
2. Launch a service that requires a high number of network resources and validate that the KPI shows a good performance but the KQI/QoE metrics, both computed and measured, don't accomplish good results.
  1. Tune the network configuration to provide additional resources.
  2. Validate that the KPI and the KQI/QoE metrics, both estimated and measured, reveal a good performance

Figure 3-7 shows the sequence which is followed by the demo.

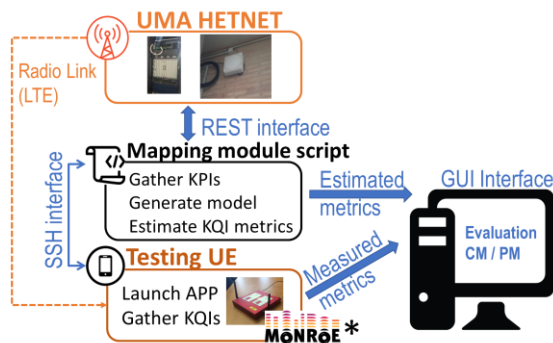


Figure 3-7. Demo sequence structure

### 3.4.5 Validation

The validation steps described above imply

- **From the translator script perspective.** Estimate the KQI from the counters and traces obtained through the REST API.
- **From the experimental UE perspective.** Launch the application and collect the KQIs.
- Check the results. The validation of the computed KQIs with the measured KQIs is the expected test output.

Different regression mechanisms for the modelling and estimation of the KQIs have been tested, including *linear regression* (LR), *step wise linear regression* (SW-LR), *support vector regression* (SVR), *decision tree regression* (DTR) and *random forest regression* (RFR) [IR+09]. DTR has been assessed as the better performing mechanism, achieving a coefficient of determination ( $R^2$ ) above 0.85 for the FTP KQIs considered (File Transfer Throughput and Total File Transfer Delay) under different bandwidth, UE positions and configurations.

In the following Figure 3-8, it can be seen the values of measured and estimated KQI as well as the root-mean-square error (RMSE) of both for the cases of the total delay and the average throughput of a file transfer under different bandwidth configurations. Here, the dashed vertical lines separate different bandwidth configurations following, left to right, the values of 5 MHz, 10 MHz, 15 MHz and 20 MHz. The figure shows how the values of the estimated KQIs are very close to the measured ones.

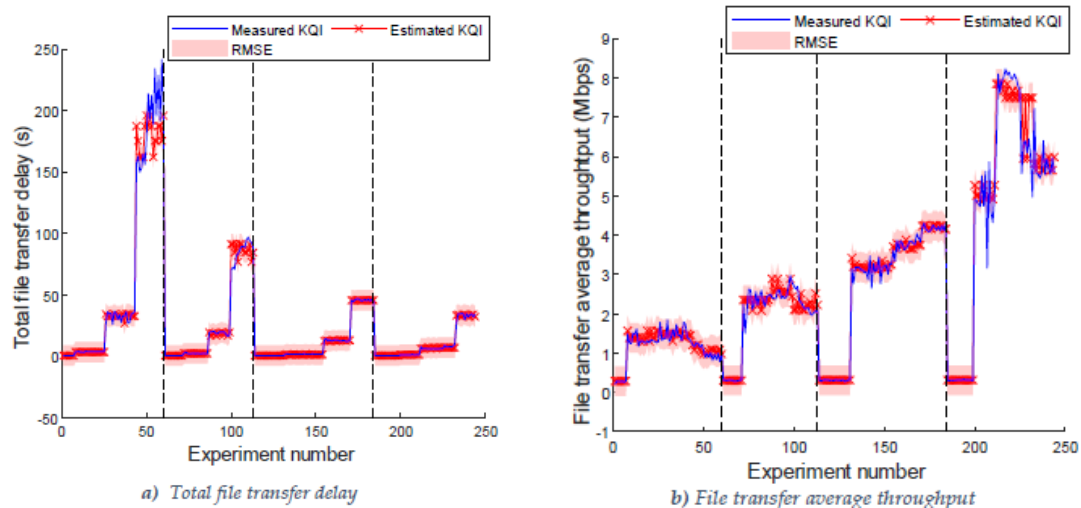


Figure 3-8. KQI prediction.

## 3.5 TeC #2.3: Prediction of network performance degradation

### 3.5.1 Overview

Two features mainly characterize the management of the upcoming standard for mobile communications (5G): its versatility, as it will have to cope with a variety of service categories, to be covered under the same 5G umbrella, and its agility since it will have to face a rapidly changing environment in terms of radio conditions and demand. In line with the latter, and in order to anticipate possible network performance degradations, which may eventually degrade the user perceived quality of experience (QoE), prediction techniques are proposed to be used on network performance indicators. With this approach, corrective and optimization-related actions may be taken before the actual performance degradation has taken place. To do so, techniques for time series forecast are implemented.

### 3.5.2 Objectives

The main objective of this TeC is to develop a tool to forecast network performance degradation based on the evaluation of performance indicators as a time series, assessing the developments reported in [ONE5G-D32, section 4.2.2.2] based on pre-stored cellular data from commercial networks. This will allow network operators to apply the pertinent corrective actions in advance, preventing users from suffering an eventual drop in the QoE.

### 3.5.3 Architecture

This TeC is conceived as a complement to traditional radio resource management (RRM) mechanisms. It has been deployed on top of the access stratum (AS), collecting network performance information, and consequently, being able to forecast the performance of all its layers: PHY, MAC, RLC, PDCP and RRC. This TeC also includes the implementation of a Matlab/Python tool in order to forecast the network behavior. The network performance indicators have been gathered using the framework described in TeC #2.2.

The technical component is set with the following interfaces:

- **REST interface.** A REST API has been defined to gather measurements from the UMAHetNet, which is described in TeC #2.2. This interface will only be used to access network performance information, stored in network databases.
- **GUI interface.** This TeC results in the forecast of the network state in terms of the expected behavior of a set of performance indicators.

The prediction tool is based on recursive deep neural networks obtained from Keras and TensorFlow libraries. The dataset used for validation has 1181 observations (experiments) performed in the network in multiple execution of FTP services, where 8 performance indicators are used to predict and only the 80% of the experiments are used to train and test the tool. Moreover, the GRU units which are used for forecasting are 512, with a batch size of 50 and a sequence length of 48. **Table 3-3** represents the inputs of the system takes and the outputs that it produces, where  $x$  is the input feature and  $t$  represents an instant in time.

**Table 3-3: Inputs and outputs of the prediction system.**

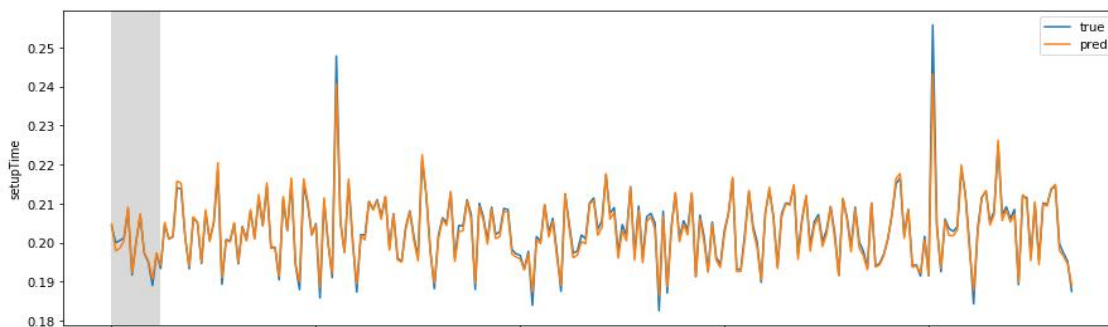
Inputs		Outputs
<b>BW values</b>	$x(t)$ $x(t-1)$ $x(t-2)$ $x(t-3)$	Setup time (t+1) Total time (t+1) Data rate (t+1)
<b>RSRP</b>		
<b>RSRQ</b>		
<b>RSSI</b>		
<b>Setup time (KQI)</b>		
<b>Total time (KQI)</b>		
<b>Data rate (KQI)</b>		
<b>File size</b>		

### 3.5.4 Test/demo scenarios

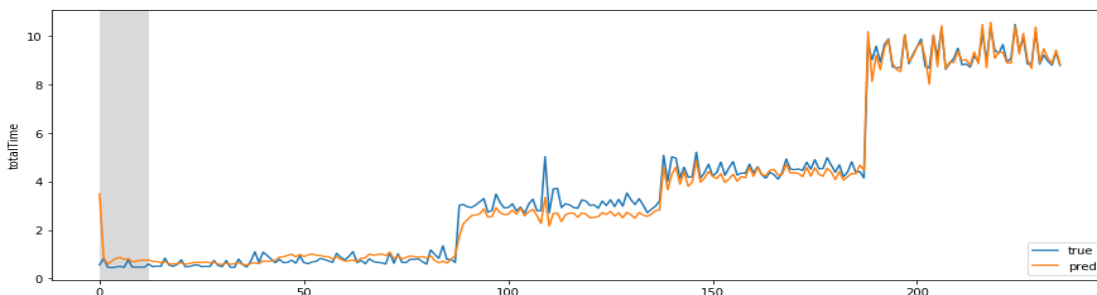
The test scenario will be similar to the one described for TeC #2.2, only using the branches/functionalities for the access to the performance and configuration (PM/CM) data in the network databases.

### 3.5.5 Validation

Figure 3-9 shows the “one step-ahead” prediction for the three output features, for the training and the test phase respectively. Here, the horizontal axis corresponds to the index of measured samples of the features and the vertical axis the value of both the measured feature (‘true’) and the estimated one (‘pred’). The good performance of the system is shown, being this able to predict indicators with high accuracy even for the test dataset not used for training.



a) Setup-time prediction



b) Total-time prediction

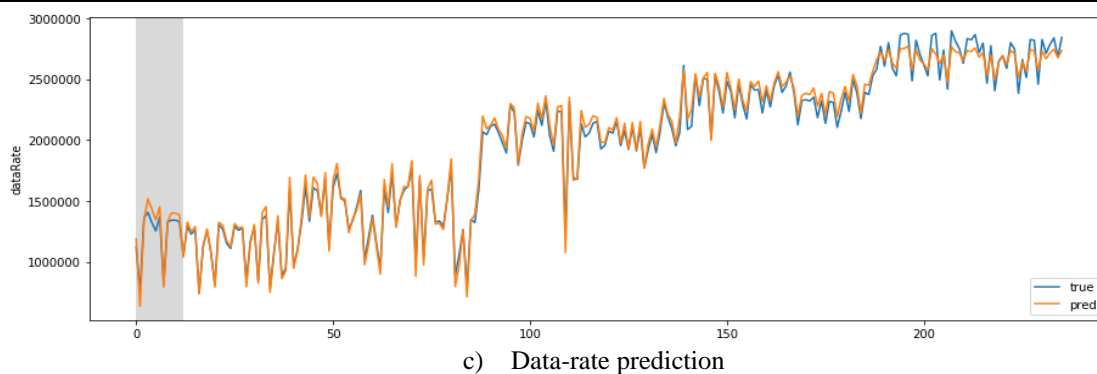


Figure 3-9. Comparison of real and predict indicators in training phase

## 3.6 TeC#2.4: Enhancement of traditional load balancing techniques

### 3.6.1 Overview

Load balancing is one of the most used techniques in order to improve service performance by sharing the load between neighboring cells. These mechanisms have been classically based on low layer indicators (e.g. cell throughput, blocked rates). However, these techniques do not offer always the best solution in order to maximize the network performance, as the relation between the Quality of Experience QoE of the users and the cell load is not straightforward, as it is analyzed in this TeC.

### 3.6.2 Objectives

The main objective of this TeC is to introduce a new driver for traffic sharing which in turn is able to improve classical Mobility Load Balancing (MLB) performance in terms of user level of satisfaction (QoE).

Classical MLB adjusts handover margins (HOM) aiming to equalize cells load (number of PRBs allocated to users). Instead of this, the proposed technique consists of the relative throughput “variation” experienced by every user when being handed. The information needed to calculate this variation is often collected in current networks via user traces. Instead of this, the mechanism introduced in this TeC consists of the relative throughput variation experienced by every user when changing between cells.

### 3.6.3 Architecture

This TeC makes use of the full indoor commercial LTE network UMAHetNet, especially focusing in the RRC layer.

The implementation of a combined Matlab/Python tool in order to calculate and collect data from the network and users which can improve balancing techniques is included in this TeC.

The interfaces which are used in this section are:

- iManager U2000 – Huawei: OSS which allows to connect with network and configurate all necessary parameters.
- TEMS Pocket software: it is used to measure the user throughput and the server cell.

### 3.6.4 Test/demo scenarios

In this scenario, which is represented in Figure 3-10, 3 different cases are modelled, where there are some active users who are downloading a heavy file meanwhile one of them is in movement between neighbor cells A and B.

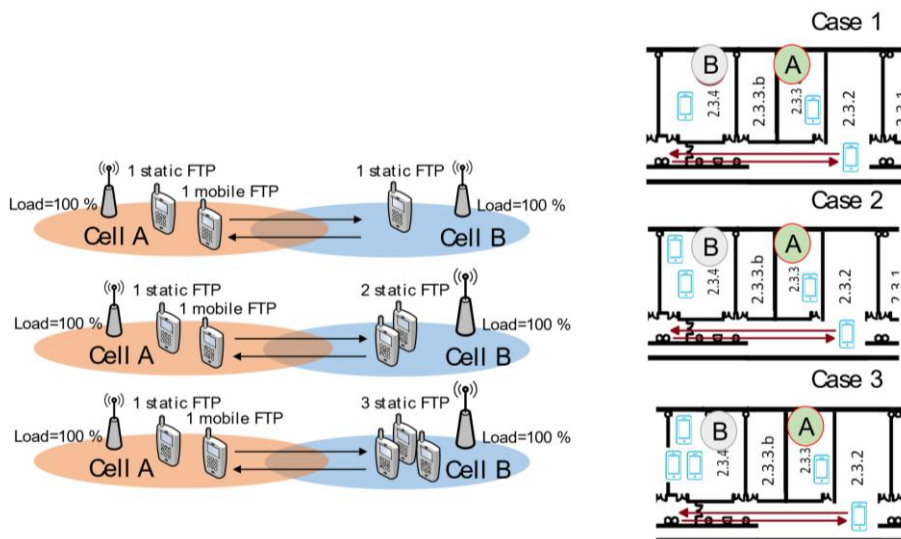


**Figure 3-10. Scenario of enhancement of traditional load balancing**

In this scenario, classic load-approaches would not properly balance the network load. Instead, a new approach based on the relative throughput variation experienced by every user is implemented.

As it is going to be shown in the validation section, in this scenario, classic load-approaches would not proper balance the network load. Instead, a new approach based on the relative throughput variation experienced by every user is implemented.

In this way, presents the average relative throughput variation experienced by handed over users, which is used in this TeC to define the new point of HO.

$$\overline{\Delta th_{UE}}(i,j) = \frac{1}{N_{HO}(i,j)} \sum_{k=1}^{N(i,j)} \Delta th_{UE}^{(k)}$$

Where,

- $\Delta th_{UE}^{(k)} = \frac{th_{afterHO}^{(k)} - th_{beforeHO}^{(k)}}{th_{beforeHO}^{(k)}}$
- $th_{beforeHO}$  = average throughput of the user calculated during a certain temporary window before HO.
- $th_{afterHO}$  = average throughput of the user calculated during a certain temporary window after HO.
- $N_{HO}$  = number of handovers
- $i$  = initial cell
- $j$  = new cell

The described expressions allow to define the proposed HO point, which is given by the cross point between  $\overline{\Delta th_{UE}}(A,B)$  and  $\overline{\Delta th_{UE}}(B,A)$  lines, as it can be seen in Figure 3-11. This new point lengthening user’s handover in the case of new cell presents a high load.

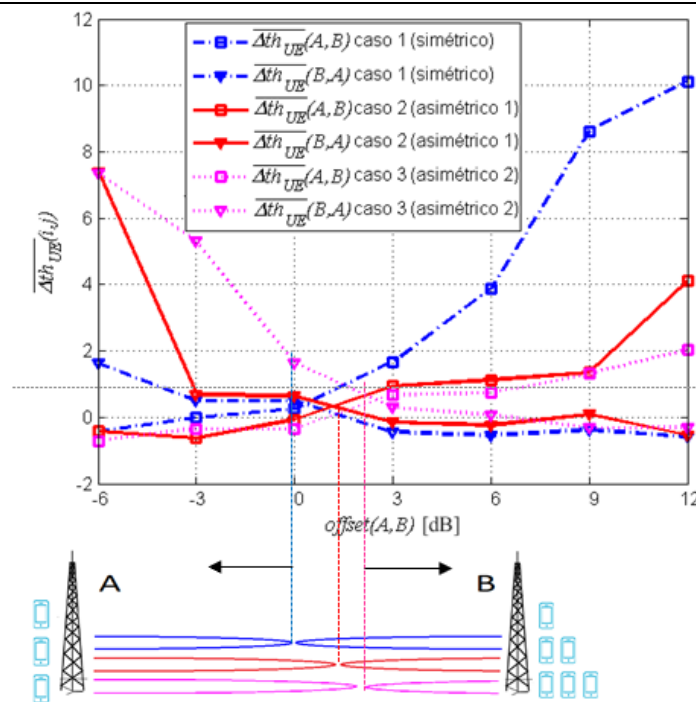


Figure 3-11. Proposed HO point

In order to validate the enhancement of traditional load balancing, the next figure of merit is used:

$$\Delta \overline{th}_{min} = \frac{\overline{th}_{min,new} - \overline{th}_{min,MLB}}{\overline{th}_{min,MLB}}$$

Where,

- $\overline{th}_{min,new}$  = mean minimum throughput obtained with the new driver
- $\overline{th}_{min,MLB}$  = mean minimum throughput obtained with the classical MLB

Table 3-4 shows throughput statistics using classical MLB and driver proposed in this TeC. Focusing on the figure of merit previously defined, it is seen how new driver performs a better enhancement in asymmetric traffic cases, such as in case 3.

Table 3-4. Throughput statistics comparison

CLASSICAL MLB VS. NEW DRIVER MINIMUM THROUGHPUT STATISTICS			
	Case 1	Case 2	Case 3
<i>offset(A,B)</i> MLB [dB]	0	0	0
$\overline{th}_{min,MLB}$ [Mbps]	1.901	1.638	1.422
<i>offset(A,B)</i> new driver [dB]	0.3	1	2.5
$\overline{th}_{min,new}$ [Mbps]	1.925	1.760	1.930
$\Delta \overline{th}_{min}$	0.0126	0.0745	0.3572

## 3.7 TeC#2.5: Service-differentiated load balancing

### 3.7.1 Overview

Traditionally, network configuration and optimization are based on KPIs but with the next generation of cellular communications, configuration and optimization of the network based on QoE appeared as a new challenge to properly tackle the need for E2E oriented optimizations.

In current scenarios, users with different services have a different impact on the network and experience different levels of QoE.

### 3.7.2 Objectives

This TeC aims at the implementation of a service-differentiated load balancing based on QoE assessing the developments performed in WP3 via simulations [ONE5G-D31, section 4.3.1]. The objective is to show the possibilities of a load balancing based on the quality of experience instead of the classical methods depending on the quality of the received signal. This method is intended to steer the users between the cells taking into account not the number of users or the load, but the service-differentiated QoE in each cell, so the QoE of all users is as satisfactory as possible. This goes beyond the previous TeC as it considers not only throughput changes but differentiated QoE for different applications.

### 3.7.3 Architecture

This TeC includes the implementation of a Matlab/Python tool in order to emulate the behavior of UEs making use of different services such as web browsing, file download or video streaming. The obtained quality of experience results are uploaded to a server through a REST interface. Moreover, a Matlab tool is implemented to get the QoE from the servers and the KPIs from the cells of the network as well as to dynamically change the configuration of the network.

The technical component is set with the following interfaces:

- **REST interface to Network.** A REST API has been defined to perform changes in the UMAHetNet, which is described in TeC #2.2.
- **REST interface to Server.** A REST API has been defined to gather QoE measurements from all cells.
- **SSH interface.** This interface is connected to the experimental UE and through it, metrics from different services can be obtained.
- **GUI interface.** This interface allows the final user to visualize the results of the experiments.

Figure 3-11 represents the proposed close-loop QoE balancing algorithm (based on fuzzy logic) which allows to change the handover margin (HOM) depending on the difference between the measured QoE ( $QoE_{diff}$ ) of each pair of cells, 'i' and 'j'. In this way,  $QoE_{diff}(i,j)$  is the input of a Takagi-Sugeno fuzzy controller [FAB+15]. Numerical values of HOM are fuzzified into linguistic values that are then the inputs for the rules defined in the inference stage. Here, it is established the linguistic rules to establish the HOM modification,  $\Delta HOM(i,j)$ , for the margins between the two cells. In this way, differences between the QoEs lead to the reduction of the area of the cell with lower QoE, so it can have more free resources to serve its users. The defuzzification phase transforms the linguistic values into numerical ones, which are then configured in the network.

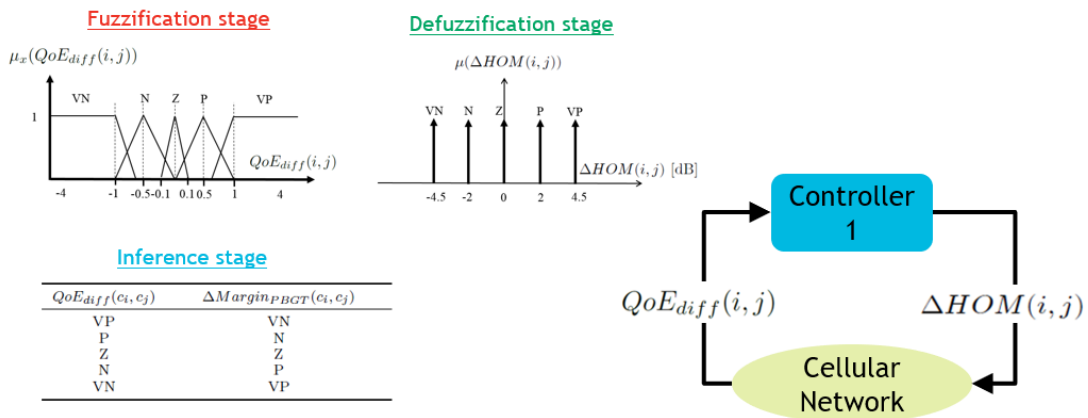


Figure 3-12. Balancing algorithm based on fuzzy logic

### 3.7.4 Test/demo scenarios

The test scenario in which this TeC is evaluated comprises the UMAHetNet, accessible through the REST API. A total of 5 testing UEs running different services in different locations are set. Besides, a remote client is running a script which compare all QoE obtained and change HOM parameters is also part of this testbed. The following Figure 3-13-b shows the distribution of users in the scenario (squared symbols), as also the service which each one is using. The color of each user represents the cell to which is connected to (circles). In this initial situation, cell 136 is highly overloaded in comparison with 131 and 139.

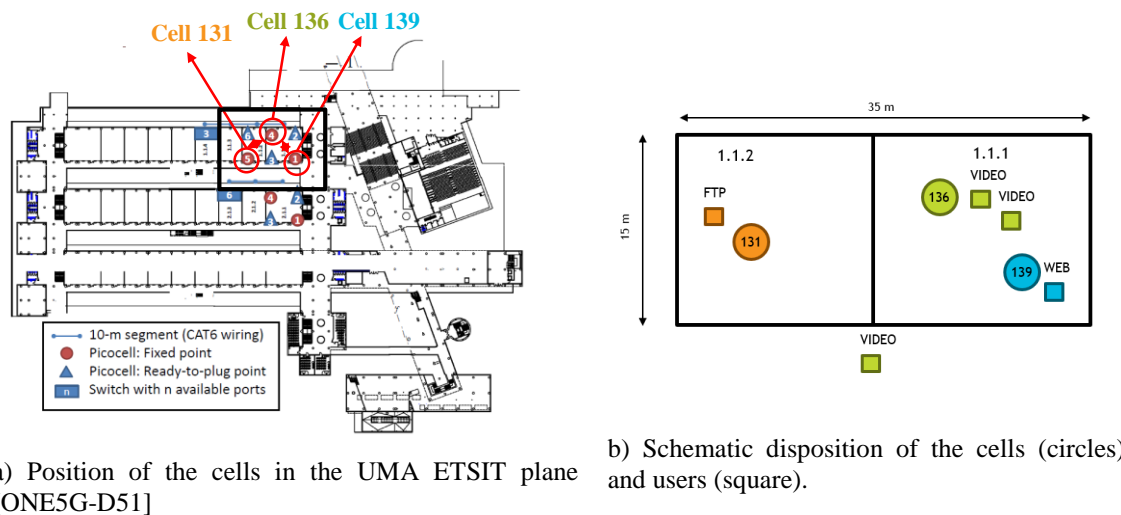


Figure 3-13. Initial scenario

In order to achieve the QoE balance and test the described algorithm, the following methodology has been adopted:

Each terminal launches a set of experiments of a service, whose QoE is evaluated by the models presented in previous sections and is uploaded to a server.

1. Once all terminals have ended running the set of experiments, remote user get from the server all measures and classifies them depends on the server cell.
2. Network is tuned with new configuration given by the algorithm and the process is repeated from step 1.

Table 3-5 the set of experiments of the services and network setting.

NETWORK SETTING		SET OF EXPERIMENTS	
Picocell BW	5MHz	VIDEO	Time: 600s. Resolution: 3840x2160. Bitrate: 14931 kbps

<b>Picocell Ref signal power</b>	-20 dBm	<b>FTP</b>	File size: 900MB
<b>Default HOM</b>	3 dB	<b>WEB BROWSING</b>	800 downloads: <a href="http://www.uma.es">www.uma.es</a>

Table 3-5. Network and experiments setting of PoC#2.6

### 3.7.5 Validation

In order to measure quality of experience of the different services, the following models have been used [NLG+10]:

$$QoE^{(FTP)} = \max(1, \min(5, 6.5 \cdot TH - 0.54))$$

$$QoE^{(Video)} = \max(1, 4.23 - 0.0672 \cdot L_{ti} - 0.742 \cdot L_{fr} - 0.106 \cdot L_{tr})$$

$$QoE^{(Web)} = 5 - \frac{578}{1 + \left(\frac{TH + 541.1}{45.98}\right)^2}$$

Where:

- $TH$  is the average user throughput
- $L_{ti}$  is the initial buffering time
- $L_{fr}$  is the average frequency of stallings
- $L_{tr}$  is the average stalling duration

being all the parameters directly measurable in the testbed. Figure 3-14 represents the distribution of the users in the scenario before (left) and after applying the mechanism (right).



Figure 3-14: Distribution of users in the scenario

The Table 3-6 shows the imbalance of the average QoE between the cells previous to the optimization of the network.

Table 3-6: Initial mean QoE of each cell

Cell	Mean QoE
131	4.25
136	1
139	5

Table 3-7 represents the mean QoE of each cell after the balance service-differentiated mechanism is applied. In it, it is observed how after the balancing the cells present a closer mean QoE between them, achieving the objective proposed in this TeC.

**Table 3-7: Balanced mean QoE of each cell**

Cell	Mean QoE
131	2.62
136	2.3
139	3

## 3.8 TeC#2.6: Traffic steering management using context, user and cell level information

### 3.8.1 Overview

Indoor areas, such as airports, malls and large offices, concentrate most part of the mobile traffic. In these areas, it is usually concentrating a large number of users that consume different services.

Moreover, the increasing capabilities of the mobile systems allow the application of context information for Operation, Administration and Management (OAM) automatic mechanisms. Also, UE localization becomes each time more pervasive, based on different technologies, such as Ultra-Wide Band (UWB), Radio Frequency Identification (RFID), cellular or a combination of multiple technologies. This is expected to be even more the case for 5G deployments. Such an environment opens the way to what we have denominated as location-aware SON ([FAB+15],[FAF+16],[FBA+15]), where the position of the UEs can highly support the management of the cellular network.

### 3.8.2 Objectives

The main objective of this TeC is to implement and validate a mechanism, evolved from the one defined in the previous TeC, which can balance network load taking into account the QoE of each cell considering different services and additionally application context information, in particular distance between the cells and user's concentrations. This provides an assessment of the development of [ONE5G-D32], section 4.2.2., which it is based on simulations of macrocell scenarios and huge user concentrations. Conversely, the TeC is tailored to indoor scenarios with smaller concentrations and terminals with different service needs. It also links with the developments of [ONE5G-D31], section 4.3.1, included in the previous TeC.

### 3.8.3 Architecture

The architecture of this TeC follows the line of the one defined in 3.7.3. The same technology is used, as well as the testbed, the UMAHetNet. The implementation of this technical component implies metrics from the application layer and also RRC.

The mechanism used for tuning the network, which is presented in Figure 3-15. Here, controller 1 is the same which has been used in previous TeC. Nonetheless, the novelty of this system lies in controller 2, whose input (radio-distance) is in charge of making more aggressive or conservative HOM changes by multiplication of both outputs. This radio-distance is estimated as the distance in dB between the edge of the cell and the higher concentration of users in the scenario. This is done considering both the transmitted power as well as the current HOM of the cell.

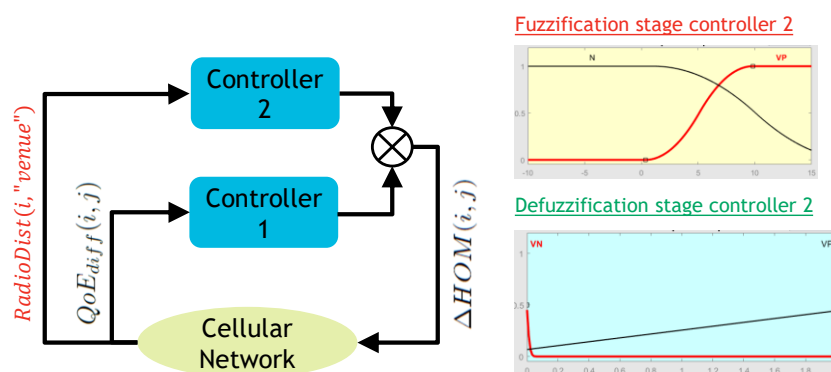


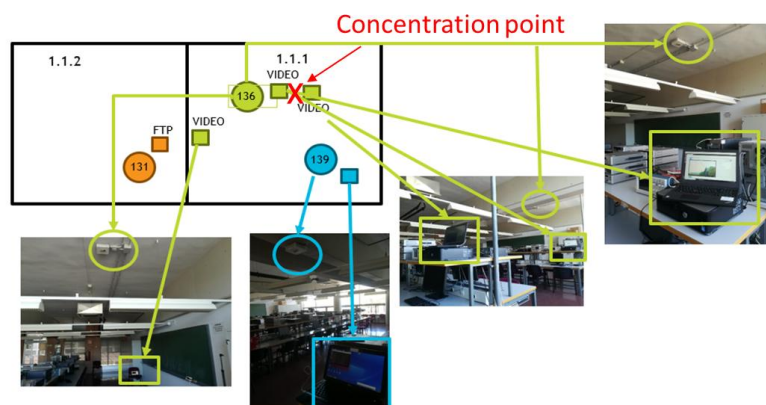
Figure 3-15. Balancing algorithm based on fuzzy logic and distance

Controller 2 fuzzy rules are quite simple: 1) if the radio-distance is very positive (VP), the output is VP; 2) if the radio-distance is negative (N), the output is VN.

Taking into account its fuzzification and defuzzification stages shown in Figure 3-15-right side, greater radio-distances to concentrations of users, are traduced in aggressive HOM changes. Once the HOMs implies a close radio-distance to the user concentration, the HOM changes are reduced, avoiding the overshooting of the process.

### 3.8.4 Test/demo scenarios

The test scenario in which this TeC is evaluated is similar to the one used in the previous TeC. The following image shows the distribution of users in the scenario, as also the service used by each of them. The concentration of users considered for the radio-distance calculations is the intermediate point (marked with an 'X') between the two close video users served by the cell 1.1.1. Such concentration points can be defined based on users demands and their positions.



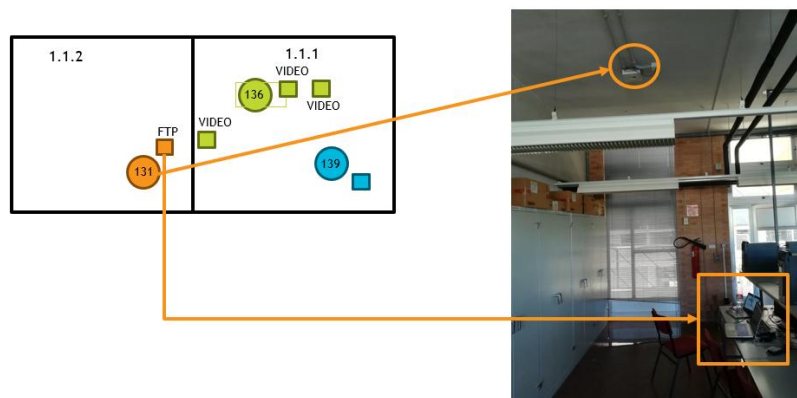


**Figure 3-16. Distribution of users in the scenario**

### 3.8.5 Validation

The validation of this TeC is done by comparing the mechanisms implemented in 3.7 and this section. To that end, the next methodology has been specified:

1. Mechanism of previous TeC is applied to the scenario
2. Mechanism of this section is applied to the scenario

In both cases, it has started from the situation represented in Figure 3-17, where there is one cell with a very bad QoE meanwhile the rest have high QoE.

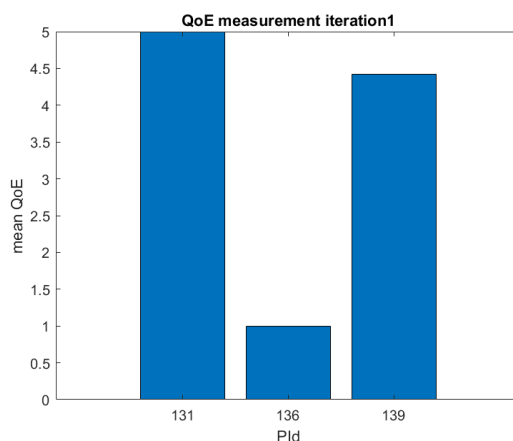


**Figure 3-17. Initial situation**

describes the evolution of QoE with both systems where, it can be seen how this mechanism (right) converges faster than mechanism which is not taking in account the contextualized information (left).

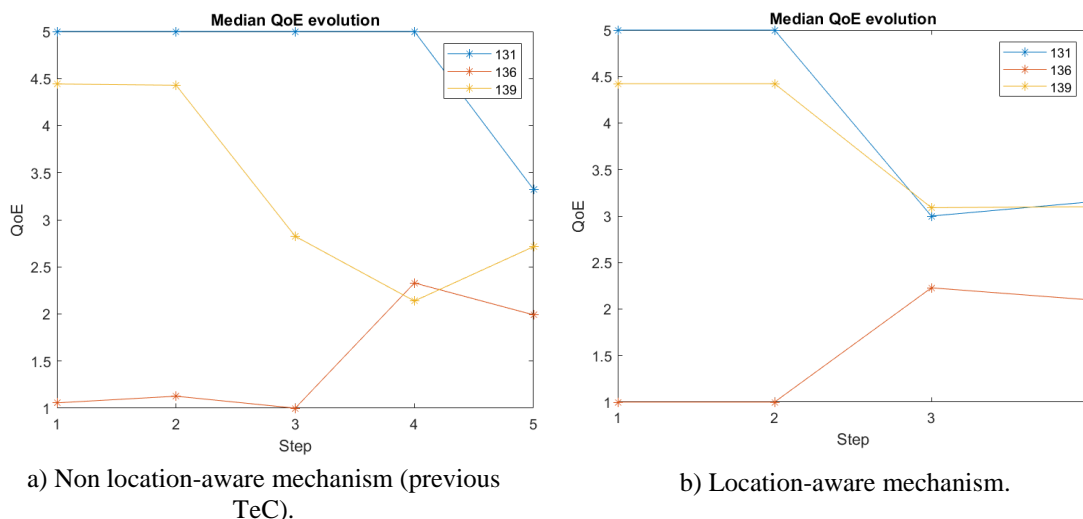


**Figure 3-18. QoE evolution of each cell.**

Additionally, the following Table 3-8 and Table 3-9 represent the evolution of HOM configuration for each loop/step of the algorithm. In them, it can be seen how by the use of contextualized information, the HOM tuning is more aggressive until the HOM value implies that the concentration of users is close to the edge of the cell 139 and 131, where the changes become more conservative and the algorithm converges, stopping the changes. In this way, it can be observed how the proposed location-aware approach reaches a more balanced QoE situation between the cells in fewer steps than the non-location-aware one.

**Table 3-8. HOM configuration mechanism from previous TeC**

STEPS	1	2	3	4	5
HOM (131,136)	3 dB	7 dB	11 dB	15 dB	17 dB
HOM (136,131)	3 dB	-1 dB	-5 dB	-9 dB	-11 dB
HOM (136,139)	3 dB	-1 dB	-5 dB	-9 dB	-9 dB
HOM (139,136)	3 dB	7 dB	11 dB	15 dB	15 dB

**Table 3-9. HOM configuration with the use of contextualized indicators**

STEPS	1	2	3	4
HOM (131,136)	3 dB	9 dB	14 dB	15 dB
HOM (136,131)	3 dB	-3 dB	-9 dB	-8 dB
HOM (136,139)	3 dB	-3 dB	-9 dB	-8 dB
HOM (139,136)	3 dB	9 dB	14 dB	15 dB

### 3.9 TeC #2.7: Ad-hoc deployment of services on edge cloud

#### 3.9.1 Overview

In the 5G era, stringent latency requirements posed by URLLC services or low latency services in general can be satisfied by introducing multi-access edge computing (MEC) technology to the cellular network architecture. Leveraging its ability to provide processing capabilities at the

cellular network's edge, an overlaid MEC deployment is expected to assist services in achieving low packet delays, due to its proximity to the end users.

This TeC focuses on the MEC topics and it is the implementation of the mechanism and algorithms presented in D4.2 [ONE5G-D42] (Section 4.4 - Optimized Functionality Placement and Resource Allocation in CRAN/DRAN Context). The implementation is realized by the development of algorithmic approach leveraging swarm intelligence and specifically built upon Particle Swarm Optimization. In addition, in order for the decisions of the algorithms to be realized on the actual testbed, a set of additional functionalities and components was implemented and integrated (described in detail in the following paragraphs).

### 3.9.2 Objectives

The main objectives of the technical component can be summarized as below:

- Demonstrate the optimized service placement between the Cloud and the MEC in order to fulfil the requirements of a newly established network slice.
- Demonstrate and validate the gains from the adoption of the approach, mainly by validating the latency KPI under the Cloud and MEC cases.
- Demonstrate that the ad-hoc migration of a service between Cloud and MEC is feasible and can be realized in an automated manner.

### 3.9.3 Architecture

The architecture of the TeC is similar to the TeC architecture presented in the "Slice Negotiation" TeC of PoC#4 presented in section 5.4 of the document, since the "Ad-hoc deployment of services on edge cloud" TeC extends this architecture with two components: the Deployment Orchestrator and the Cloud Deployment Manager. The TeC architecture is illustrated in Figure 3-19. The Deployment Orchestrator is responsible to decide between the Cloud and MEC deployment of a service. The decision is based on the characteristics of the requested network slice (e.g. latency thresholds). The Cloud Deployment Manager is responsible to realize the decision received by the Deployment Orchestrator. In case of a MEC deployment, the Cloud Deployment Manager is using the MEC Agent for the deployment of the selected service on the MEC. We assume that the service is available as container, therefore the MEC Agent deploys the service as a new container in the MEC using the Docker framework. In case of a Cloud deployment, the same approach is utilized, but at this time the Cloud Agent is responsible to deploy the service as container in the Cloud Server.

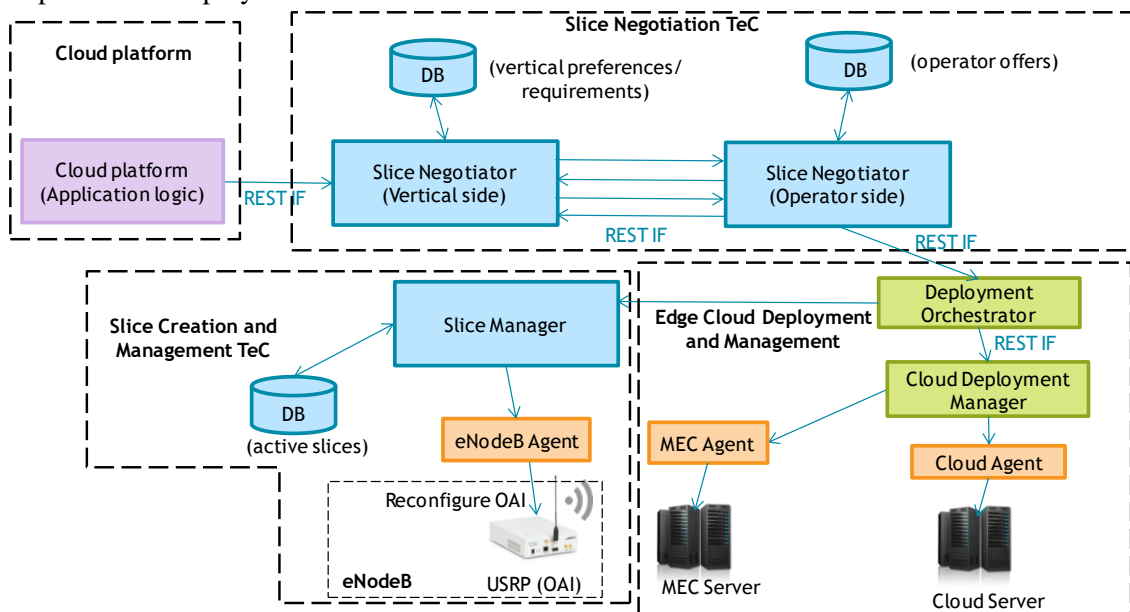


Figure 3-19. TeC Architecture

### 3.9.4 Test/demo scenarios

The test scenario in which this TeC was integrated and demonstrated is similar to the test/demo scenario described in section 5.4.4 of the document ("Slice Negotiation" TeC of PoC#4). In addition, to the aforementioned scenario, the functionality of the different components of the "Edge Cloud Deployment and Management" TeC was tested, while the latency KPI was validated. In detail two cases were tested: a) the application is executed in the Cloud; b) the application is executed in the MEC.

### 3.9.5 Validation

The TeC was validated through lab experimentation and testing in the "Platform for vertical service delivery through 5G - IoT and big data- technologies" testbed, as well as through the demonstration in EuCNC2019.

In addition, the Round Trip Time (RTT) Latency KPI was measured and validated for different executions of the experiments (using ping commands). The latency results for two cases: a) IPF in the Cloud; b) IPF in the MEC are depicted in the following table. In this table the latency benefit of using IPF on the MEC is demonstrated.

**Table 3-10. Latency results**

Scenario	Min Latency (RTT) (ms)	Avg Latency (RTT) (ms)
<b>IPF in the Cloud</b>	<b>29ms</b>	<b>48ms</b>
<b>IPF in the MEC</b>	<b>12ms</b>	<b>21ms</b>

## 3.10 Conclusion

The present PoC has served to test and evaluate multiple novel approaches for cellular management, with focus on QoE and E2E monitoring/modelling as well as context-awareness and slice negotiation procedures.

As can be appreciated from the results obtained from the implementation of TeCs, KQIs can be properly estimated as well as forecasted based on low-layer metrics. Also, load balancing algorithms supported by QoE estimation or direct measurement allow to highly improve the performance in the network. Moreover, adding context information relative to the position of the users increases these benefits, validating it as a solid option for the development of new standards of cellular network management.

In addition, this PoC codes and decodes a High Throughput bit stream compatible with the standardization (NR or WiFi) and fully compatible with any MCS. The validation of the system shows a slow reconfiguration of the component with no packet loss.

Finally, it includes mechanisms for serving megacity areas through the ad-hoc deployment of services on edge cloud demonstrating the efficiency of 5G technologies in supporting the mass and high requirements in computing/storing power of the highly populated areas.

## 4 PoC#3: Enhanced massive MIMO Proof-of-Concept

### 4.1 Brief description of the PoC

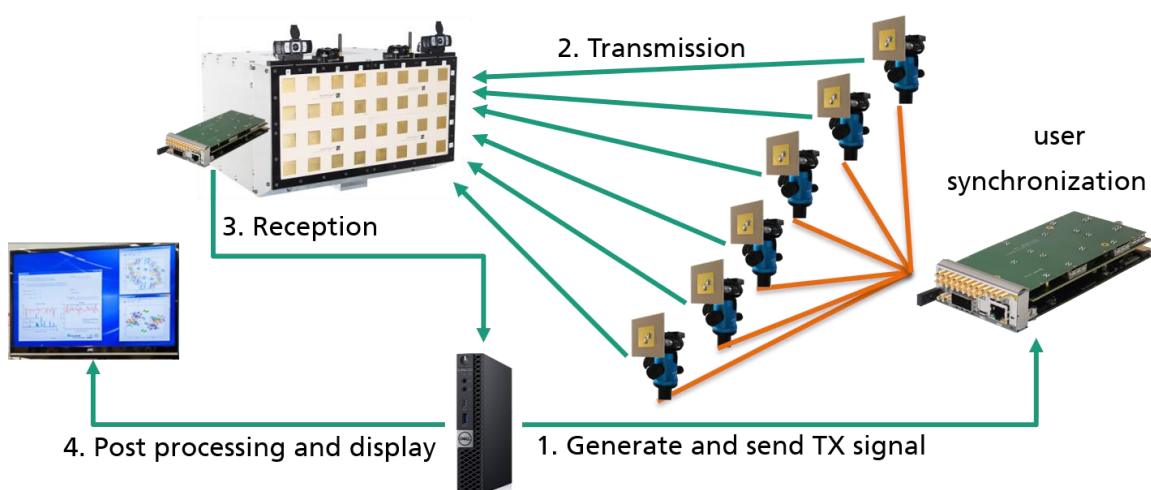
Non-orthogonal multiple access (NOMA) schemes in connection with massive MIMO technology have the potential for additional performance gains in a multi-user and multi-cell environment over the orthogonal access schemes. This PoC demonstrates a machine learning based adaptive NOMA uplink scheme. For the demonstration in this PoC a dual polarized uniform rectangular antennas array of  $[4 \times 8]$  is used as a receiver in the uplink transmission, see **Figure 4-1**. On the transmitter side, we use 6 single antennas, of-the-shelf commercially available hardware, with different locations and transmit powers to emulate different path-losses as in a real cellular systems.

In a classical orthogonal transmission system, the pilots for channel estimation for each user should be mostly interference-free, which is normally achieved by allocating orthogonal resources. This inevitably leads to pilot contamination and estimation errors, when the number of users becomes very large and pilot reuse must be employed. Additionally, large number of resources are wasted during channel estimation. In our machine learning based scheme, no such explicit channel estimation procedure is required.

In some cell-less systems, e.g. CRAN, the number of available antennas at the RRHs is limited due to cost considerations. This means that the number of users to be detected can be larger than the number of available antennas. In this case linear receive beamforming techniques cannot deal with the resulting excessive multiple-access interference adequately. Therefore, our PoC is based on a nonlinear receive filtering technique. Unlike other nonlinear methods, our technique has a remarkably low-complexity and it involves only inexpensive computations.

Our machine learning algorithm learns the multiple-access interference during the training phase. The training and detection for each user can be performed independently for each user. This allows accelerated execution on parallel hardware architectures such as multicore processors, graphics processing units (GPUs) and field programmable gate arrays (FPGAs).

For the evaluation in the PoC we used a hardware in the loop approach with offline processing for the modulation and decoding for the uncoded bits, see Figure 4-1.



Martin Kurras

**Figure 4-1. NOMA Uplink System Model Setup for the PoC**

Our machine learning algorithm is also able to learn certain hardware impairments, like different phases at the antenna ports of the receiver, introduced by different track length on the printed circuit board (PCB) or connected cables. Therefore, our technique can potentially not only avoid the classical signal processing blocks, such as channel estimation and equalization, but also the calibration step for phase coherent reception in the receiver path. Furthermore, we observed that the machine learning algorithm was able to learn (and correct for) certain hardware impairments in the receiver if these impairments are slowly changing which is often the case. An example is the low-frequency oscillation (LFO) mismatch between the receiver and the transmitter which often cannot be fully corrected for in inexpensive traditional receivers. This makes our overall receiver design simpler and potentially cheaper than traditional systems.

## 4.2 List of technical components (TeCs) used in the PoC

The following TeC developed in WP4 is used in this PoC:

- **Machine learning-based adaptive nonlinear receive filtering in non-orthogonal multiple access (NOMA)** that is titled as "Nonlinear Mechanisms in Cell-Less Systems" in Section 4.3.4 in the final WP4 Deliverable 4.2 [ONE5G-D42]. It should be mentioned that the "cell-less" aspect is not addressed in this PoC. The "cell-less" aspect is an extension of the proposed schemes such that uplink signals can be received at any (multiple) BSs and combined in a central processing unit, considering limited backhaul. However, before demonstrating the "cell-less" extension part, the basic scheme needs to be demonstrated and verified which was the goal in this project and has been successfully achieved, as presented in the following paragraphs.

## 4.3 TeC #3.1: Machine learning-based adaptive nonlinear receive filtering in non-orthogonal multiple access (NOMA)

### 4.3.1 Overview

Massive connectivity, e.g., in the context of mMTC communications, is an important part of the 5G wireless technology. In these systems, a massive number of low-rate devices transmit information (sensor data, health updates, etc.) to a single BS or multiple BSs. The design goal of such low-data rate networks is to achieve reliable communication (e.g., in terms of a low BER) at a fixed transmission rate. To enhance system throughput, many users share the same time-frequency resources, and they therefore experience multiple-access interference.

Though in general non-linear receive filters (or beamformers) achieve a better BER performance than their linear counterparts do, they are often avoided because of their higher complexity and their larger sensitivity to changes in the wireless propagation environment or interference situation.

Against this background, we develop a low-complexity robust nonlinear beamforming technique for 5G NOMA uplink. Our technique is also suitable for operation in cell-less *multi-connectivity* scenarios. The suitability of our technique for cell-less operation results from the fact that low-cost BSs (e.g., in CRAN) may have only a few antennas, so that nonlinear techniques are required when the number of users becomes large.

Our technique has several attractive *features*:

1. The receive filter consists of a mixture of linear and nonlinear component functions and the amount of nonlinearity (and linearity) of the aggregate filter can be controlled by a weighting factor. This flexibility allows us to adapt the nonlinearity of the receive filter to various environments. For example, in contrast to weak users, users with good receive SINR may not require a highly nonlinear receive filter. In addition, in dynamic environments where users are either not perfectly synchronized or they transmit

- sporadically, one can decrease the nonlinearity in the system (or increase the linearity) to make the system more robust.
2. Our machine learning based technique does not require channel and parameter estimation, which are susceptible to errors. The errors become more severe when the number of user channels is larger than the number of available orthogonal pilots. In this case, pilot reuse causes interference between pilots and degrades the quality of channel estimation.
  3. Our technique has the potential of overcoming certain hardware impairments like frequency offset between transmitter and receiver local oscillators that cause a gradual change in the overall channel. Therefore, our technique simplifies receiver design.
  4. All users are detected independently in parallel, and various other aspects of our signal processing technique make it suitable for parallel computing platforms.
  5. Our technique has low complexity, which is comparable to that of standard linear techniques.

For more details, please see Section 4.1.4 in [ONE5G-D41], Section 4.3.4 in [ONE5G-D42] and in the technical papers in [ACY+18], [ACS1+18], and [ACS2+18].

### 4.3.2 Objectives

The objective of this TeC is to demonstrate and verify features discussed in the previous section. To demonstrate the nonlinearity aspect of our design we show that our technique outperforms a standard technique when the number of users (transmitting simultaneously at the same time-frequency resource) to be detected is larger than the number of available antennas at the receiver. We show that, unlike standard receivers that require channel estimation, which is susceptible to errors, our technique can detect user modulation symbols directly which simplifies the receiver design. Furthermore, all users are detected independently in parallel, which reduces complexity and delay. By exploiting the computationally attractive frameworks of reproducing kernel Hilbert spaces (RKHS) and the adaptive subgradient projection method, we can compute high-dimensional complex nonlinear functions in a computationally efficient way. We compare the performance of our technique with a standard detection method in terms of user Symbol Error Rate (SER), total system throughput, and execution time complexity.

### 4.3.3 Architecture

Our technology is positioned in the PHY layer of the protocol stack. The TeC architecture consists of several user terminals transmitting modulation symbols simultaneously at the same frequency to a single BS. The NOMA uplink is shown in Figure 4-2 for the case when user 1 is the desired user. It is assumed that the number of users may be larger than the number of antennas. All users are allocated independent training sequences. During training, the BS learns how to cancel multiple-access interference and noise for each user independently in parallel. The memory and processing limitations of the receiver are considered during the computation of the nonlinear filter. After the training is completed, data is detected for each user in parallel.

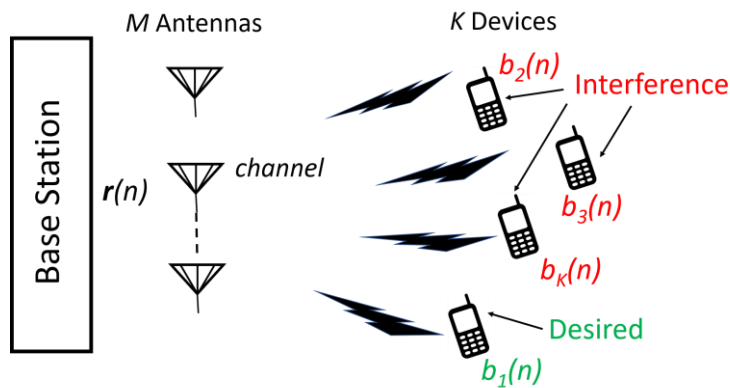


Figure 4-2. NOMA Uplink System Model

This PoC uses the Flexible Massive MIMO testbed, which is described in the ONE5G document D5.1 [ONE5G-D51]. Briefly, the BS in our test bed is equipped with a mMIMO array. We can use up to eight antennas on the array. Up to six users are equipped with a single antenna, and they are placed at distance of few meters from the BS. All base band processing takes place in a desktop computer. See [Appendix A.4, ONE5G-D51] for further information.

#### 4.3.4 Test/demo scenarios

Up to six users are placed at different locations and height transmit simultaneously on the same frequency to the BS, see Figure 4-3. Users are multiplexed in the power domain with a resolution of 3 dB. In the lab setup, the distance between BS and users is approximately 4 meters and the users height is between 0.5 and 1.5 meters. The training period is followed by data transmission. The signal is transmitted at 2.44 GHz carrier frequency in the unlicensed WiFi band with a bandwidth of  $\frac{30.72 \text{ MHz}}{16} = 1.92 \text{ MHz}$ . The 16 in the denominator indicates that an oversampling factor of 16 was used in order to emulate a frequency flat narrowband channel. This results to symbol length of  $\approx 0.5 \mu\text{s}$ . For modulation and ease of demonstration a BPSK waveform was used. After each burst of data, we can calculate the uncoded SER and total user sum throughput to monitor the detection performance.

##### 4.3.4.1 Live Demo

The demo setup at HHI Berlin MIMO laboratory is shown in Figure 4-3 and Figure 4-4. In the graphical user interface (GUI) shown in Figure 4-5, we adjust the main algorithm configuration parameters like the number of transmit (users) and receive antennas, the number of used training samples, the weights settings between linear and non-linear kernel. We also monitor various aspects of the reception and performance.



Figure 4-3. NOMA demonstration setup – array view

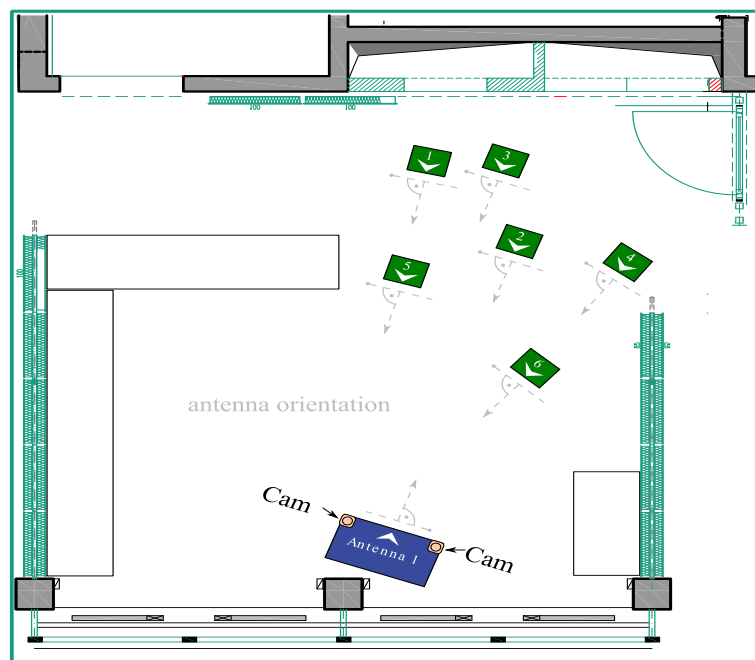


Figure 4-4. NOMA demonstration setup – bird-eye's view

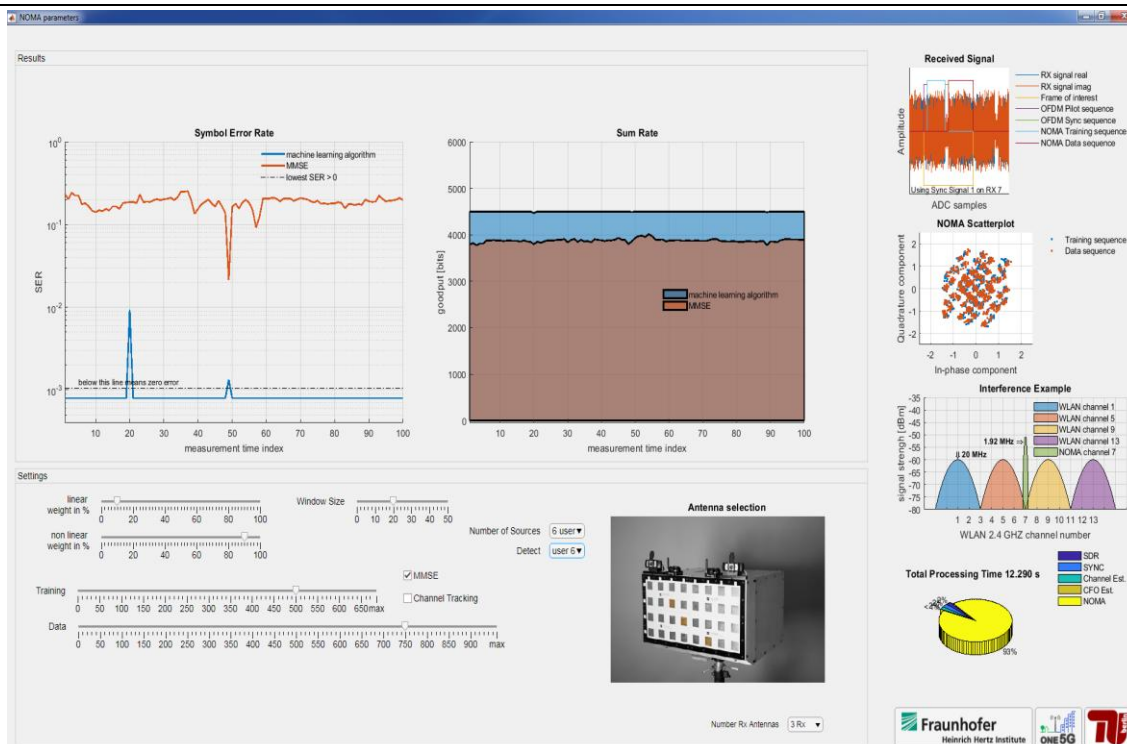


Figure 4-5. Graphical user interface for the NOMA MIMO testbed

### 4.3.5 Validation

We now present the results of our experiments performed in the demo with various settings. The results from different settings are shown in Figure 4-6, Figure 4-7 and Figure 4-8.

In the top plot of Figure 4-6 the SER performance of our method and the standard MMSE method for the strongest user is shown. Since a finite number of bits, denoted by  $N^{(\text{bits})}$ , is transmitted in the data-transmission phase, the lowest detectable SER is determined by  $1/N^{(\text{bits})}$ . This threshold is given by the dashed line in Figure 4-6. If zero symbol errors are detected no statement about the actual SER can be derived, therefore this regime is below the dashed line. For visibility reasons, the lines of the NOMA and reference scheme are drawn as non-overlapping if both SERs are zero. Despite the NOMA line being above the reference scheme, if both lines are below the threshold they have the same value of SER zero.

In the bottom plot, the total sum good put achieved by our method and the standard MMSE method. In this configuration 5 users are active in the system and 3 receive antennas are used at the BS. For all measurements, we used 500 training samples and 1000 test samples and used 0.5 and 0.5 for nonlinear weights and linear weights, respectively. The takeaway message here is, that this algorithm allows a tuning of robustness for adaptation to changing conditions in the cell-environment.

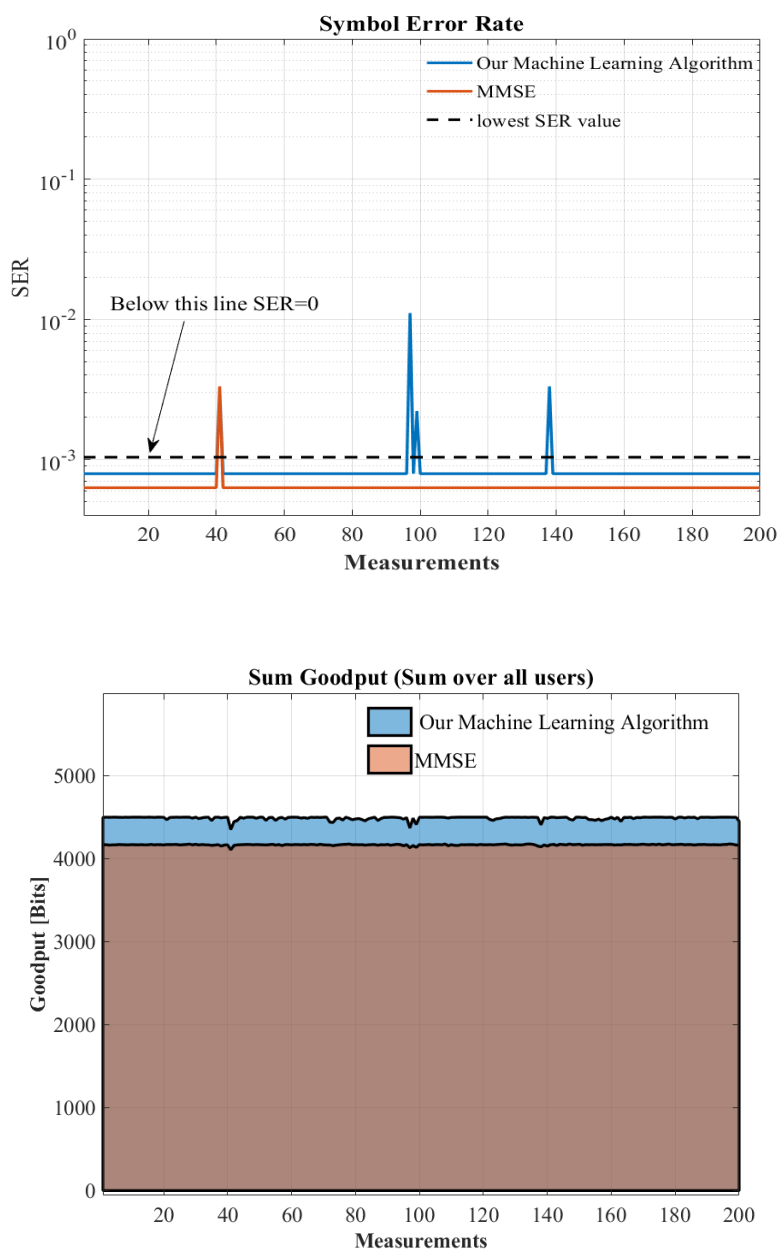


**Figure 4-6. Result 1 - (top plot) SER performance, (bottom plot) total sum goodput**

For the next result we alternate the weights to 0.9 and 0.1 for nonlinear weights and linear weights, respectively. All other configurations are the same, as in the previous configuration. There are 5 users in the system and 3 receive antennas at the BS. For all measurements, we used 500 training samples and 1000 test samples. We show in Figure 4-7 the SER performance (top plot) of our method and the standard MMSE method for the weakest user and the total sum good put achieved by our method and the standard MMSE method in the bottom plot.

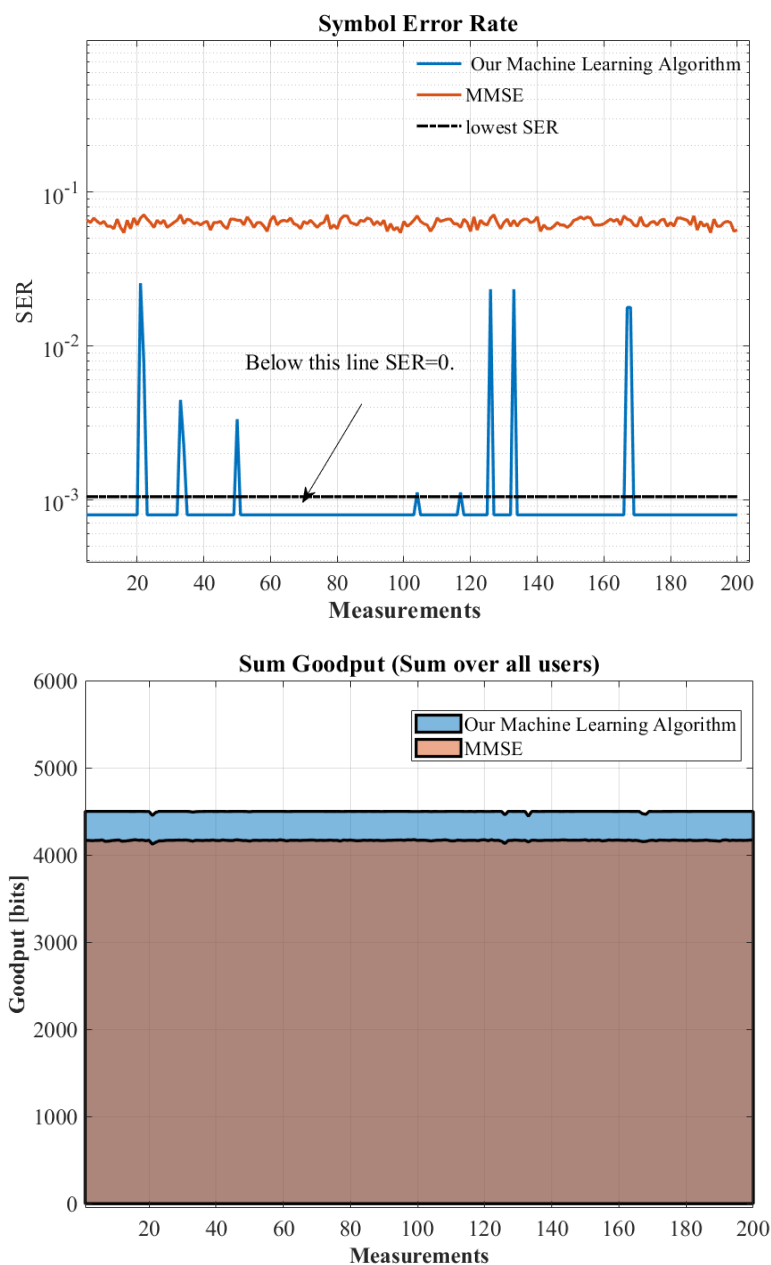


**Figure 4-7. Result 2 - (top plot) SER performance, (bottom plot) total sum goodput**

In the next experiment, we reduce the number of users to 3, which equals to the number 3 receive antennas at the BS. We also change the weights to 0.2 and 0.8 for nonlinear weights and linear weights, respectively. For all measurements, we used 500 training samples and 1000 test samples. In Figure 4-8 the SER performance of our method and the standard MMSE method for the weakest user with this configuration is shown in the top plot. Moreover, in the bottom plot we display the total sum good put achieved by our method and the standard MMSE method.

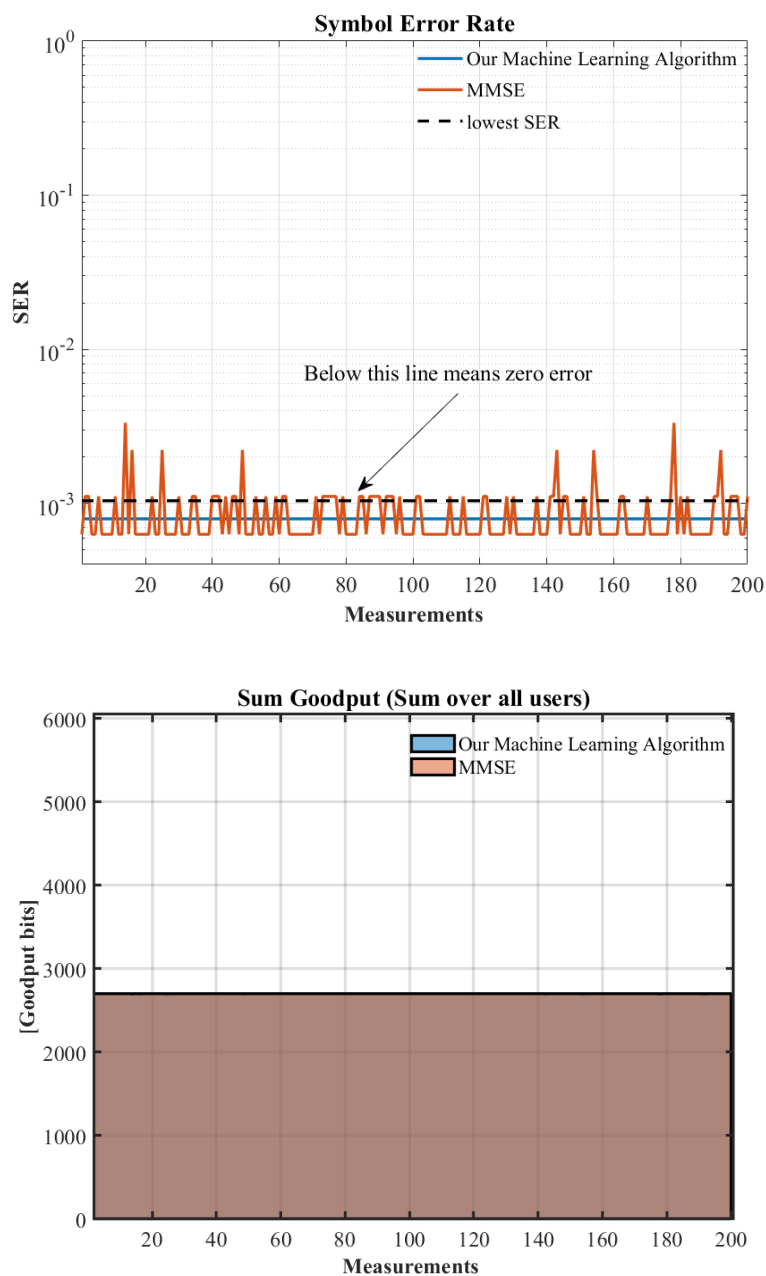


**Figure 4-8. Result 3 - (top plot) SER performance, (bottom plot) total sum good put**

The results shown in Figure 4-6, Figure 4-7 and Figure 4-8 paint a clear picture. When the number of users exceeds the number of antennas at the base station, the standard MMSE technique is unable to detect weak users sufficiently well. This effect is clearly visible in terms of SER in Figure 4-7 and the sum goodput in Figure 4-6 and Figure 4-8. In contrast, by increasing the nonlinearity weight (see the GUI in Figure 4-5) in our method from 0.2 and 0.5, respectively, in Figure 4-6 and Figure 4-8 to 0.9 in Figure 4-7, we are able to decrease the SER to almost zero.

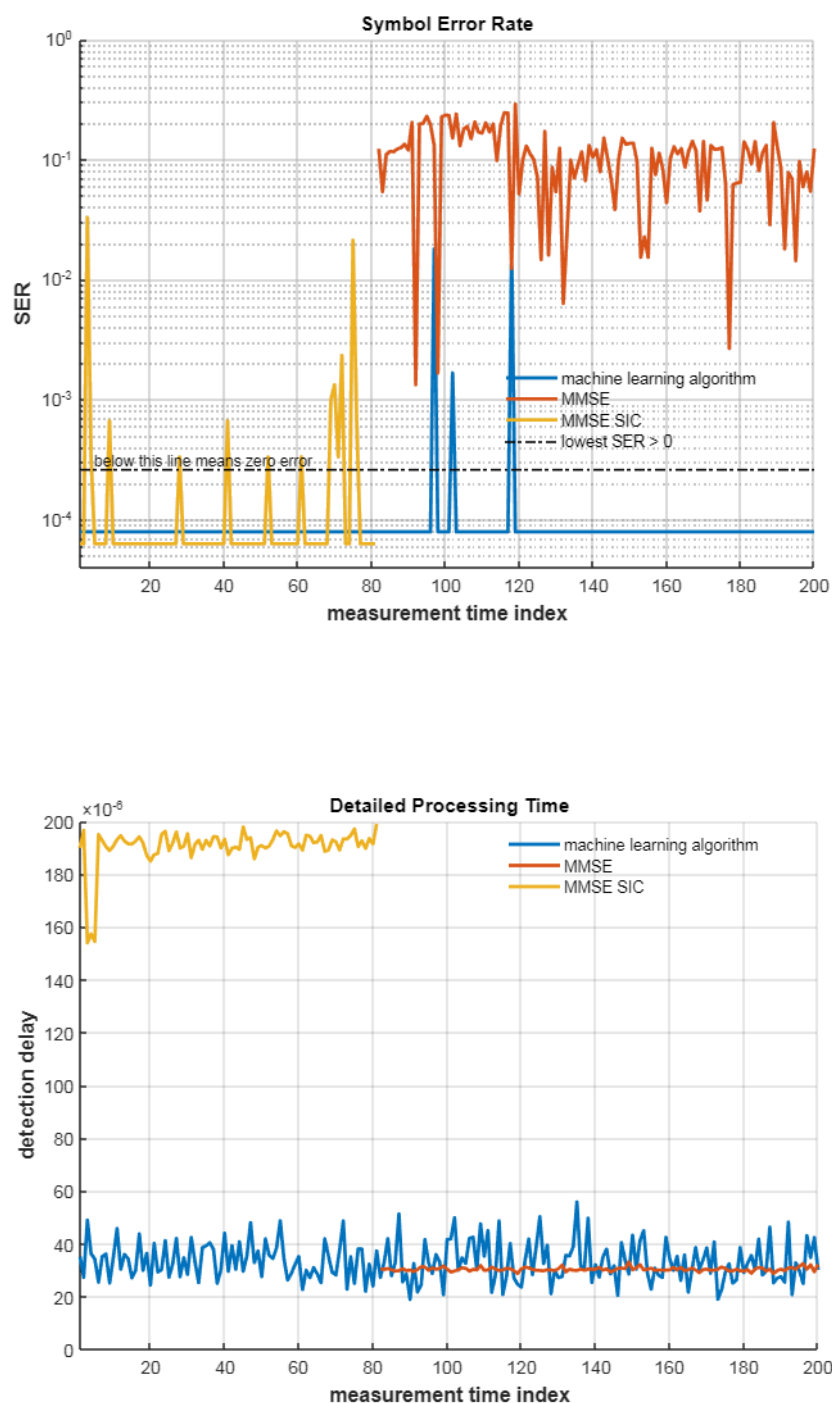


**Figure 4-9. Result 4 - (top plot) SER performance, (bottom plot) processing time**

The results in Figure 4-9 of our NOMA demonstration address the linear and non-linear kernel. We also add MMSE-SIC (non-linear) to compare with MMSE (linear) and NOMA. In this experiment, 5 users were active and we use 3 receive antennas to detect user 3. We show the symbol error rate (SER) of this user and the detection delay in  $\mu\text{s}$ . In the top plot you can see that the performance of MMSE-SIC outperforms MMSE because the number of receive antennas is less than the number of transmit antennas. And it is also in the region of NOMA because we use the weights of 0.6 and 0.4 for nonlinear weights and linear weights, respectively. In the bottom plot of this figure, we see that MMSE-SIC had a bigger delay

---

compared to MMSE and NOMA, because successive interference cancelation (SIC) need the calculation of the stronger users (user 1 and 2 in our case) to detect user

### 4.3.6 Conclusion

Based on results from our live Demo we conclude that our machine learning method shows a sufficiently convincing performance gain over the standard MMSE based receiver. Moreover, our technique has the flexibility to adapt the nonlinearity and linearity of the receive filter based on intuition and experience. This is achieved by simple weighting of the components. This feature is important since nonlinear systems are less robust against small changes in the channel or hardware degradation.

By introducing linear components in the design we make our technique suitable to be used on real-life slowly-changing wireless channels. Note that in real wireless systems, perfect symbol-synchronization of users required by many estimation techniques is not guaranteed. In this case, purely nonlinear systems can be unreliable. Similar situation is met in machine-type communications where users transmit sporadically, and they may leave or enter the system in a random fashion. Such an environment was simulated inherently in the Demo because all transmissions took place in the unregulated WIFI band. This meant that all random WIFI transmissions that took place in the vicinity of the Demo caused interference to all users. This effect manifests itself in terms of spikes in Figure 4-7, less number of spikes in Figure 4-6, and lack of these spikes in Figure 4-8. In a purely nonlinear system (see [ACY+18] for a direct comparison with purely a nonlinear filter), these spikes may be much higher than those seen in our robust technique. This shows that by adding linear components, the overall detection becomes more robust to sudden changes or interferences in the wireless environment.

We clearly observe in the demo that the greatest gains over MMSE are achieved when the number of users exceeds the number of available antennas and we detect the weakest user in the system. In this case the MMSE fails because it is not able to sufficient enhance the SINR of the weakest user. Furthermore, by detecting all users in parallel, an inherent feature of our technique, we observed a significant speed-up.

We showed that NOMA symbol error rate (SER) performance is in the region of non-linear algorithms like MMSE-SIC, whereas the detection delay remains in the linear region. This performance can be explained by the fact that NOMA is directly able to separate noise and interference caused by all other users from the signal of a desired user. This feature allows the desired users to be detected in parallel, which is another advantage of our NOMA algorithm. This decisive advantage is very helpful in a massive connectivity scenario where hundreds of users are active and sharing the same resources.

Moreover, with our machine learning based NOMA scheme we demonstrated that we reliably serve a significantly higher number of users than antennas are available at the same time-frequency resource, thus this technique fits neatly to the massive connectivity use case.

## 5 PoC#4: Underserved areas Proof-of-Concept

### 5.1 Brief description of the PoC

Highly populated areas, namely "Megacities" encompass districts of high interest for operators to provide 5G as early as possible, as these districts are promising to be profitable right from the beginning. In these areas, very high throughputs and connection densities are of highest importance. In addition to persons with smartphones and other connected wearables, these areas will include in the near future a large quantity of wireless connected machine type communication (MTC) devices. In "Megacities", various services will be intermixed to an extremely high degree, and a main challenge for 5G will be to efficiently deliver the expected quality of service/experience to all these services.

Nevertheless, less densely populated areas should also benefit from the opportunities that 5G is about to offer. These "Underserved Areas" will involve different challenges to be addressed, with a considerably lower density of devices and traffic, but longer communication ranges to cover, in an environment often constrained by a limited availability of resources (e.g. power sources) and/or infrastructure (e.g. backhaul). In their majority, those regions are not covered by traditional networks due to an insufficiently attractive business case, either because the population density is not high enough to provide sustainability for deploying and operating mobile networks infrastructure in these regions.

The main objective of this PoC is to design, develop and implement a low-cost network for underserved areas use cases. The targeted vertical scenario is large underserved areas with agricultural applications.

The PoC implements and integrates solutions for the flexible and fast reconfigurable hardware targeting the reduction of the cost of network deployment and operation, especially in underserved areas. In addition, it includes network slice negotiation and management solutions targeting to establish network slices in the underserved areas in a per request manner.

Two testbeds are used in this PoC:

- Flexible and reconfigurable HW/SW testbed
- Platform for vertical service delivery through 5G – IoT and big data - technologies

### 5.2 List of technical components (TeCs) used in the PoC

The following TeCs are used in this PoC:

- **Rx and Tx Digital Front Ends (Rx/Tx DFE).** This TeC is related to "Flexible and Fast Reconfigurable HW Architecture for Multi-Service Transmission" (section 3.6.2 of D4.2 [ONE5G-D42]).
- **Slice negotiation between the vertical side and the operator side.** This TeC is related to "Time-variant optimal slicing negotiations" (section 3.2.3 of D3.1 [ONE5G-D31]).
- **Network slice creation supporting the vertical requirements in an area-based and time-based manner.** This TeC is related to "Network slice management based on mobility and traffic patterns" (section 4.2.3 of D3.2 [ONE5G-D32]).

### 5.3 TeC #4.1: Rx and Tx Digital Front Ends (Rx/Tx DFE)

#### 5.3.1 Overview

The Rx/Tx DFE is part of the "Flexible and fast reconfigurable" hardware IP initially proposed in ONE5G document D5.1 [ONE5G-D51]. The Rx/Tx DFE is able to handle multi-bands and allows up or down conversion from/to base band by removing unwanted images.

The Rx DFE is parametrized to support the NB-IoT protocol, which is a good candidate for underserved areas MTC verticals.

The Tx DFE is generic and can support both NB-IoT protocol and LTE.

### 5.3.2 Objectives

The main objective of this TeC is to isolate bands after analog-to-digital conversion and to remove unwanted images when performing digital-to-analog conversion.

Isolating bands is necessary to allow the coexistence of more than one radio protocol or separate resource blocks in the frequency domain. For underserved areas PoC scenario, the DFE will be used jointly with the NB-IoT protocol. NB-IoT can be implemented in three different categories of bands:

- a. In-Band,
- b. Guard-Band,
- c. Stand-alone.

In our implementation, the ‘a’ option, in-band mode, is used.

### 5.3.3 Architecture

#### 5.3.3.1 Rx DFE

In the reception chain, the Rx DFE is located right after ADCs. It is made of a CIC (cascaded integrator–comb filter) for sampling rate adaptation, followed by a FIR (Finite Impulse Response) filter which is a low pass filter that rejects high frequency image products. The resulting signal is down-sampled by a factor of 2. Then, the signal is split and sent to a poly-phase sine cardinal filter that feeds an FFT whose size is the number of filtered bands. Resulting output is a set of channels, each one corresponding to a subdivision of the sampling frequency spectrum. Figure 5-1 shows the flowchart of the Rx DFE.

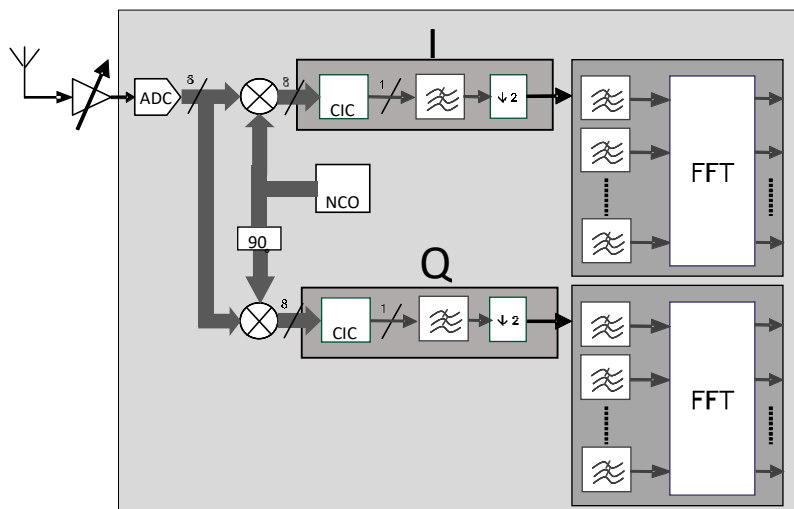


Figure 5-1. Rx DFE overview

To support NB-IoT protocol, the FFT will be tuned to have filtered bands of 180 kHz bandwidth.

Figure 5-2 shows an example of NB-IoT subband with filtered region represented in green.

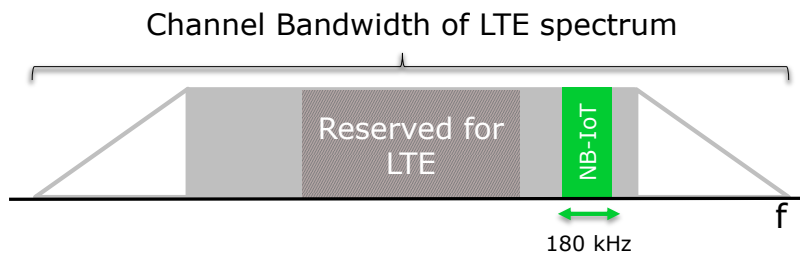


Figure 5-2. NB-IoT implemented in In-band.

Table 5-1 describes the number of allocated NB-IoT resource block depending on the carrier bandwidth.

Table 5-1. Resource blocks per NB-IoT bands

	LTE carrier BW					
	1,4 MHz	3 MHz	5 MHz	10 MHz	15 MHz	20 MHz
NB-IOT Carrier Above DC		2	2, 7	4, 9, 14, 19	2, 7, 12, 17, 22, 27, 32	4, 9, 14, 19, 24, 29, 34, 39, 44
NB-IOT Carrier Below DC		12	17, 22	30, 35, 40, 45	42, 47, 52, 57, 62, 67, 72	55, 60, 65, 70, 75, 80, 85, 90, 95
Total Resource Block	6	15	25	50	75	100
NB-IoT Channel number		2	4	8	14	18
FFT size	128	256	512	1024	1536	2048
Sample rate (MHz)	1.92	3.84	7.68	15.36	23.04	30.72

Let’s consider the 10MHz NB-IoT band for example. The filter bank included in the Rx DFE will filter incoming signal and extract only spectrum in NB-IoT sub-bands. The remaining spectrum is then demodulated with smaller FFTs, significantly improving global signal processing time. The OAI framework will be modified accordingly to support this hardware acceleration. Nonetheless, to simplify the PoC demonstration, only NB-IoT resource blocks will be processed. LTE resource blocks will be ignored. This is depicted in Figure 5-3 where NB-IoT resource blocks are represented in green.

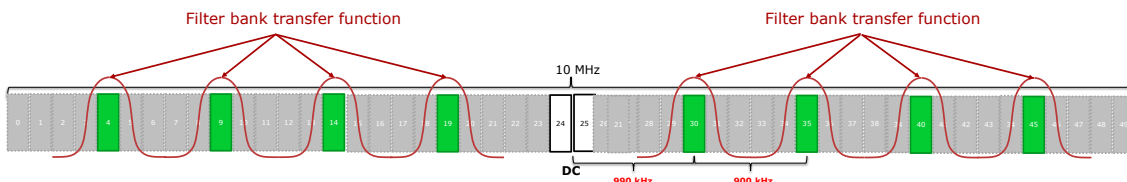


Figure 5-3. Filter bank transfer function

The main drawback of this architecture is the limitation of the filter bank that requires regular gaps between each resource block.

NR 5G aims at addressing, for the same user, several kinds of services simultaneously. This goal requires having a very fast reconfigurable HW architecture allowing a very flexible HW

implementation. The Rx Digital Front End (Rx DFE) adapts the data stream to the antenna considering the RF impairments. The Rx DFE targets the filtering of the RF bands and the reduction of data rate. According to the underserved areas verticals, that needs long range coverage and low data rate, the Rx DFE studies mainly focused on NB-IoT standard. The reception part aims at the selection of the NB-IoT carriers from the ADC samples. It encompasses the following processes:

- The ADC signal is scaled with an Automatic Gain Control;
- The signal is filtered on two stages;
  - A first combination of a CIC and a FIR filter adapts the bandwidth to the LTE band;
  - A second operation provides a fine adaptation of the sampling rate;
- Each NB-IoT resource block is extracted and converted in Base-Band;
- Each NB-IoT channel is filtered.

Figure 5-4 shows the data processing steps.

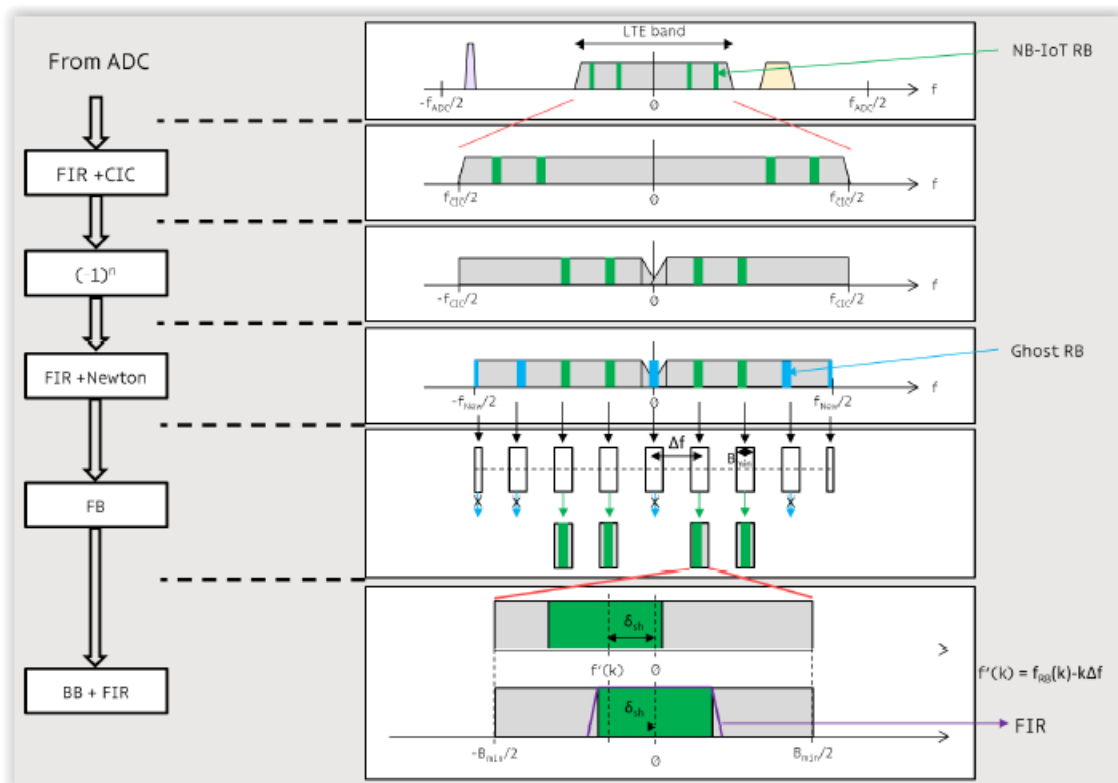


Figure 5-4. NB-IoT Digital Front End – Rx side

### 5.3.3.2 Tx DFE

The Tx DFE is much simpler than Rx DFE. It just consists in a succession of filters associated with factor 2 up-samplers. Each I and Q path is modulated using 8-phases NCO, with a phase shift of 90° for the Q path. Then I and Q paths are added together and send to the power amplifier.

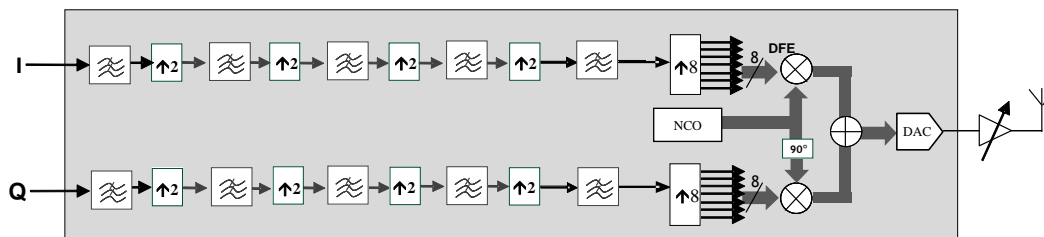


Figure 5-5. NB-IoT Digital Front End – Tx side

5.3.3.3 Associated testbeds

The Rx and Tx DFEs are currently ported to the BCOM Multi-RAT testbed with an input and output sampling rate of 1966.08 MHz. The Multi-RAT testbed is also connected to the OAI framework.

5.3.3.4 Position of the TeC in the protocol stack

The Rx DFE is part of the physical layer on the Rx link. It is located just after analog-to-digital conversion stage. Its inputs are connected to the ADC outputs whereas its outputs are connected to the upper part of the physical layer.

The Tx DFE is also part of the physical layer. It is located just before the digital-to-analog conversion stage. Its inputs are connected to the IFFT outputs whereas its outputs are connected to the DAC.

Position of Rx and Tx DFEs in the protocol stack is represented on Figure 5-6.

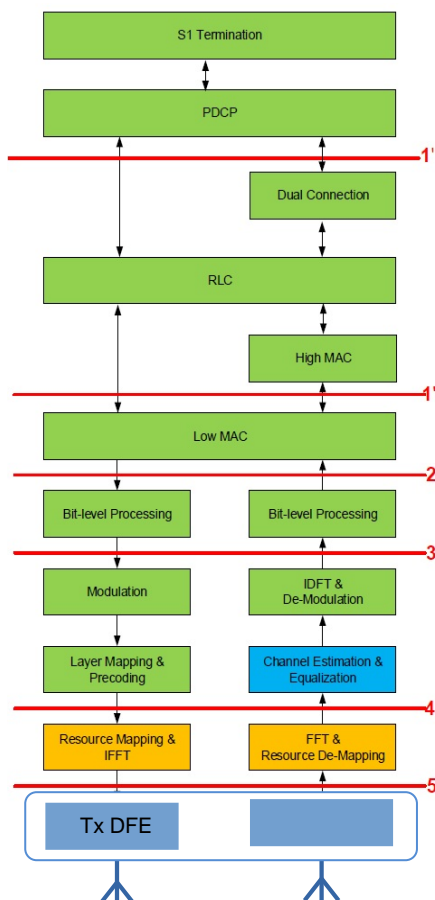


Figure 5-6. Position of the Rx and Tx DFE in the protocol stack

### 5.3.3.5 Technology used

This block is coded in VHDL. It does not use manufacturer specific hardware. All memories and logic are directly generated from VHDL. It can be compiled with either Intel (Formerly Altera) or Xilinx tools.

### 5.3.3.6 Interfaces

The Rx and Tx DFEs use only one master clock and are interfaced to the external world by means of versatile data interfaces. These interfaces are compatible with Intel Avalon streaming or ARM AXI4 streaming buses. Modules have also a CPU compatible interface for configuration.

## 5.3.4 Test/demo scenarios

### 5.3.4.1 Test overview

For this scenario, a modified version of the OAI framework supporting NB-IoT will be used. The scenario consists in communicating with one NB-IoT UE as shown on the figure below. Short messages will be sent by the eNodeB to the UE which sends back the response to the eNodeB afterwards. This setup has been tested successfully using USRPs as RF frontend and is currently tested on our Multi-RAT platform. The goal is to show that our Multi-RAT platform combined to our Rx & TX DFEs can efficiently replace USRPs frontends when combined with OAI framework. And that our platform can be a good candidate to support multi-band/multi-link services in the future. Scenario is illustrated in Figure 5-7.

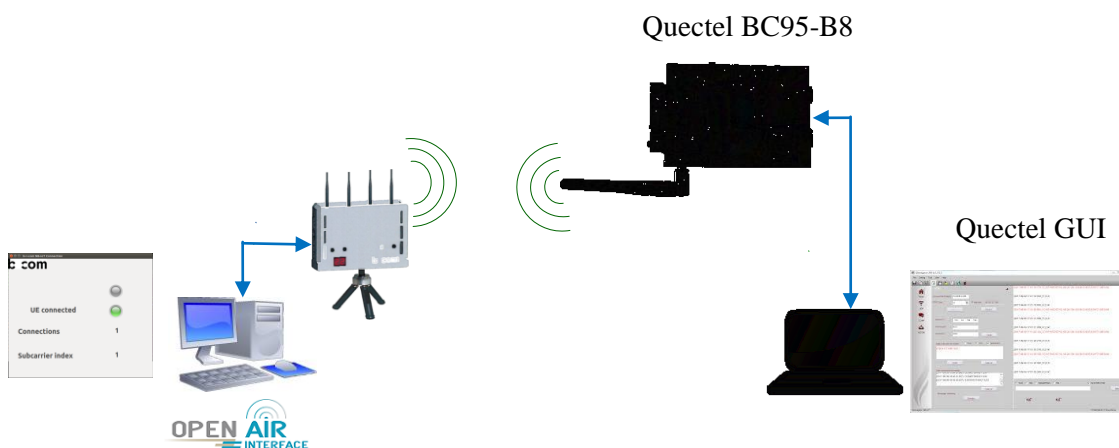


Figure 5-7. Test scenario

### 5.3.4.2 Test setup parameters

Below are described the parameters/configuration used for playing our scenario:

- eNodeB side:
  - the OAI framework running on Ubuntu 18.04 low latency,
  - the OAI framework configured with the following parameters:
    - Mode: In-band
    - Band: 8 (900MHz) or 28 (700MHz)
    - half FDD
    - Resource-blocks: 22
    - Band occupation: 180 kHz (12x15 kHz)
    - Data rate: 50 kbps.

- A graphic tool is used to show logs, statistics and signals extracted from OAI framework.
- UE side: Quectel BC95-B8
  - The UE is connected to a graphic tool to show logs.

### 5.3.5 Validation

Validation was done on the BCOM Multi-RAT platform. It consists in exchanging messages for random access procedure (RACH):

1. Cell search,
2. Synchronization between UE and eNB,
3. Random access (RACH),
4. User data transmission uplink/downlink with low data rate,

Tests were run in band #8 and band #28 with success during hours. Next step will be to use optical links to take advantage of our large acquisition spectrum over USRPs.

## 5.4 TeC #4.2: Slice negotiation between the vertical side and the operator side

### 5.4.1 Overview

In order to cope with the challenges of underserved areas, a more flexible and easily sustainable mobile type of network should be adopted in comparison to the traditional mobile network. This flexibility can be provided by the adoption of dynamic slicing and resource orchestration functionalities.

In addition, the legacy resource negotiation process is not efficient because of the dynamic nature of the network, and a dynamic resource negotiation scheme should be followed. In underserved areas, in which the needs of the verticals may be sparse and sporadic, the vertical entities can benefit from automated negotiation mechanisms in order to get lower prices for the needed resources of a network slice.

In general, negotiation is the primary form of interaction of two or more parties for the formulation of an agreement ([LAH04], [SKD+05], [JPL+01]). The slice negotiation mechanisms and algorithms proposed in the project are reported in [ONE5G-D31] and [ONE5G-D32], while in this document the technical component generated from the implementation of the proposed mechanisms is described, also the results from its integration into the testbed are presented. The technical component implements mechanisms for the automated negotiation of price offers for providing certain quality levels of services for the “under-served areas” scenarios. Furthermore, the negotiation process was extended to provide a certain price levels by taking into account environment heterogeneity, variable user aspects (e.g. density, distribution etc.), variable service/traffic demand (e.g. accommodating eMBB, URLLC, mMTC) and network aspects (e.g. cell layout, bands etc.).

### 5.4.2 Objectives

The focus of the technical component is on a rural (or suburban area), whose economy is based on agriculture. A set of sensors is deployed in the area. Some of these sensors are constantly active, while others become active when certain events are detected (e.g., an agricultural disease, a fire, a flood, etc.). So there are constantly sensors capable of detecting such events,

while a camera (drone) is an example of an additional sensor needed, when events are detected. Moreover, the 5G network is contacted, in order to support the additional information flow (e.g., by activating a slice that will be appropriate for transferring the information also from the additional sensors that are needed).

The main objectives of the technical component can be summarized as below:

- To demonstrate the efficiency of 5G technologies in supporting the requirements in rural and suburban areas (underserved areas) and in the management of critical infrastructures.
- To demonstrate the advantages of the design, development and deployment of a flexible and powerful network for underserved areas use cases.
- To showcase an underserved areas scenario, in which the network can cover large areas (cell of around several kilometres radius) with allocation of narrow bandwidth (few RBs), and in a low-cost manner, having also a low energy fingerprint. It will be also capable to provide the needed capabilities, in order to serve 5G use cases, upon demand, where and when needed.
- To demonstrate an efficiently reconfigurable network, in terms of communication and cloud resources, to address the multi-services (mMTC and URLLC) requirements.

### 5.4.3 Architecture

The high-level architecture is illustrated in Figure 5-8. The architecture includes the cloud platform component, the slice negotiation technical component and the slice management technical component as illustrated in the figure.

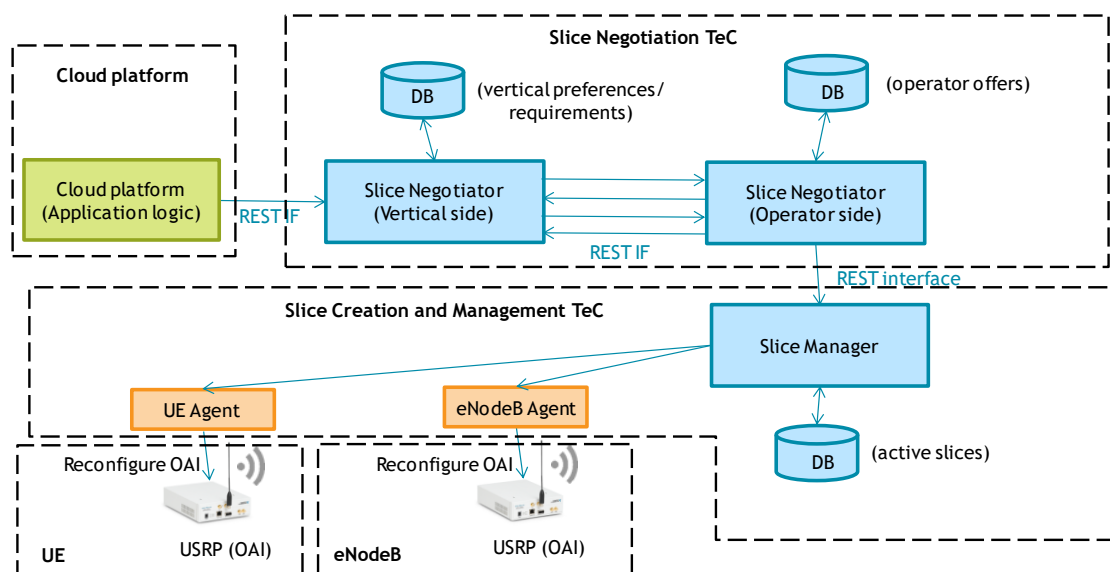


**Figure 5-8. Architecture and interfaces of Slice Negotiation TeC**

The cloud platform component includes the application logic of the vertical. The slice negotiation technical component is comprised of two parts: one located in vertical side and the other located in the network side. These two software components are both implemented using the Java programming language. The communication between the two parts is realized using the Representational State Transfer (REST) software architectural style, while the data format follows the JSON (JavaScript Object Notation) format. Since the REST interface is used for the communication between the two entities, the two parts can potentially be implemented using different programming languages or frameworks (e.g. Java and C++).

The slice management component includes the implementation of Slice Manager and a set of RAT Agents which are responsible for the realization of the RAT configuration decided by the Slice Manager. The Slice Manager is implemented in Java, while the RAT Agents are

implemented in C/C++. The communication between the Slice Manager and the RAT Agent are realized using the REST interface, while the data format follows the JSON format. The Agents communicates directly with the Open Air Interface (OAI) framework [OAI] (currently with the MAC layer of OAI) and enforce the decided reconfiguration actions.

Regarding the interfaces, the slice negotiation component has one internal interface for the communication between the two parts of negotiator and two external interfaces, as illustrated in Figure 5-8. The first external interface is located between the slice negotiator (vertical side) and the applications of the vertical. In the testbed a vertical application is implemented, which sends the vertical application requirements toward the slice negotiator (vertical side) using the REST interface. The second external interface is located between the slice negotiator (network side) and the network management entity which is responsible to configure the network (the OAI framework in our case). In a real network, this interface will be established between the slice negotiator (network side) and the Network Management System (NMS).

Regarding the interfaces of the slice manager, it has one internal interface for the communication between the Slice Manager and the Agents. In addition, it has one external interface toward the Slice Negotiator (on the network side). The Slice Negotiator (on the network side) is responsible to negotiate with the Slice Negotiator (on the vertical side) the characteristics of the new slice. When this negotiation process is finalized, the Slice Negotiator informs the Slice Manager about the request of the new slice, its type (e.g. mMTC, eMBB, URLLC) and their requirements (KPIs).

#### 5.4.4 Test/demo scenarios

The test scenario in which this TeC was integrated and demonstrated is titled "Serving underserved areas through 5G (IoT and big data) technologies: a critical infrastructure and agricultural use case". The overall scenario architecture is depicted in Figure 5-9. The architecture includes: a) the agricultural or critical vertical infrastructure which includes the sensors, actuators and different end devices; b) the 5G infrastructure including the 5G RAN, the slice orchestration and management and the service management functionalities; c) the analytics parts in which the data collection, management and analysis resides, as well as predictions of important insights (e.g. critical events); d) the dynamic dashboard which is responsible to visualize important aspects of the system like real-time or historical data, critical events or impacts of selected actions.

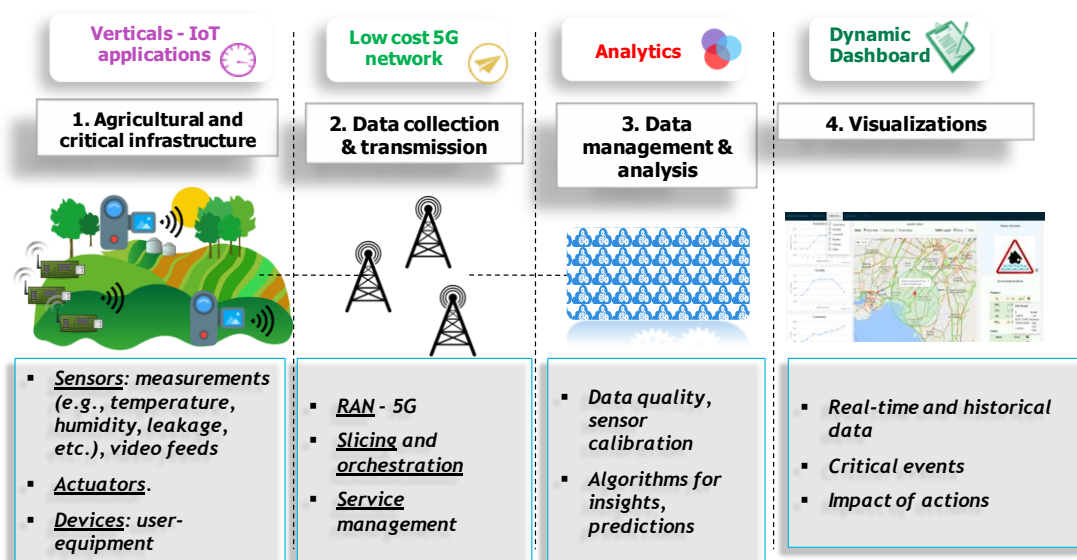
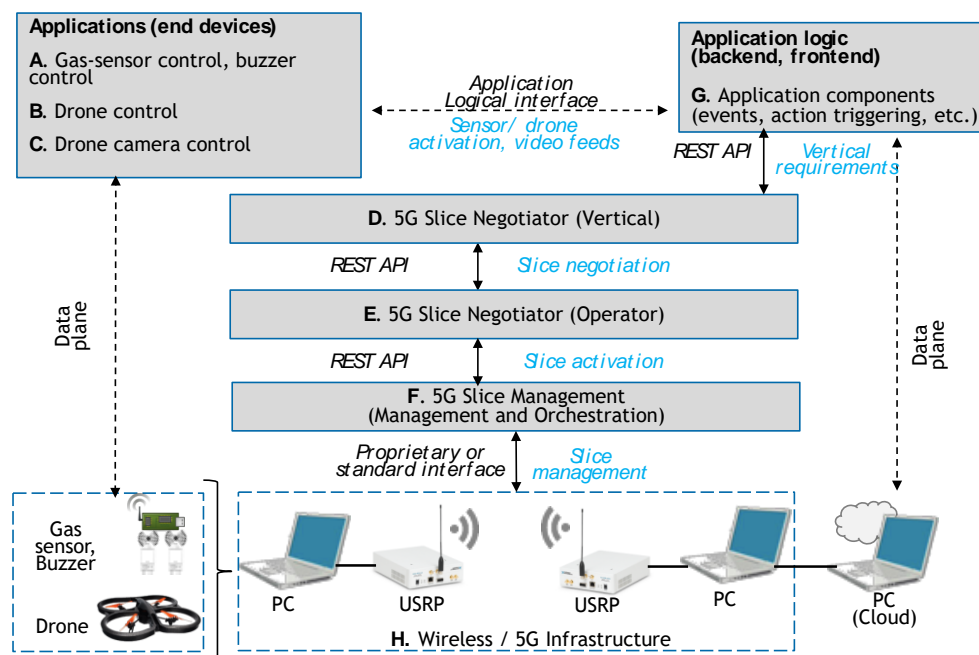


Figure 5-9. Overall scenario architecture

### 5.4.5 Validation

The Slice Negotiation technical component was validated through lab experimentation and testing in the "Platform for vertical service delivery through 5G - IoT and big data-technologies" testbed, as well as through the demonstration in high impact conferences including the MWC2018, EuCNC2018, MWC2019 and EuCNC2019.

The demonstration system comprises a set of sensors monitoring certain "problematic" events, a camera which become active on cases of "problematic" events, a set of USRPs ([USRP-B],[USRP-X]) serving as the 5G network deployment for rural and suburban areas (underserved areas) and a set of laptops having the roles of servers. The demo architecture, as well as the demo script (sequence of events) are illustrated in Figure 5-10.



**Figure 5-10. Experimentation/demonstration architecture**

According to the demo script, initially a set of sensors which are assumed to be constantly active, are monitoring for certain events (e.g., assuming a gas leakage event, an agricultural disease, a fire, a flood, etc.). These context data (of mMTC service type) are delivered using the 5G infrastructure (USRPs) to the 5G cloud platform for analysis and event identification. The USRPs are equipped with the 5G Open Air Interface framework.

When an event of interest is identified, the system decides to activate an additional service for capturing video data in order to further investigate the event and take any counter measurements. This new service is considered to have specific requirements (eMBB or even URLLC service), therefore a new slice is needed to be created in order to fulfill them. In order a new slice with specific characteristics (allocation of resources), to be activated, the slice negotiator at the vertical side (user of the service) negotiates with the slice negotiator at the operator side. This decision is further delivered to the 5G infrastructure (USRPs) in order to allocate the new resources, while a camera activation message is delivered to the video sensor.

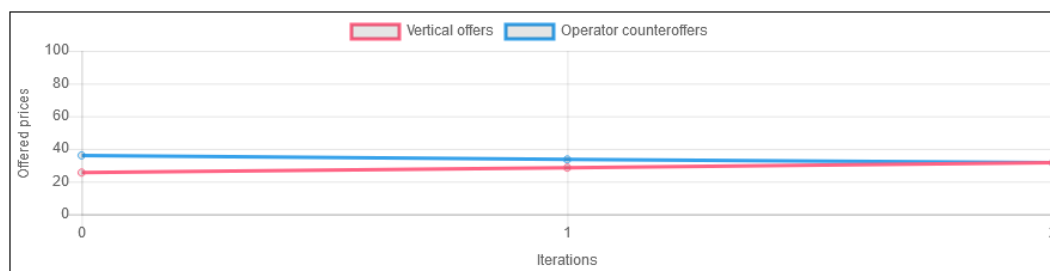
A description related to the role of the software components is the following:

- Sensors are covering an underserved area (rural, agricultural) and/or a critical infrastructure
- There is also a camera in the area
- A sensor catches some issue in an agricultural context, e.g., disease, etc. (mMTC) or a failure in the Critical Infrastructure (URLLC).

- A message is sent to a critical infrastructure management application or to an agricultural area monitoring application that has some frontend
- The application notifies a Slice Negotiator on vertical side
- The Slice Negotiator on vertical side negotiates with the Slice Negotiator on operator side
- The Slice Negotiator on operator side cooperates with further operator mechanisms and eventually a slice is established, i.e., the cell (USRP) aggregates a carrier so as to enable higher bit rates and lower latencies.
- Based on the deployed slice, our system enables the timely reception of video streams from the camera and/or the reception of more data from the massive number of sensors.

Results from the slice negotiation process of two indicative scenarios are illustrated in Figure 5-11 and Figure 5-12 respectively. In the first scenario named "service update scenario" (Figure 5-11), initially the vertical entity requests the available resources for the control of a drone for 1h and for downloading photos from the drone for 5min. The operator counteroffers with an updated offer which include video streaming (instead of the outdated photo downloading application) and for a specified offered price. The dynamic negotiation process continues until we reach to a consensus (same offered price from both entities). In the second scenario named "service counteroffers" (Figure 5-12), the vertical requests an initial service, which does not conclude to a consensus (iteration 2). In response to this, the vertical requests a lower but acceptable quality of service for a lower price. After a number of iterations, the negotiation comes to a consensus as illustrated in Figure 5-11 (iteration 6).

**Slice Negotiation: Offered prices**



**Slice Negotiation: Message Exchange**

entryId	verticalId	direction	type	verticalServiceSet	operatorServiceSet	iteration	offeredPrice
1	122	Vertical->Operator	Offer	Drone control for 1h and Photo downloading for 5m		1	25.5
2	122	Operator->Vertical	Counteroffer	Drone control for 1h and Video streaming for 5m	mMTC medium quality for 1h and eMBB medium quality for 5m	1	36
3	122	Vertical->Operator	Offer	Drone control for 1h and Video streaming for 5m		2	28.5
4	122	Operator->Vertical	Counteroffer	Drone control for 1h and Video streaming for 5m	mMTC medium quality for 1h and eMBB medium quality for 5m	2	33.5
5	122	Vertical->Operator	Offer	Drone control for 1h and Video streaming for 5m		3	31.5
6	122	Operator->Vertical	Counteroffer	Drone control for 1h and Video streaming for 5m	mMTC medium quality for 1h and eMBB medium quality for 5m	3	31.5

**Figure 5-11. Slice negotiation process - scenario 1**

### Slice Negotiation: Offered prices

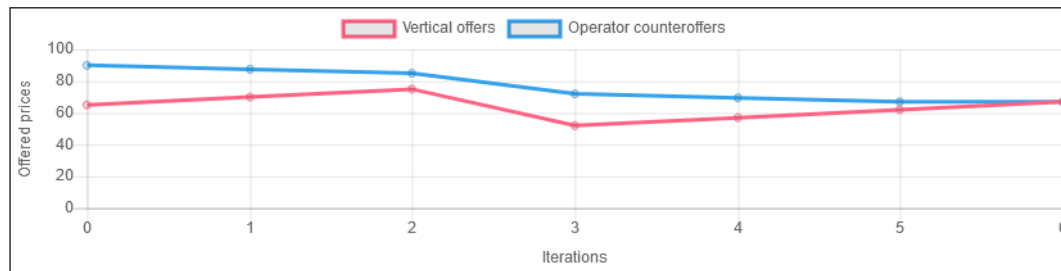


Figure 5-12. Slice negotiation process - scenario 2

## 5.5 TeC #4.3: Network slice creation supporting the vertical requirements in an area-based and time-based manner

### 5.5.1 Overview

The concept of network slicing is driven from a business rather than a technology perspective and targets a group of business customers with specialised connectivity requirements, also known as verticals. A single network slice spans across all network domains and is composed of a collection of network functions and specific RAT settings combined together for the specific use case or business model.

In addition, due to mobility and service demand variations the traffic levels change in time and space and this would require for the network slices characteristics to follow these fluctuations as well. Such traffic load fluctuations may occur in an area-based or time-based manner. For example the user movements from their houses to their offices creates area-based and time-based fluctuations of the traffic load, since traffic demands shifts from residential areas to office areas during the morning, while they shift back to residential areas during afternoon. In this direction, network slice management should be extended to proactively create network slices according to required service demands and ongoing network characteristics. In addition, such a flexible creation/management of slices will result to allocations that do not have to be always enabled and at every location all the time (which would lead to resource inefficiency). The mechanisms and algorithms for the creation of slices in an area-based and time-based manner proposed in the project are described in detail in D3.2 [ONE5G-D32] (Section 4.3.2 - Network slice management based on mobility and traffic patterns), while this section presents the actual implementation of the proposed solution as technical component and then the integration of this component into the testbed.

### 5.5.2 Objectives

The main objectives of the technical component can be summarized as below:

- Demonstrate the creation of eMBB, mMTC and URLLC slices, which are realised by the allocation of resources in the RAT and the realisation of the appropriate RAT configuration.
- Demonstrate the creation of network slices in an area-based or/and time-based manner
- Demonstrate that already established network slices can be updated based on the foreseen traffic characteristics, which are estimated based on traffic load and mobility patterns.
- Demonstrate the feasibility of the proposed technical solution on providing savings in resource utilization in residential and office areas compared to the over-provisioning case.

Currently, the TeC creates RAT slices, but the proposed implementation approach can be extended in order to be able to create end-to-end slices including RAT resources, EPC resources and cloud resources.

### 5.5.3 Architecture

The architecture of the TeC is similar to the architecture presented in the "Slice Negotiation" section, since this TeC extend the previous architecture with slice creation and management capabilities which can be applied in a time-based and area-based manner. The TeC, as illustrated in Figure 5-13, includes the Slice Characteristics Estimation component and Slice Creation and Management component.

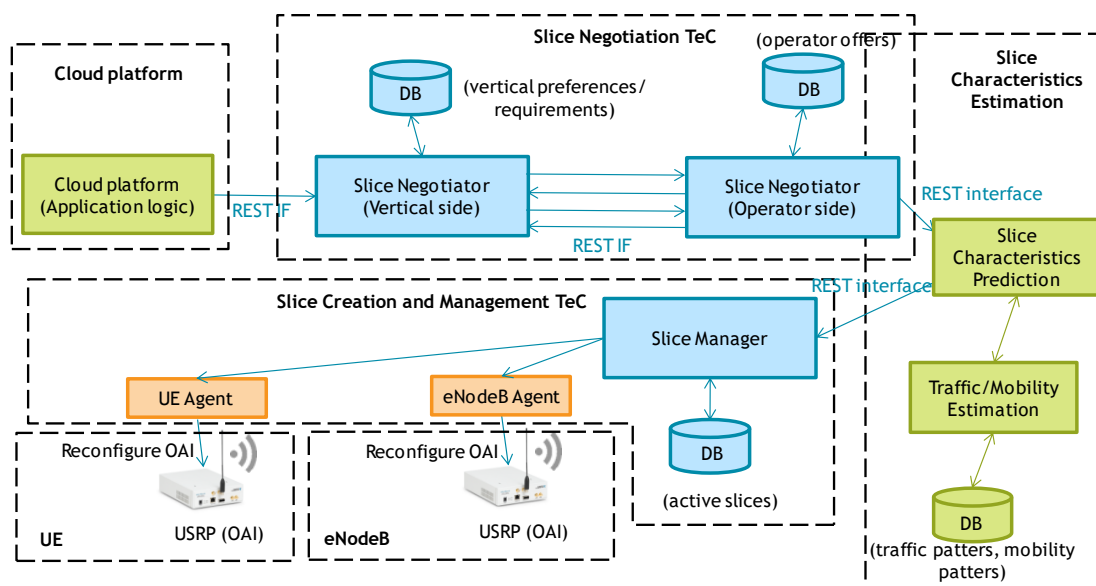
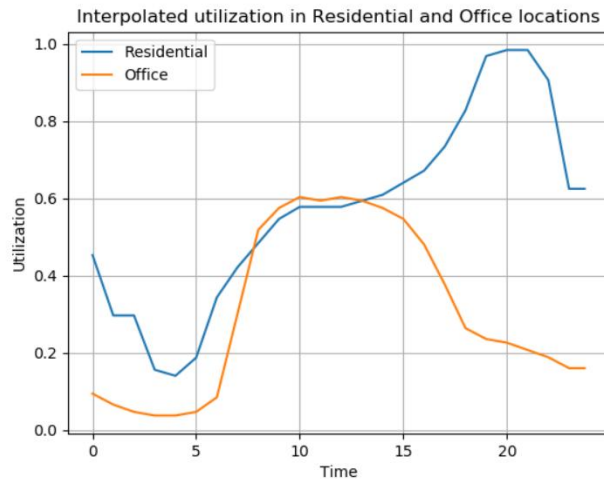


Figure 5-13. Architecture and interfaces of TeCs

The Slice Characteristics Estimation component is responsible to estimate the traffic load and mobility for the time period denoted by the network slice request arrived from the Slice Negotiator (Operator side). Then, the Slice Characteristics Predictor estimates the foreseen traffic load for the specific period by using the functionalities of the Traffic / Mobility Estimator. The Traffic / Mobility Estimator calculates the traffic load for a specific time frame using machine learning techniques based on a set of traffic and mobility patterns.

Figure 5-14 illustrates the traffic load patterns used in the case of residential and office areas respectively ([ZMF+17], [WHX+15]). From the figure it becomes obvious that the time periods in which high loads are observed are different for these two selected different areas. In offices the high loads emerge during the morning and midday, while in residential areas during afternoon and night times respectively.



**Figure 5-14. Traffic load patterns for the residential and office areas respectively**

The Slice Characteristics Estimation component is responsible to estimate the traffic load during the requested network slice establishment period for two reasons: a) in order to decide if the new network slice can be accommodated by the network (without to degrade the performance of the already established network slices); b) to affect the actual price offered by the Slice Negotiator (Operator side) to the Slice Negotiator (Vertical side) in the sense that a network slice with specific characteristics can be offered with lower or higher prices to the verticals in under-utilized or over-utilized network time periods respectively.

The Slice Characteristics Predictor is implemented in Java, while the Traffic / Mobility Estimator is implemented in Python and uses Python machine learning (ML) libraries for the realization of the ML functionality.

The Slice Creation and Management component performs the actual establishment of the network slice with the characteristics defined by the Slice Characteristics Estimation component. The implementation of this TeC includes the implementation of Slice Manager and a set of RAT Agents which are responsible for the realisation of the RAT configuration decided by the Slice Manager. The Slice Manager is implemented in Java, while the RAT Agents are implemented in C/C++. The communication between the Slice Manager and the RAT Agent are realised using the Representational State Transfer (REST) protocol, while the data format follows the JSON (JavaScript Object Notation) format. The Agents communicates directly with the Open Air Interface (OAI) framework (currently with the MAC layer of OAI) and enforce the decided reconfiguration actions.

### 5.5.4 Test/demo scenarios

The test scenario in which this TeC was integrated and demonstrated is similar to the test/demo scenario described in section 5.4.4 of the document. The test/demo scenario is entitled "Serving underserved areas through 5G (IoT and big data) technologies: a critical infrastructure and agricultural use case". The only difference to the scenario described before, is the additional testing and validation of the new components integrated into the testbed.

### 5.5.5 Validation

The TeC was validated through lab experimentation and testing in the "Platform for vertical service delivery through 5G - IoT and big data- technologies" testbed, as well as through the demonstration in EuCNC2019.

Some indicative results of the validation process are illustrated in Figure 5-15. In the inlet table the negotiation process is executed for two selected time periods and for both the residential and office areas. The results in the table demonstrate that the offered price by the operator is highly affected by the estimated traffic during the requested network slice period. In the office case,

low prices can be achieved during the afternoon, while at the same time, the requested slice cannot be accommodated in a residential area.



Figure 5-15. Slice negotiation results

## 5.6 Conclusion

The PoC implements and integrates solutions for the flexible and fast reconfigurable hardware targeting in lowering the network deployment and operation cost in underserved areas. In addition, it demonstrates network slice negotiation and management solutions targeting to fulfil the network requirements of the verticals in a cost effective way by requesting network slices in an ad-hoc manner. The PoC was validated through testing and demonstration in high quality conferences (MWC18, MWC19, EuCNC18, EuCNC19).

## 6 PoC#5: Automotive Proof-of-Concept

### 6.1 Brief description of the PoC

In the automotive industry, Tele-operated driving (ToD) is a recent application in which a remote operator controls a fully or partially automated vehicle over a wireless telecommunication network. The vehicle's cameras and sensors send live video streams and sensor data to the operator control desk which are used to control the vehicle's motion including steering, acceleration and braking. Hence ToD technology combines the human or cloud-based Artificial Intelligence (AI) capability for fast and accurate scene understanding with the benefits of automated technology inside the car. ToD is a complementary technology to autonomous driving and represents a shift in driving intelligence from the local vehicle (human or autonomous) to the remote cloud with the goal of enhancing driving safety, comfort and efficiency.

- In near-term, the ToD can help to solve complex traffic situations (temporary construction, traffic sign is unclear or even distorted, jam or conflicting traffic flows) which are not solvable by local human (passenger who is not able to drive) or local AI (considering Level 4/5 autonomous driving in any road condition with local AI is still far from being mature).
- In a more futuristic scenario, if all the vehicles are tele-operated with unified cloud-side AI, the whole road traffic system will become highly coordinated, and as a result, highly efficient and safe.
- The ToD is also applicable to professional areas such as freight hub and mining, in which large numbers of vehicles move and cooperate with each other; however, the direct field operation of human should be minimized due to safety and economic reasons.

In both ToD and cloud robotics concepts, the URLLC connectivity is crucial to guarantee that the controlling signal from the remote operator or cloud can reach the vehicle or robot reliably within low-latency constraint, considering the highly dynamic natures of the traffic environment and the factory automation process. Meanwhile, the eMBB capability is also desired to share the sensor information to the remote operator or cloud-side AI in real-time, which is the input for fast decision making.

The PoC #5 Automotive – ToD is developed by Huawei with its 5G research prototype (also applied in PoC #1 Tec #1.4 Cloud Robot) and supported by the Institute of Automotive Technology, Technical University Munich (TUM) with its ToD research platform [TeleDrv] including a real vehicle and driving control station.

The 5G prototype is designed to offer low-latency connectivity with high reliability for limited number of terminals, enabled by short and scalable frame structure, on-the-fly reconfigurable numerology, pilot density, bandwidth and MCS, etc., which is implemented with highly optimized software radio architecture.

For the PoC of ToD, the terminal node of the 5G prototype is installed into a real experimental car and interconnected with the car's driving control onboard unit (OBU) while the BS node of the prototype will be interconnected with the driving station with steering wheel, gas/brake pedals and large display showing the video sent back from the vehicle. The 5G prototype and the vehicular system are integrated in order to achieve the real ToD driving in a closed testing area and expect that the driving experience based on low-latency 5G link will outperform the experience via existing commercial cellular network. It should be noted that the 5G PoC prototype is not capable of real eMBB with data throughput of hundreds Mega of or even Giga bit per second. However, the maximum throughput of 8Mbps is able to handle the TOD video with sufficient quality.

## 6.2 List of technical components (TeCs) used in the PoC

The following TeCs are used in this PoC:

- **Flexible SDR Architecture Supporting Joint Performance-Complexity Optimization.** This TeC is specific to WP5. No direct relation with the technical WPs.
- **Short Packet Structure for Ultra-Reliable Machine-type Communication.** This TeC is related to "URLLC Enabled by GF Access, HARQ, and Frame Design" (section 2.2 of D4.2 [ONE5G-D42]).
- **Multi-connectivity beamforming for enhanced reliability.** This TeC is related to "URLLC Enabled by GF Access, HARQ, and Frame Design" (section 2.2 of D4.2 [ONE5G-D42]).
- **Tele-operated Driving Solution.** This TeC is specific to WP5. No direct relation with the technical WPs.

## 6.3 TeC #5.1: Flexible SDR Architecture Supporting Joint Performance-Complexity Optimization

### 6.3.1 Overview

The core of the flexible SDR architecture consists of a real-time processing environment and a reference simulation environment which mutually configure and validate each other as illustrated in Figure 6-1. The real-time processing environment is further integrated with SDR frontend, the configuration and scheduling entity and external application (e.g. the ToD vehicle and driving station) through the flexible data interface.

#### Real-time processing environment

In this environment, the real-time processing in both low and high layers are implemented in C/C++ on real-time Linux OS. The real-time constraint must be fulfilled that the overall processing time must be less than the actual flow time of a data unit (e.g. the time length of a signal frame). Therefore, aggressive optimization of processing efficiency has been done based on:

- Single Instruction Multiple Data (SIMD) feature of the CPU
- Multi-core joint processing of the CPU
- Real-time feature of the Linux OS
- OS/Hardware fine tuning

Meanwhile, the processing software is highly flexible in terms of applying different numerology, bandwidth, frame structure, modulation and coding schemes. High modularity is designed in the software with object-oriented programming for the ease of mapping and validation with the reference simulation environment.

#### Reference simulation environment

Developed in Matlab, this simulation environment provides an exact functional mapping of the real-time processing environment's core part. The fast prototyping and validation of algorithm and frame structure designs is achieved thanks to Matlab's ease of use and powerful libraries. Besides, the reference environment is also used to validate the over-the-air captured signal using the real-time processing environment and the RF frontend.

#### High layer configuration and scheduling entity

This entity provides the configuration and scheduling for the identity, admission and the static resource scheduling to multiple users.

#### SDR RF Frontend

Currently, we use the NI USRP X310 and N210 products as the SDR RF Frontend thanks to its sufficiently good RF quality and maturity in hardware and software support.

### Flexible data interface

The flexible data interface has been developed supporting both IP and Ethernet traffic for transparently delivering data traffics from vertical applications.

## 6.3.2 Objective

The SDR architecture is aiming at using the same software framework to support different vertical application scenarios with different setup and performance requirement. For example, in the tele-operated driving scenario, high data throughput and high mobility is required which can be supported with more power baseband server and RF frontend. In the cloud robot scenario, described in PoC#1, TeC#1.4, the data and signal bandwidth requirement is relatively lower while the form-factor and power consumption is more limited. We support both PoC scenarios with the same SDR software architecture but just different configurations.

## 6.3.3 Architecture

The architecture is illustrated in Figure 6-1. This TeC is associated with Huawei's 5G research testbed, which is used in both PoC#5 Automotive (Tele-operated Driving) and PoC #1 TeC #1.4 Cloud Robot. This TeC ranges from the physical layer (L1), medium access layer (L2) up to the IP layer or Ethernet MAC layer.

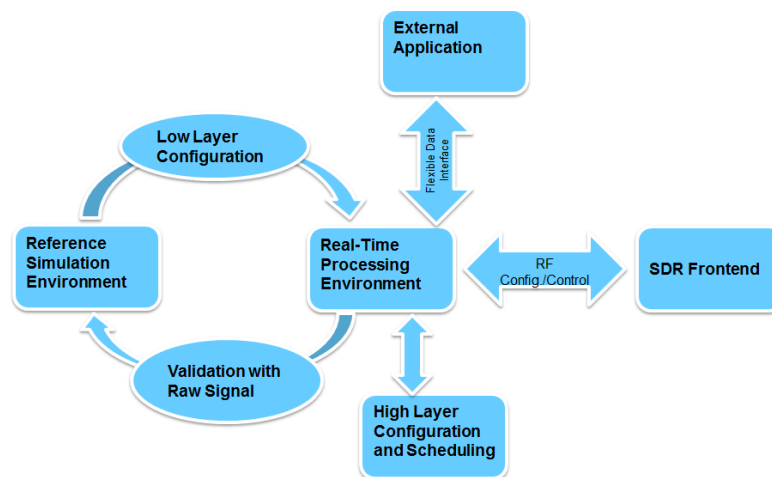


**Figure 6-1. Flexible SDR Architecture**

### Key radio access technologies

The HWDU radio testbed supports the TDD connection between one terminal and cloud side services, with different latency, reliability and bandwidth requirements. The following features are supported:

- PHY data throughput ranging from 300kbps ~ 5Mbps
- Latency ranging from 1ms to 5ms
- 99.999% PHY reliability achievable at SNR as low as 1dB
- 1 Tx by 2 Rx with receive diversity for reliability enhancement
- Signal bandwidth: 1MHz to 10MHz
- Frame length: 0.25ms ~ 5ms
- Subcarrier spacing: 30kHz, 60kHz, 120kHz
- Reference signal density: every 2 to 12 OFDM symbols
- Cyclic-prefix ratio: 0.08 ~ 0.5 length of DFT window
- ZF or MMSE channel equalization

- Coding rate  $1/9 \sim 0.9$
- Live query of SNR, BLER
- Live display of QAM constellation and signal PSD
- PHY parameter reconfiguration on-the-fly
- Defining and simulating frame structures in Matlab reference chain
- PDCP size: 42 ~ 600Bytes
- PCAP & IP tunnel based interface: supporting both Ethernet and IP traffic
- Diagnostic with self-transmitted signal

#### Versatile Data Interface Supporting Different Vertical Applications

The flexible SDR architecture supports a versatile data interface for either IP, Ethernet or raw data traffic.

- Ethernet Frame Interface Carrying Ethernet frame as the payload can achieve full transparent communication for the application system without caring the MAC/IP address conversion. Besides, for industrial automation application based on Ethernet, the extended information in the Ethernet frame header (e.g. 802.1Q extension) is needed. However, the disadvantage is that the Ethernet header will consume 14bytes or more in the payload of wireless system. The Ethernet frame interface is implemented using the PCAP library which can capture and inject raw frames from/to the Ethernet adapter.
- The IP Packet Interface Carrying only IP packet can save the overhead of Ethernet frame. However, it may require reconfiguration of the network topology of the application system for avoiding network switching over the wireless link.

### 6.3.4 Test/demo scenarios

This TeC lays the basic framework of the 5G research testbed. The demo showcases that how a customizable frame structure can be generated from a simulation environment and fast loaded into a real-time communication environment, which reflects different latency and reliability goals in the real-world V2X and industrial automation communication use cases.

### 6.3.5 Validation

The flexible SDR architecture was validated through observation of framing behavior with a spectrum analyzer (in zero-span mode). Besides, the real-time environment has the self-check capability for validating whether the RAN configuration is logically correct, for example, whether the time length of the OFDM symbols exceed the slot length, whether reference signal's structure is sufficient for the MIMO configuration, whether guard period is can sufficiently accommodate the RF chain's switching time, etc.

## 6.4 TeC #5.2: Short Packet Structure for Ultra-Reliable Machine-type Communication

### 6.4.1 Overview

For the tele-operated driving (current scenario) and cloud robot PoC, the reliable communication considering the high mobility scenario is supported from the following aspects in the physical layer:

- Flexible Numerology
- Flexible Self-contained Frame Structure
- Advanced Modulation/Coding/Diversity

This TeC is rooted from WP3's work documented in D3.2 [ONE5G-D32] Section 2.3.1 Short Packet Transmission with Reliability-Latency Constraints.

## 6.4.2 Objective

The high mobility nature of automotive application requires reliability enhancement for combating the very fast fading of the wireless channel.

## 6.4.3 Architecture

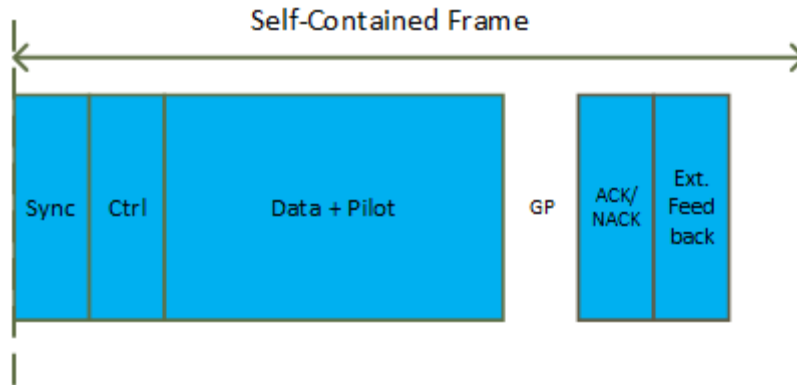


**Figure 6-2. Self-contained Frame Structure**

The frame structure implemented and integrated in the PoC consists of the following parts:

### Synchronization Preamble

In a high mobility scenario, especially for direct communication, the timing of the radio frame from different nodes is very dynamic. Therefore, an always available synchronization preamble is necessary. According to different reliability or distance requirement, the length of the synchronization preamble can be flexibly configured.

### Control Signaling

The control signaling part carries the numerology information (subcarrier spacing, CP length, modulation order, coding rate, etc.) for the receiver side to correctly decode the data part.

### Data

The numerology and the density of the reference pilot signal can be flexibly configured on the fly adapting to different requirements of reliability/data throughput and the channel conditions.

### Acknowledgement / Non-acknowledgement

It is used for acknowledging the success or failure of decoding the data in order to decide further retransmission process.

### Extended Feedback

It provides feedback information to assist advanced link adaptation, e.g. the channel delay spread and Doppler frequency spread for assisting the optimal selection of sub-carrier spacing and CP length.

This TeC is implemented in Huawei's 5G research testbed. This TeC is mainly positioned at the physical layer of the 5G research testbed. The following technologies are applied in this TeC:

- Flexible numerology, which enables the short frame structure (down to 0.125ms length) and adaptation to wireless channel, especially in high mobility
- Self-contained fast feedback, which allows for latency reduction when ACK/NACK feedback and CSI feedback are needed
- Configurable reference signal (RS) structure, which could provide the optimal trade-off between robustness and spectrum efficiency according to the mobility and traffic demand
- Fast-switch RF transceiver, which enables the fast over-the-air Tx/Rx switch within the short frame time.

- The 5G testbed has utilized the pulse-shaped OFDM (P-OFDM) waveform which has been proved being more robust than the conventional cyclic-prefix OFDM (CP-OFDM). The details of this waveform modulation scheme can be found in [P-OFDM].
- The testbed supports both turbo code and polar code while the later has superior performance especially for short packet.

#### 6.4.4 Test/demo scenarios

In the tele-operated driving scenario, this TeC enables both the low-latency and high uplink video data throughput required by the application system.

#### 6.4.5 Validation

This TeC was validated by

- Over-the-Air (OTA) observation using a spectrum analyzer in zero-span mode which indicates the frame periods from the changing of power over time
- E2E ping test which indicates the scale of latency. It should be noted that the latency also includes:
  - Signal processing time at both transmitter and receiver sides
  - The multiple access pending time, as the arrival time of application packet is not aligned with the available resource and time slot of the transmission

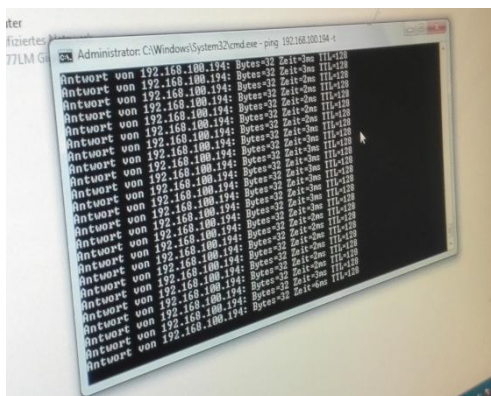


Figure 6-3. End-to-end ping to test the round-trip end-to-end delay

### 6.5 TeC #5.3: Multi-connectivity beamforming for enhanced reliability

#### 6.5.1 Overview

The reliability enhancement with multi-connectivity beamforming is implemented in the 5G research testbed at the receiver side. Basically, the receiver tracks track the channel and applies apply the optimal coefficients to its multiple receiving antenna. In this way, physically, the main lobe of a virtual beam is aimed to the transmitter side, which maximize the post-processing signal power at the receiver and enhances the reliability. User-specific beamforming is applied in a multi-connectivity scenario.

This TeC is rooted from WP3's work documented in D3.2 [ONE5G-D32] Section 4.3.2 Multi-connectivity beamforming for extreme reliability and massive multiple access. It is implemented in Huawei's 5G research testbed,

#### 6.5.2 Objectives

The main objective of the TeC is to enhance link reliability using multi-connectivity beamforming, supporting high QoE in tele-operated driving applications.

### 6.5.3 Architecture

This TeC is associated with Huawei's 5G research testbed, which is used in both PoC #5 Automotive (Tele-operated Driving) and PoC #1 TeC #1.2 Cloud Robot. This TeC is mainly positioned at the physical layer of the 5G research testbed.

The main technologies used in this TeC include:

- Reliable channel estimation algorithm with adaptive noise cancellation based on channel delay spread
- Maximum ratio combining (MRC) and minimum mean square error (MMSE) based Rx beamforming
- SIMD instruction based efficient algorithm implementation for realtime processing

### 6.5.4 Test/demo scenarios

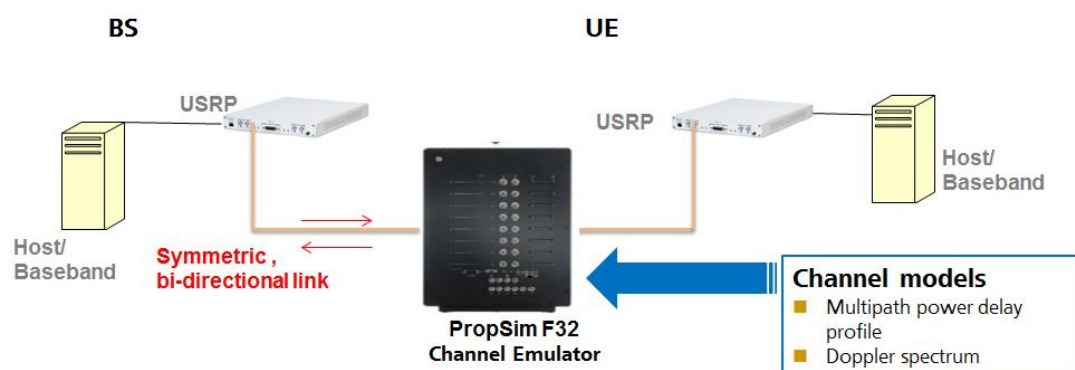


Figure 6-4. Setup for performance evaluation with real-time channel emulator



Figure 6-5. Field test of air interface performance

The TeC is tested both in our and lab and in the field:

- The lab test relies on a PropSim F32 real-time channel emulator for generate the V2X MIMO multi-path channel in real-time. The 5G research testbed runs in real-time and collect the BLER results in different antenna configurations.
- In the field test, a car carrying the UE driving along fixed path and collect the BLER results.

### 6.5.5 Validation

The testbed currently supports 2x2 transmission and reception. The transmitting diversity is applied at the transmitter side and the beamforming at the receiver side. Significant performance gain over single-antenna transmission has been shown by simulation, test with real time channel emulator and field test.

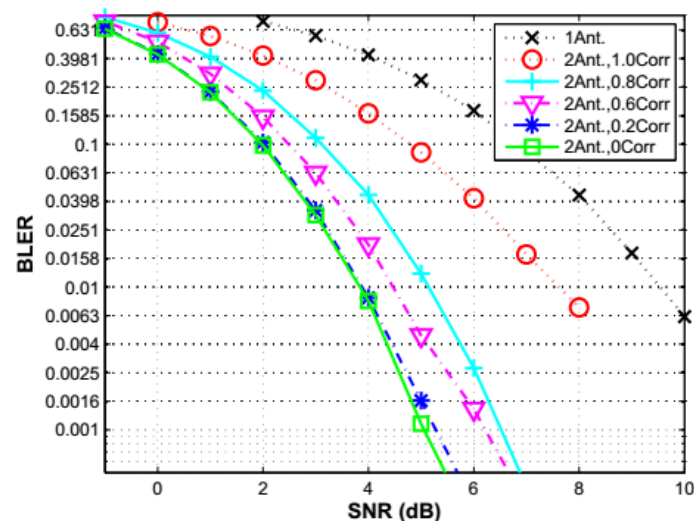


Figure 6-6. Performance gain with Rx MRC diversity

Figure 6-6 shows the test results of the 5G testbed by using a realtime channel emulator to generate MIMO channel with different correlation factors. In the fully correlated case (correlation factor of 1), about 2dB array gain can be obtained by Rx beamforming. When the channel correlation factor is less than 1, more significant diversity gain is expected, even when the correlation factor is still large. For example, the performance of correlation factor 0.6 is nearly the same as the fully uncorrelated case.

## 6.6 TeC #5.4: Tele-operated Driving Solution

### 6.6.1 Overview

The Institute of Automotive Technologies (FTM) from Technische Universität München (TUM) supplied Huawei the ToD research platform for integration with 5G testbed and joint testing. The ToD platform includes a real car modified to be fully controllable (steering, acceleration and brake) from an external onboard controller over the drive-by-wire system. Cameras and LiDAR is installed for environmental awareness. The 5G research testbed is installed in the car and interconnected to the onboard controller providing the remote connection to a driving station which is composed of driving wheel with haptic feedback, acceleration/brake pedals and HD display

### 6.6.2 Objective

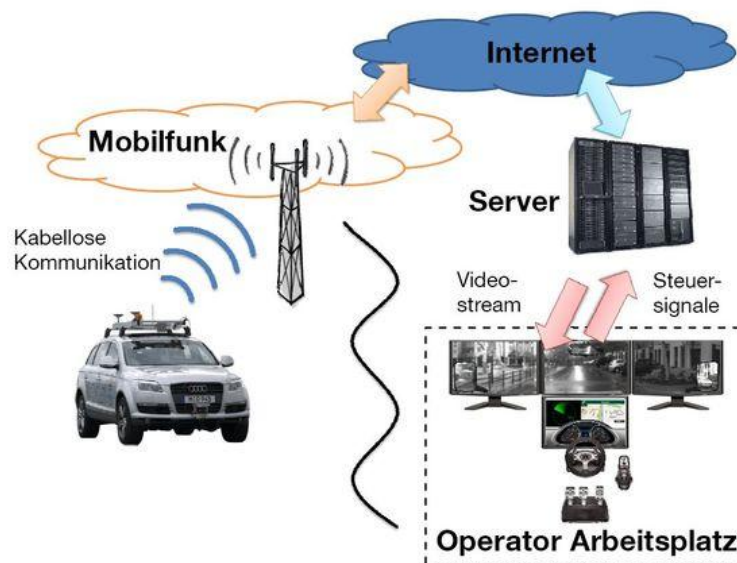
This TeC provides the complete solution of remote driving based on a real vehicle and complete camera, sensor and driving control sub-systems.

This TeC is integrated with Huawei's 5G research testbed. This TeC is positioned as the end-to-end application system on top of the 5G communication system. The ToD system consists of

- A car with the full capability of lateral (steering) and longitudinal (acceleration/deceleration) controls by digital command as well as environmental awareness by optical camera, LiDAR, mmWave radar, etc.
- A driving station equipped with steering wheel, accelerating/braking pedals and displays
- IP based data interface for communicating sensor and control data traffic.

For details, please refer to [TeleDrv].

### 6.6.3 Architecture



**6.6.4** Figure 6-7. The overall architecture of the Tele-Operated Driving System from TU München Demo/Test scenario

The vehicle transmits multiple video streams (front/side views) to the driving station and accept the steering, acceleration or braking command from the driving station given by the remote driver. The remote driver can obtain a similar experience as driving in the car, thanks to the low-latency and reliable connectivity provided by the 5G testbed.



**Figure 6-8. Tele-Operated Driving Research Platform**

### 6.6.5 Validation

The tele-operated driving test has been performed in a test ground with marked road tracks and barriers. The test shows that the vehicle can be driven normally without touching the barrier and the track border at the speed of 50km/h.

### 6.7 Conclusion

The PoC#5 Tele-operated Driving integrates the TeC of low-latency frame structure, reliability enhancement with multi-connectivity beamforming, flexible SDR architecture and the ToD application system to build a complete tele-operated driving system enabled by 5G's key

---

services of URLLC and eMBB. Through the lab and field validation, the ToD concept has been proved to be feasible if the latency, reliability and bandwidth requirement can be fulfilled with continuous coverage.

## 7 Integrated PoCs

The integrated PoC (IPoCs) realise the integration among different partner testbeds and among individual PoCs already described in the previous sections. The purpose of integration is mainly to demonstrate that: a) TeCs from different partners can be integrated toward a common target; b) different testbeds can be integrated in order to support different verticals using a common infrastructure; c) a central entity can manage in a unified way two or more testbeds located in different places.

### 7.1 IPoC#1: Serving megacities and industrial areas through 5G technologies

#### 7.1.1 Description

The main goal of the integrated PoC is to prove the suitability of 5G technologies in supporting the requirements in two challenging environments: a) industrial areas with large factories; b) highly populated areas, namely "Megacities". The PoC demo presented the validity and performance of technical components developed in ONE5G and their feasibility through prototyping into megacity and industrial contexts. Specifically, the main objectives of the PoC can be summarized as below:

- To demonstrate small cells 5G multi-connectivity for reliability enhancement in industrial environments.
- To demonstrate E2E monitoring schemes based on the actual user quality of experience (QoE) as enablers for the future network management solutions.
- To demonstrate slice negotiation and management functionalities in the industrial and megacities scenarios.
- To demonstrate the advantages of the design, development and deployment of a flexible and powerful network for megacity and industrial use cases.
- To demonstrate the validity and performance of technical components developed in ONE5G, and the corresponding gains for Megacities and industrial verticals
- To demonstrate their feasibility through prototyping into megacity and industrial contexts

In "Megacities" use case, the PoC is presenting innovative E2E Network management for 5G infrastructures using Key Quality Indicators (KQIs, characterizing E2E performance) monitoring. The PoC demo demonstrates the enhancements of QoE metrics in terms of achieving a proper assessment of the network status by proper translation of low-level indicators into higher layer performance metrics.

In industrial use case, the PoC focuses on the reliability aspects of the URLLC services. The PoC demonstrated small cells multi-connectivity for reliability enhancement. The PoC verifies the potential of multi-connectivity schemes (PDCP packet duplication, Single Frequency Network, Coordinated multi-point transmission) in improving the link quality of "smart" user equipments in industrial scenarios.

In addition, to the above functionalities, the IPoC includes a slice negotiation and management functionality, which interconnects the PoCs of the two areas ("Megacities" and industrial) and demonstrate that the network slices of both areas can be managed in a unified way.

In the PoC showcase we addressed the aforementioned use cases, through 5G and associated management technologies, as well as relevant services.

## 7.1.2 Architecture

Figure 7-1 illustrates the high-level architecture of the PoC. The PoC architecture includes:

- A 5G Infrastructure corresponding to an industrial environment including a set of smart cells (located in AAU testbed).
- A 5G Infrastructure emulating a megacity environment including a set of small cells (located in UMA testbed)
- The 5G URLLC Manager is responsible to realise the URLLC related decisions (e.g. multi-connectivity parameters, cell selection parameters) for the industrial infrastructure. For demonstration purposes, the 5G URLLC Manager was deployed in a PC and located in the conference booth (e.g. Booth in MWC19) , and communicated via the internet with the industrial infrastructure.
- The 5G KPI to KQI modelling component is responsible for managing the megacity infrastructure using KPI/KQI monitoring and estimation. For demonstration purposes, the component was deployed in a PC and was located in the conference booth. Then it was communicating through the internet with the megacity infrastructure.
- The 5G slice negotiation and management component is responsible to perform the negotiation process between the vertical side (vertical requirements) and the operator side (operator capabilities and availability) and to forward the decisions of the negotiation process to the slice manager which is responsible to create the new slices by interacting with the two management entities (industrial and megacity). Both entities are deployed on WINGS testbed.

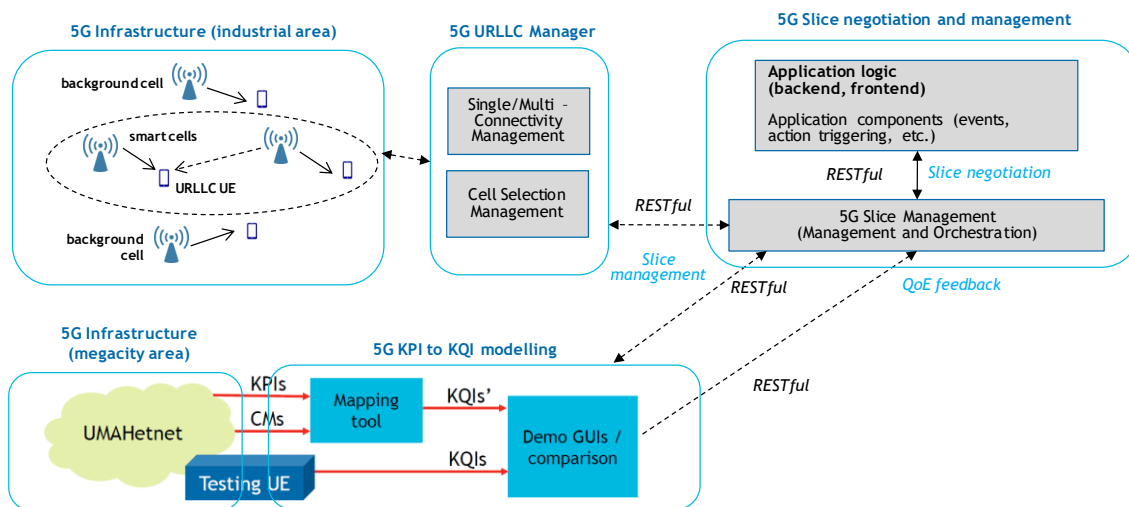


Figure 7-1. IPoC#1 architecture

## 7.1.3 Test/demo scenarios

### 7.1.3.1 Megacity scenario

Traditionally, optimization techniques have been based on improving the quality of service based on KPIs. However, classic KPIs are not enough to fully optimize and grasp the network status. In this sense, service-oriented analysis and its metrics, the KQIs, are key features to consider in the management of 5G networks.

However, the continuous gathering of KQIs presents also important challenges: the use of secure HTTP and any high-layer encrypted protocols limits the traffic inspection to measure the

KQIs. The access to application layer KQIs is also very limited at both ends of the communication, being the application user-experience generally out of reach of the cellular management monitoring. In this sense, this PoC implements tools required for the prediction of the KQIs based on cellular low-layer performance metrics and configuration parameters. This can be decomposed in two main objectives:

- Representation of KPIs and the associated service KQIs under different circumstances, comparing estimated and directly measured KQI values.
- A baseline network optimization to show the capabilities of this approach.

The test scenario comprises the UMAHETNET (a full indoor LTE network deployed in the Telecommunication Engineering School of the University of Málaga), accessible through a REST API, a testing UE and a remote client, running a mapping script. **Figure 3-7** shows the Megacity architecture. The mapping script translates, in real time, low-layer metrics collected from the network to service KQIs. To do so, in a previous offline stage, the service performance is monitored in order to build the relationship between the network metrics and KQIs, using regression techniques. Then, once the model is built, it can be used for optimization and prediction purposes. For example, using the model is possible to predict the KQIs for different services even when no user is making use of them at a specific moment.

### 7.1.3.2 Industrial scenario

The objective of this scenario is to verify the potential of multi-connectivity in improving the link quality of UEs demanding reliable communication compared to traditional single link connection. We consider a dense scenario characterized by 4 small cells located in an industrial scenario, each cell featuring 1 AP and 1 UE. Each node (AP or UE) is multi-antenna capable. Out of the 4 cells, two are “smart” cells (supporting the ONE5G technology components for multi-connectivity) and the others are background cells, i.e. meant for assessing the overall network throughput. The focus is on the downlink only, with 1 “smart” UE (benefiting from multi-connectivity), and 3 UEs associated to 3 cells in single cell mode. The UEs can be set to operate with Maximum Ratio Combining (MRC) or Interference Rejection Combining (IRC) receivers.

The targeted scenario represents a harsh interference environment given the close proximity of the cells, which may compromise the link performance in case of single connectivity. Introducing multi-connectivity is expected to lead to significant performance improvement for the UEs suffering from harsh fading or interference conditions. The smart UE selects the two cells that will provide multi-connectivity depending on their receive signal strength. Different multi-connectivity techniques are analyzed: PDCP packet duplication, Single Frequency Network (SFN), and coherent Joint transmission (JT). All the nodes are controlled by a testbed server, which also collects the relevant measurement reports by the UEs, calculates the relevant KPIs and display them live in a GUI. The goal of the demo is to assess the benefits of multi-connectivity in terms of Signal to Interference plus Noise Ratio (SINR) improvement for the smart UE, and its impact on the overall network throughput. In particular, multi-connectivity aims at ensuring that the receive SINR by the smart UE is always above a minimum threshold which guarantees the data connection. The scenario execution is shown in Figure 2-2.

### 7.1.4 Validation

The PoC was validated through the demonstration of the PoC during the MWC2019 in the 5G IA Booth. The demonstration was mainly addressing the following KPIs: reliability and network throughput. For the industrial (multi-connectivity) demonstration, reliability was estimated as the rate of occurrence of SINR dropping below a minimum threshold which guarantees data connection. For the Megacity demonstration the metrics taken into account are: RSRP, RSRQ, RSSI from the UE side and the available bandwidth and the current network load from the

network side. Moreover, the demonstration illustrated how 5G can be used for efficiently support of challenging use cases and scenarios in industrial and megacity areas.

The video from the MWC2019 demonstration can be found here:

[https://one5g.eu/wp-content/uploads/2019/03/one5g-@-mwc19\\_compressed.mp4](https://one5g.eu/wp-content/uploads/2019/03/one5g-@-mwc19_compressed.mp4)

## 7.1.5 Conclusion

The PoC is an integrated PoC between three testbed owners (partners): AAU, UMA and WINGS. The PoC includes a set of TeCs integrated into an industrial and megacity environment deployed on AAU and UMA testbed respectively, managed by a slice management entity deployed in WINGS testbed. In the industrial environment small cells 5G multi-connectivity for reliability enhancement for URLLC in industrial environments was demonstrated. The demo showcases that E2E monitoring schemes based on the actual user quality of experience (QoE) can become enablers for the future network management and optimization solutions in megacities environments. The PoC demo showcases the reliability improvements in industrial area and network throughput improvements in megacity area, while an automated process of slice negotiation and management was also demonstrated.

## 7.2 IPoC#2: Wireless control of industrial production

### 7.2.1 Description

This integrated PoC demonstrates the usage of prediction techniques to improve communication's reliability in industrial scenarios.

A key feature of industrial processes in the FoF is the high customization degree that the end products may have. This requires easily reconfigurable production lines, made up of easily rearrangeable modules. Still, such modules require connectivity, and often, the connection must fulfill a certain quality of service. Connectivity is traditionally provided to such modules by cabled connections. Nevertheless, the use of cables is opposed to the objective of having rearrangeable modules. This drives the idea of using wireless connectivity in industrial scenarios, as shown in PoC 1.

The industrial processes in the FoF sometimes interchange mission-critical messages, such as safety alarms, that have very stringent end-to-end network requirements. In 5G, these types of communications are mapped in URLLC service class, where QoS is given by ensuring certain maximum values for latency and packet loss. To do this, usually redundant resources are used, for instance, with techniques such as packet duplication, which reduce the probability of loss. Nevertheless, assigning additional resources to URLLC may come at a penalty for other coexisting service classes (such as eMBB or MMTC), causing a cost of opportunity which may or may not prove necessary, depending on the conditions.

URLLC comes, therefore, at a cost that can be reduced if resources can be reserved only in the case that the probability of packet loss and/or a high delay is significant. Usually, these values can only be measured "a posteriori", that is, after a packet has been sent. This integrated PoC uses prediction techniques to estimate the expected end-to-end latency and packet loss probability "a priori", so that the transmitter can decide whether to use redundant resources or to save the extra expense. For the estimation, this integrated PoC uses the KPI to KQI mapping developed in PoC 2, where the latency and packet loss are the KQIs and the radio interface KPIs are RSRP, RSRQ, SNR and RSSI.

The KPI to KQI mapping uses ML to train an estimator. Therefore, in the operation of the mapping method, there are two distinct phases; firstly, there is a training phase, where the relations between the KPIs and KQIs is drawn and the estimator is adapted to the environment conditions; and secondly, there is an exploitation phase where the estimator is used to actually

do the translation from KPIs to KQIs. These two stages can be superimposed in time (online learning) or done in different times (offline learning).

ML is a computationally costly process, that requires large datasets. In this integrated PoC, the ML is outsourced to a centralized location, where it acts as a service. It can be defined as a Machine Learning as a Service (MLaaS) [RGC+15] scheme, where the client sends the training samples to the server and receives an updated estimator. This has advantages both for the client and the server. The client is released from the burden of the computational cost, since it only needs to run the already trained estimator (which is usually a low computational cost process). The server can benefit from receiving datasets from many clients, therefore improving the accuracy of the training process. Since the estimator is in the machine that uses the estimation of the KQI, only the processing delay is added to the URLLC communication. The communication between the client and the MLaaS server only occurs when the model is updated, so its delay does not add up to the end-to-end latency. The MLaaS scheme also allows for continuous improvement, since upgrading the ML algorithms and software in the server does not affect the clients. In this integrated PoC, a prototype for both the client and the server have been developed, demonstrating the validity of the scheme.

## 7.2.2 Architecture

This integrated PoC is made up mainly of two components: a MLaaS server and a client installed in an industrial terminal. Figure 7-2 shows the overall architecture of the integrated PoC, identifying the TeCs implemented in each part. The two parts can be briefly described as follows:

- Server (located in the UMA testbed): it composes the core of the MLaaS scheme. It contains an aggregated dataset received from the clients and the ML logic that, using that dataset, produces a set of optimal parameters for the estimator block running in the clients. The server uses an HTTP interface that needs to be accessible through a public network interface (IP and port combination).
- Client (located in the AAU testbed): it is run in the end equipment, where the estimation is required. Since the samples that need to be estimated, as well as the KPIs that are used by the estimator, are only available in the client, the task of training data collection also relies on the client. It can be gathered in a separate training phase, where dummy packets are sent over the interface, their KQIs measured and joined with the KPIs; or in a live manner, where production packets are measured, and their data accumulated over time. The data is then sent to the MLaaS component through the HTTP interface. In order to minimize the computation delay, the estimator component runs in the client. This estimator has a set of configurable parameters that optimize its behavior, and they are set by the MLaaS component.

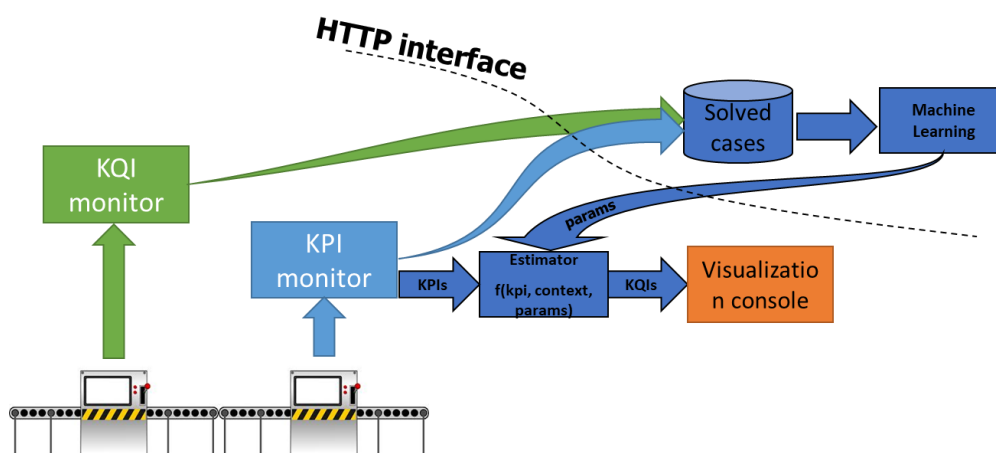


Figure 7-2. General overview of the proposed MLaaS scheme.

Apart from the advantages in computation load in the client and the possibility of using large dataset in the server, this scheme has a practical advantage for the development and deployment. Since the client and the server communicate through an HTTP interface, which is a standard supported by many platforms, their development can be decoupled; allowing the development of clients for many different platforms and also as modules that are components of larger systems.

### 7.2.2.1 Data gathering for ML

Data gathering is a key task in any ML problem. It consists in gathering, appropriately formatting and sending the data that will be used by the ML method for producing the optimized output.

The data gathering component measures the network conditions and target KQIs for a specified time interval. Specifically, the following measurements are taken:

- KQIs: average end-to-end latency and packet loss probability.
- KPIs: average RSRP, RSRQ, RSSI and SNR.

In each of the measured intervals, the component executes a routine where a set of dummy packets are sent to a server and the round-trip time is measured, as well as the number of lost packets. At the same interval, the wireless KPIs are measured. It then creates a data vector that is accumulated in a dataset, which is sent at predetermined intervals to the server to update the estimator.

This component runs in the UEs described in PoC 1, TeC 2, which act as gateways for production line modules.

### 7.2.2.2 Machine Learning

The ML task models the processes that take place when a wireless transmission is performed, considering the radio conditions. The type of ML algorithm will depend on the type of available data. If the available data only covers the input space, only unsupervised learning can be applied, which mainly looks for common patterns among the data. If both input and output data of the modeled process are available, then supervised learning can be used, effectively establishing a relation between input and output that imitates the modeled system. In this integrated PoC, the target is a mapping mechanism that models the end-to-end behavior of a service running on a wireless UE under different radio conditions; such that when it is fed with the radio KPIs, it returns an estimation of the end-to-end delay and packet loss probability.

The ML algorithm used in this integrated PoC is a random forest regressor [B+01]. Random forests are an ensemble technique that can be used both for regression and classifying. Internally, they have a set of decision trees that are trained independently on a subset of the training data in a procedure called Bootstrap Aggregation [HL+03]. Once the training is completed, a set of trees that can estimate a value for the output given a set of input values are obtained.

The testbed associated to this process is described in Section 2.4.

### 7.2.2.3 Estimator

The estimation task consists in the exploitation of the model returned by the MLaaS component. It is a low computational cost operation where the estimator is fed with the measured radio KPIs and returns the estimation for the end-to-end delay and the packet loss probability at the current instant. This operation allows the client to decide which resources to use based on the estimated latency and packet loss probability. Since the estimator runs locally, the computing time overhead is minimal. No communication between client and server is required for the estimation task.

The estimator is a random forest, as described in the previous section. In the exploitation stage the trees are fed the input values (KPIs), each returning a different value for the estimation of

the output variable (KQI). The output of the regressor is the average of the output of all the trees. In this integrated PoC, a total of 1000 trees are trained and used for estimation.

This component runs in PoC 1, where it acts as a predictor background process.

### 7.2.3 Test/demo scenarios

This integrated demo is oriented towards connectivity in industrial scenarios. The development of novel industrial processes and paradigms is increasingly creating the demand for wireless connectivity in factories, with increasingly tight requirements. Specifically, in URLLC, upper bounds in latency below 10 ms are expected, as well as a packet loss probability below  $10^{-5}$ . Nevertheless, in industrial scenarios, the conditions for propagation are very harsh, mainly due to two reasons:

- Presence of large metallic structures that cause shadowing and therefore reduce the received power. These structures may be moving (for instance, moving vehicles or growing stockpiles), so it is also difficult to compensate their effects with network planning.
- Large number of connected devices in small areas that cause interference.

These two phenomena reduce the signal to noise ratio and generally cause an increase both in packet loss probability and latency (in part, because packet loss at lower layers causes retransmissions). Therefore, in industrial scenarios, URLLC requirements are both in high demand and especially challenging.

As described earlier, the demo has been developed as two separate entities: a client and a server. The client has been deployed in the wireless gateway of a production line at Aalborg University premises as described in PoC 1, while the server has been deployed in a remote location in the University of Málaga.

#### 7.2.3.1 Client

To better assess the behavior of the module in a controlled environment, the antenna port of the LTE modems in the gateway have been connected through a programmable wideband attenuator, as shown in Figure 7-3. The attenuator is used to easily illustrate the behavior of the system in different emulated scenarios in a demo setup, but it can be removed in a production setup.

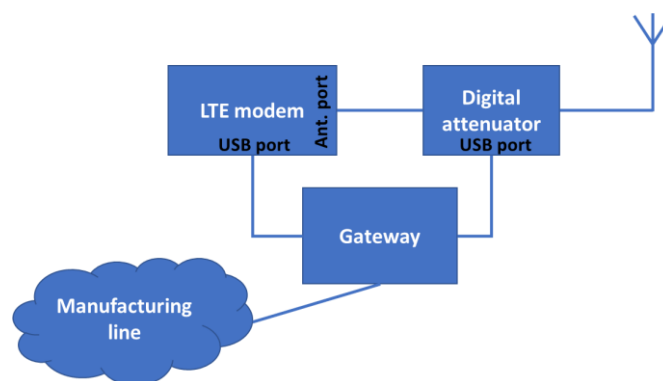


**Figure 7-3. Hardware connections in a demo setup.**

The client software has been developed in Python, as a set of independent modules connected through a RabbitMQ [RMQ] server. The RabbitMQ server acts as a message broker where the modules can publish data (such as KPI readings or KQI estimations) and send commands to other modules. Each module will subscribe to the channels that are relevant to it. The modules (Figure 7-4) that make up the setup are the following:

- Estimator: performs the task of estimating end-to-end latency and packet loss probability. It reads a RabbitMQ queue that contains the KPIs and also the updated parameters for the random forest.
- KPI gatherer: collects the KPIs from the radio interface and sends them through a RabbitMQ exchange.
- Training modules: a set of four modules that orchestrate and collect the training set:
  - Dummy packet generator: generates dummy packets in groups of configurable length. Specifically, pings of a configurable size are sent to a predefined IP. Creates a file for each group where all the IP traces.
  - KQI measurer: reads the file dumped by the packet generator and measures the average RTT and the proportion of lost packets. It then sends these measurements through a RabbitMQ exchange.
  - Training data collector: joins the data generated by the KQI measurer and the KPI gatherer and accumulates them over time in a file.
  - Training orchestrator: Coordinates the rest of the training modules, starting and stopping the KQI measurer when required, and interacting with the attenuation module in order to obtain data from different scenarios. The orchestrator can also work in a production environment where the attenuator is not present; and in that case it coordinates a passive data collection for a manually defined time period.
- Attenuator control: sets the attenuation of the wideband attenuator through its USB interface. It reads the attenuation commanded by the training orchestrator from a RabbitMQ queue. It is only used in the demo setup.
- MLaaS client: reads the dataset accumulated by the training dataset collector and sends it to the MLaaS server. When a response is received, it sends the parameters to the estimator module.
- Terminal GUI: displays the measured KPIs, real ("a posteriori") KQIs and estimated ("a priori") KQIs. The GUI is based on a Python server that collects the values to be displayed from a RabbitMQ queue, and a JavaScript client which displays the graphs on a web browser.

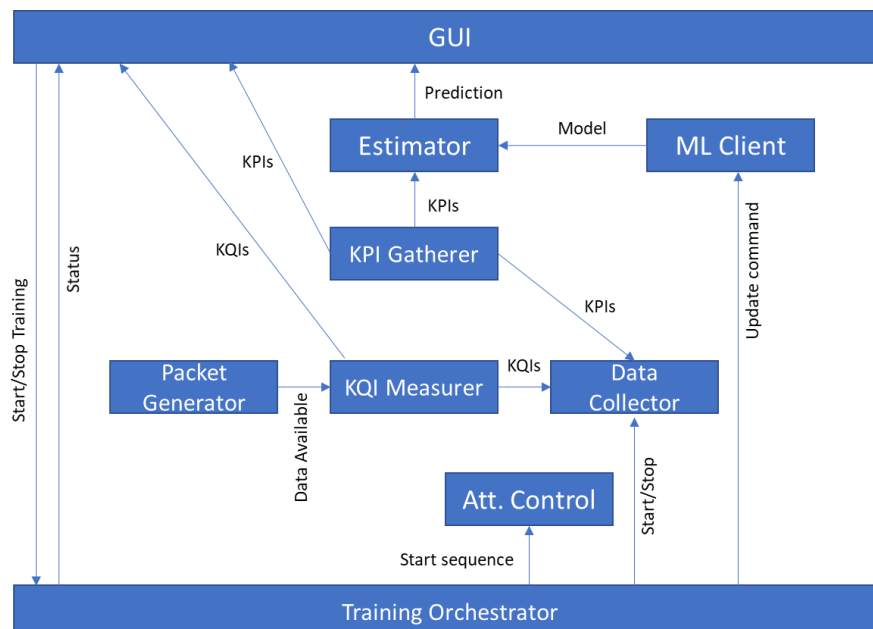


**Figure 7-4. Client Modules**

The client software can be operated for learning (both in production and demo setups) and for emulating different scenarios when the attenuator is connected (only in the demo setup). In the learning phase of a demo setup, the training orchestrator will command increasingly high

attenuations for a certain period, while the dummy packet generator, the KQI measurer, the KPI gatherer and the training data collector accumulate the training data. Once the full sweep of predefined attenuations is performed, the orchestrator will stop data collection and command the MLaaS client to send the data to the server and will update the estimator once the response is received. In a production setup, there is no attenuation sweep. The orchestrator will start and stop the data gathering on demand. Once the data gathering is stopped, it will command the interaction with the server and update of the estimator.

To test the trained model live, in demo setups, the attenuation can be set manually through the GUI, emulating different scenarios and eliciting a response from the estimation module. The GUI is made up mainly of the following components:

- Live prediction graph (Figure 7-5): shows if the estimated "a priori" end-to-end latency and packet loss rate are above a certain predefined threshold. The intervals where the estimation is above the threshold are painted in red. It also represents the values measured "a posteriori" (as a line graph), demonstrating the prediction capability of the system. In Figure 7-5 both the "a priori" estimation (blue) and "a posteriori" measurements are shown.
- ML controls (Figure 7-6): two different ways for data gathering can be commanded from the GUI:
  - Automated data gathering based on an attenuation sweep.
  - Manual start and stop of data gathering, associated with a production setup. In this case, the attenuation is not modified, therefore, this mode works both with and without the presence of the attenuator.

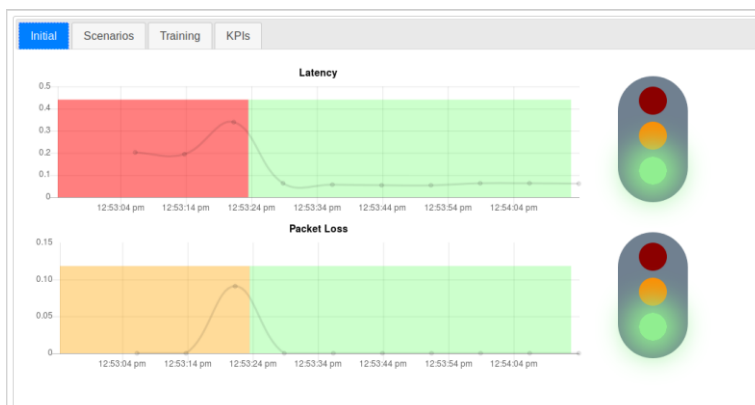


**Figure 7-5. Live prediction in the client GUI.**



**Figure 7-6. Training and demo controls.**

### 7.2.3.2 Server

The server is implemented as a Flask [FLASK] service that runs a single function, which is performing the ML process on a dataset received through an HTTP POST request. Once a

dataset is received, it will train a random forest with 1000 trees using the Scikit-learn library [SLL], with the default parameters, and return the results as a response to the POST request. This functionality can be extended in the future with functions such as additional preprocessing, data accumulation from different clients, optimization of the ML parameters, etc.

## 7.2.4 Validation results

This demo has been executed during EuCNC2019. The client was installed in the equipment in Aalborg University and accessed by remote desktop; while the server was running in the University of Málaga. The client measured in real time the KPI and KQI conditions and estimated the "a priori" values of the KQIs after the ML was done in the premises of UMA.

Additionally, some measurements of the accuracy were made over a dataset of 6983 samples collected over 15 hours. These measurements are summarized in Table 7-1. The system predicts 99.8% of the time correctly when the latency is going to be above or below a threshold settled at 120 ms, with a false positive (i.e. predicting that the latency will be above 120 ms and then obtaining a lower latency in the "a posteriori" measurement) rate of 0.16% and false negative rate of 2.85%. For the packet loss rate, the success rate is lower, 88.57%, with false positive rate of 11.43% and false negative rate of 10.71%. The higher error in the packet loss estimation is due to a low number of occurrences of packet loss in the training sets. In order to obtain better results, a more prolonged training time is required. Table 7-1 also shows the MSE error of the "a posteriori" estimation for both end-to-end delay and packet loss.

**Table 7-1. Accuracy measurements.**

E2E KQI	MSE	False-negative	False-positive	Success rate
Latency (target: < 0.120 s)	0.00264	2.85 %	0.16 %	99.8%
Packet loss probability (target < 10 <sup>-5</sup> )	0.00018	10.71 %	11.43 %	88.57 %

## 7.2.5 Conclusion

This integrated PoC proposes a MLaaS scheme to deploy a mechanism that can predict "a priori" the end-to-end delay and packet loss probability of a mission critical message in a wireless gateway that provides connectivity for an industrial equipment.

In this MLaaS scheme, the client runs a software that estimates the delay and packet loss using a random forest regressor. The client also gathers samples for training this regressor, but instead of performing the ML locally, it sends the measurements to a remote service where ML is performed and an updated set of parameters for the regressor are sent back. This offers two advantages: for the client, it means a reduction in computational cost; and for the server, a larger rich dataset gathered from many clients.

A demo using elements of PoCs #1 and #2 has been developed, where the estimated "a priori" KQIs are compared with the measured "a posteriori" values. The results show that the system can predict with a high degree of success when additional resources are required to guarantee a certain quality of service in an industrial scenario. These figures can be improved in the future by preprocessing the training sets or fine-tuning the ML process. Thanks to the MLaaS scheme all these improvements can be done without any modification on the client, therefore reducing the cost of upgrades in the service.

## 8 Conclusion

In this final WP5 deliverable, we presented the final version of the PoCs that were defined, implemented, integrated and demonstrated throughout the ONE5G project with the aim of realizing in hardware and software the main innovations of the project, proposed in the two technical WPs (WP3 and WP4) of the ONE5G project.

In Chapter 1 of the deliverable an introduction was presented, in which the five PoCs and the two integrated PoCs were presented together with the list of TeCs implemented and integrated in each PoC. We presented the technological proposals included in each TeC and the testbeds in which these proposals were integrated. We also presented and explained the integrations between testbeds and the motivation for such integration activities.

Then, in Chapters 2 to 6 we presented in detail the five PoCs of the ONE5G project: 1) Industrial PoC; 2) Smart Megacity PoC; 3) Massive MIMO PoC; 4) Underserved Areas PoC and; 5) Automotive PoC. In each chapter, we presented the main innovations and the included TeCs. Then, for each TeC we provided its main objectives, the architecture, the testing scenarios under which each specific TeC was tested and validated, and finally the validation results in terms of KPI improvements in lab scenarios or demonstration during important events (e.g. MWC18, MWC19, EuCNC18, EuCNC19).

In Chapter 7 we presented the two integrated PoCs, resulted by the integration of different testbeds. The first IPoC demonstrated the suitability of 5G technologies in supporting in a unified way the requirements in both industrial and "Megacities" areas, while the second IPoC deals with a wirelessly controlled production line, addressing the capabilities of different radio technologies in supporting the latency demands.

In short, the main findings of the prototyping activities can be summarized below:

1. In industrial scenarios, the adoption of multi-connectivity solutions in improving the reliability of the communication link has been assessed. Different multi-connectivity solutions have been demonstrated; physical layer solutions such as SFN and non-coherent JT, as well as higher layer duplication. Results prove the capability of multi-connectivity solutions in improving the receive SINR especially in scenarios characterized by high LOS probability. Physical layer multi-connectivity solutions outperform high layer duplication, at the expense of a higher computational cost. The penalty of multi-connectivity in terms of maximum throughput in the considered network has also been estimated.
2. In Megacity scenarios, multiple novel approaches for cellular management, with focus on QoE and E2E monitoring/modelling as well as context-awareness and slice negotiation procedures were prototyped and validated. Higher layer KQIs can be properly estimated as well as forecasted based on low-layer metrics. Also, load balancing algorithms supported by QoE estimation or direct measurement allow to highly improve the performance in the network. Moreover, adding context information related to the position of the users increases these benefits, validating it as a solid option for the development of new standards of cellular network management.
3. In Megacity scenarios, mechanisms for the ad-hoc deployment of services on edge cloud improve latency and minimizes the throughput between the BS and the Cloud.
4. In Megacity scenarios, machine learning can replace some building blocks of wireless NOMA receivers in the regime of having more UEs than receive antennas at the BS. A practical nonlinear machine learning based technique that works with short training and a small number of antennas was demonstrated and validated, outperforming conventional methods with fewer antennas.
5. Underserved Areas solutions for the flexible and fast reconfigurable hardware can be used in order to lower the network deployment and operation cost. In addition, the adoption of slice negotiation and management solutions helps in fulfilling the network requirements of the verticals in a cost-effective way by requesting network slices in an ad-hoc manner.

- 
6. In automotive scenarios, the following solutions improve the latency in URLLC services: low-latency frame structure, reliability enhancement with multi-connectivity beam-forming and flexible SDR architecture. The improvements were demonstrated using a complete tele-operated driving system.

## References

- [3GPP-38212] 3GPP TS 38.212- Release 15 - NR; Multiplexing and channel coding. September 2017.
- [ACS1+18] D. A. Awan, R. L.G. Cavalcante and S. Stanczak, "A robust machine learning method for cell-load approximation in wireless networks", IEEE International Conference on Acoustics, Speech, and Signal Processing (ICASSP), Calgary, Alberta, Canada. April 2018.
- [ACS2+18] D. A. Awan, R. L.G. Cavalcante and S. Stanczak, "Set-theoretic learning for detection in cell-less C-RAN systems". 6th IEEE Global Conference on Signal and Information Processing, California, USA, Nov. 26-18, 2018.
- [ACY+18] D. A. Awan, R. L.G. Cavalcante, M. Yukawa, and S. Stanczak, "Detection for 5G-NOMA: An Online Adaptive Machine Learning Approach", IEEE International Conference on Communications (ICC), May 2018
- [B+01] L. Breiman, «Random forests,» Machine learning, 2001.
- [CEN+10] E. J. Candes, Y. C. Eldar, D. Needel, P. Randall, "Compressed sensing with coherent and redundant dictionaries", Applied and Computational Harmonic Analysis, no. 31, pp. 59-73, 2010.
- [Cisco-FaM] Cisco 2017, "Cisco Visual Networking Index: Forecast and Methodology, 2016-2021". September 15, 2017. Available at: <https://www.cisco.com/c/en/us/solutions/collateral/service-provider/visual-networking-index-vni/complete-white-paper-c11-481360.html>
- [CWS+17] B. Chen, J. Wan. L. Shu, P. Li, M. Mukherjee, B. Yin, "Smart Factory of Industry 4.0: Key Technologies, Application Case, and Challenges", IEEE Access, vol.6, pp. 6505-6519, December 2017.
- [FAB+15] S. Fortes, A. Aguilar-García, R. Barco, F. B. Barba, J. A. Fernández-Luque and A. Fernández-Durán, "Management architecture for location-aware self-organizing LTE/LTE-a small cell networks," in IEEE Communications Magazine, vol. 53, no. 1, pp. 294-302, January 2015.
- [FAF+16] S. Fortes, A. Aguilar Garcia, J. A. Fernandez-Luque, A. Garrido and R. Barco, "Context-Aware Self-Healing: User Equipment as the Main Source of Information for Small-Cell Indoor Networks," in IEEE Vehicular Technology Magazine, vol. 11, no. 1, pp. 76-85, March 2016.
- [FBA+15] Sergio Fortes, Raquel Barco, Alejandro Aguilar-García, Pablo Muñoz, Contextualized indicators for online failure diagnosis in cellular networks, Computer Networks, Volume 82, 2015, Pages 96-113, ISSN 1389-1286.
- [FLASK] Pycocoo, «Flask,» Available: <http://flask.pocoo.org/>.
- [FSP+19] Fortes, S.; Santoyo-Ramón, J.A.; Palacios, D.; Baena, E.; Mora-García, R.; Medina, M.; Mora, P.; Barco, R. The Campus as a Smart City: University of Málaga Environmental, Learning, and Research Approaches. Sensors 2019, 19, 1349.

- [HL+03] T. Hothorn y B. Lausen, «Double-bagging: combining classifiers by bootstrap aggregation,» Pattern Recognition, vol. 36, nº 6, pp. 1303-1309, 2003.
- [HW+18] S. Gangakhedkar, H. Cao, A. R. Ali, K. Ganesan, M. Gharba and J. Eichinger, "Use Cases, Requirements and Challenges of 5G Communication for Industrial Automation," 2018 IEEE International Conference on Communications Workshops (ICC Workshops), Kansas City, MO, 2018, pp. 1-6.
- [IEEE-80211ac] IEEE 802.11ac-2013 - Part 11: Wireless LAN Medium Access Control (MAC) and Physical Layer (PHY) Specifications--Amendment 4: Enhancements for Very High Throughput for Operation in Bands below 6 G. January 2013.
- [JPL+01] N. R. Jennings, P. Faratin, A. R. Lomuscio, S. Parsons, C. Sierra and M. Wooldridge (2001) "Automated negotiation: prospects methods and challenges" Int. J. of Group Decision and Negotiation 10 (2) 199-215.
- [KAB+19] E. J. Khatib, D. Assefa, G. Berardinelli, I. Rodriguez, P. E. Mogensen, "Multi-Connectivity for Ultra-Reliable Communication in Industrial Scenarios", VTC-Spring 2019, April 2019.
- [LAH04] Haifei Li, D. Ahn and P. C. K. Hung, "Algorithms for automated negotiations and their applications in information privacy," Proceedings. IEEE International Conference on e-Commerce Technology, 2004. CEC 2004, pp. 255-262.
- [MLL+18] N. H. Mahmood, M. M. L. Lechuga, D. Laselva, K. Pedersen, G. Berardinelli, "Reliability Oriented Dual Connectivity for URLLC services in 5G New Radio", 15th IEEE International Symposium on Wireless Communication Systems (ISWCS), August 2018.
- [MPT+13] P. Mogensen et al. "5G small cell optimized radio design", Global Communication Conference 2013, December 2013.
- [MRB+19] R. S. Mogensen et al. "Implementation and Trial Evaluation of a Wireless Manufacturing Execution System for Industry 4.0", submitted to VTC Fall 2019.
- [NLG+10] "J. Navarro-Ortiz, J. M. Lopez-Soler, and G. Stea, "Quality of experience based resource sharing in IEEE 802.11e HCCA," in 2010 European Wireless Conference (EW), April 2010, pp. 454–461."
- [OAI] Open Air Interface (OAI), Website: <http://www.openairinterface.org/>
- [ONE5G-D21] ONE5G Deliverable D2.1 " Scenarios, KPIs, use cases and baseline system evaluation", Dec. 2017
- [ONE5G-D31] Deliverable D3.1 "Preliminary multi-service performance optimization solutions for improved E2E performance"
- [ONE5G-D32] Deliverable D3.2 "Recommended multi-service performance optimization solutions for improved E2E performance"

- [ONE5G-D41] Deliverable D4.1 “Preliminary results on multi-antenna access and link enhancements”
- [ONE5G-D42] Deliverable D4.2 “Final results on multi-antenna access and link enhancements”
- [ONE5G-D51] ONE5G Deliverable D5.1; Definition of the PoC scenarios
- [OTL+16] "P. Oliver-Balsalobre, M. Toril, S. Luna-Ramírez, and J. M. Ruiz Avilés, “Self-tuning of scheduling parameters for balancing the quality of experience among services in LTE,” EURASIP Journal on Wireless Communications and Networking, vol. 2016, no. 1, p. 7, Jan 2016."
- [RGC+15] M. Ribeiro, K. Grolinger y M. A. M. Capretz, «MLaaS: Machine Learning as a Service,» de IEEE 14th International Conference on Machine Learning and Applications (ICMLA), 2015.
- [RMQ] Pivotal, «RabbitMQ,». Available: <https://www.rabbitmq.com/>.
- [Robotino] Robotino mobile robot system from Festo: <http://wiki.openrobotino.org/>
- [SKD+05] V. Stavroulaki, A. Katidiotis, G. Dimitrakopoulos, P. Demestichas and S. Buljore, "Negotiation and selection of equipment reconfigurations in beyond 3G systems," 2005 IEEE 16th International Symposium on Personal, Indoor and Mobile Radio Communications, Berlin, 2005, pp. 1969-1973 Vol. 3
- [SLL] Scikit-learn library, Available: <https://scikit-learn.org/>.
- [SW+18] S. Stefanatos and G. Wunder, "Performance Limits of Compressive Sensing Channel Estimation in Dense Cloud RAN," IEEE International Conference on Communications (ICC18), May 2018.
- [TeleDrv] Gnatzig, Sebastian; Frederic Chucholowski, Tito Tang and Markus Lienkamp: A system design for teleoperated road vehicles. ICINCO 2013 - Proceedings of the 10th International Conference on Informatics in Control, Automation and Robotics, 201410th International Conference on Informatics in Control, Automation and Robotics, ICINCO 2013, 231-238
- [U2000] U2000, Huawei network commercial management tool, <https://support.huawei.com/enterprise/es/network-management/manager-u2000-pid-15315>
- [USRP-B] USRP B210, Website: <https://www.ettus.com/all-products/UB210-KIT/>
- [USRP-X] USRP X310, Website: <https://www.ettus.com/product/details/X310-KIT>
- [WHX+15] Wang, Huandong, Fengli Xu, Yong Li, Pengyu Zhang, and Depeng Jin. "Understanding mobile traffic patterns of large scale cellular towers in urban environment." In Proceedings of the 2015 Internet Measurement Conference, pp. 225-238. ACM, 2015.
- [ZMF+17] Zhang, Mingyang, Haohao Fu, Yong Li, and Sheng Chen. "Understanding urban dynamics from massive mobile traffic data." IEEE Transactions on Big Data (2017).